

DIPLOMARBEIT

Titel der Diplomarbeit

Development of a phosphonic acid pseudo-peptide
based monolithic chiral stationary phase for
capillary electrochromatography

Verfasserin

Stefanie Buchinger

angestrebter akademischer Grad

Magistra der Naturwissenschaften (Mag. rer. nat.)

Wien, 2009

Studienkennzahl lt. Studienblatt: A 419

Studienrichtung lt. Studienblatt: Chemie

Betreuerin / Betreuer: ao. Univ.-Prof. Mag. Dr. Michael Lämmerhofer

TABLE OF CONTENTS

I. CHIRALITY MATTERS	1
I.A. WHY DOES CHIRALITY MATTER?	1
I.B. WHAT IS CHIRALITY?	1
I.C. HOW CAN ENANTIOMERS BE SEPARATED?	1
I.C.1. INDIRECT APPROACH	3
I.C.2. DIRECT APPROACH	4
<i>I.C.2.1. Chiral mobile phase mode.....</i>	<i>4</i>
<i>I.C.2.2. Chiral stationary phase mode.....</i>	<i>4</i>
 II. OBJECTIVE OF THE PRESENT WORK	 6
 III. SELECTOR SYNTHESIS	 7
III.A. MULTICOMPONENT REACTIONS AND COMPOUND LIBRARIES.....	7
III.B. ADOPTION OF AN UGI REACTION FOR SELECTOR SYNTHESIS	8
III.B.1. THE UGI REACTION – RETROSPECTION AND PROSPECTS	8
III.B.2. MECHANISTIC CONSIDERATIONS	9
III.B.3. EXPERIMENTAL CONDITIONS	12
<i>III.B.3.1. Microwave irradiation</i>	<i>12</i>
<i>III.B.3.2. Reactant concentration</i>	<i>17</i>
<i>III.B.3.3. Solvent.....</i>	<i>19</i>
<i>III.B.3.4. Temperature.....</i>	<i>23</i>
III.B.4. SYNTHESIS PROTOCOL OF THE PRIMARY TEST COMPOUND	24
III.C. PRIMARY TEST COMPOUND CHARACTERIZATION	24
III.C.1. RPLC-UV-ESI-MS	25
III.C.2. ENANTIOMER SEPARATION.....	27
III.C.3. STEREOCHEMISTRY	28
<i>III.C.3.1. Absolute configuration determination of the aminophosphonic acid building block.....</i>	<i>28</i>
<i>III.C.3.2. Optical rotation of the stereoisomers of obtained Ugi product</i>	<i>29</i>
III.C.4. STABILITY	30

III.D. MONOESTER CLEAVAGE.....	31
III.D1. EXPERIMENTAL	31
<i>III.D.1.1. Ester cleavage with TMSBr</i>	<i>31</i>
<i>III.D.1.2. Hydrolysis with HBr</i>	<i>32</i>
<i>III.D.1.3. Hydrolysis with NaOH, KOH, NaHCO₃, KHCO₃.....</i>	<i>33</i>
III.E DESIGN OF SELECTORS FOR CEC USAGE	35
III.E.1. OUTLINE	35
III.E.2. VARIATION OF THE ACID COMPONENT	37
III.E.3. VARIATION OF THE ALDEHYDE COMPONENT.....	40
<i>III.E.3.1. Synthesis of 4-allyloxy-3,5-dibromobenzaldehyde and 4-allyloxy-3,5-dimethoxybenzaldehyde.....</i>	<i>40</i>
<i>III.E.3.2. Ugi reaction with 4-allyloxy-3,5-dibromobenzaldehyde and aminophosphonic acid.....</i>	<i>43</i>
III.F. CONCLUSION	44

IV. IMMOBILIZATION CHEMISTRY 45

IV.A. INTRODUCTION TO HPLC, CE AND CEC	45
IV.A.1. HIGH PERFORMANCE LIQUID CHROMATOGRAPHY	45
IV.A.2. CAPILLARY ELECTROPHORESIS.....	47
IV.A.3. CAPILLARY ELECTROCHROMATOGRAPHY	50
IV.B. MONOLITHIC CAPILLARY COLUMNS AS CHROMATOGRAPHIC SUPPORT	53
IV.B.1. ORGANIC POLYMER MONOLITHS	53
IV.B.2. INORGANIC SILICA-BASED MONOLITHS.....	54
IV.C. PREPARATION OF FUNCTIONALIZED MONOLITHS	55
IV.C.1. PREPARATION OF GMA-co-EDMA MONOLITHS.....	55
<i>IV.C.1.1. Vinylization of the plain fused silica material.....</i>	<i>55</i>
<i>IV.C.1.2. Preparation of GMA-co-EDMA organic polymer monoliths.....</i>	<i>55</i>
<i>IV.C.1.3. Thiolization of the monolithic surface.....</i>	<i>56</i>
<i>IV.C.1.4. Selector immobilization.....</i>	<i>57</i>
IV.C.2. SELECTOR LINKAGE TO AN EPOXY-MODIFIED SILICA MONOLITH	57
IV.C.3. MONOLITH DATA FOR OPMs AND SILICA MONOLITH	57
IV.D. COMPARISON OF THE SILICA-BASED AND ORGANIC POLYMER MONOLITHS	58
IV.D.1. EXPECTATIONS	58
IV.D.2. EVALUATION OF THE TOTAL ELECTROLYTE CONCENTRATION	59
IV.D.3. ORGANIC MODIFIER	61
IV.E. CONCLUSION AND EVALUATION OF THE SILICA MONOLITH	63
IV.E.1. OVERLOADING OF THE SILICA MONOLITH	63

IV.E.2. SEPARATION OF ARYLOXY CARBOXYLIC ACIDS.....	64
---	----

V. SELECTOR EVALUATION 66

V.A. PREPARATION OF THE CHIRALLY FUNCTIONALIZED SILICA MONOLITH..... 66

V.A.1. SELECTOR IMMOBILIZATION..... 66

V.A.2. MONOLITH DATA 67

V.B. EVALUATION OF THE FUNCTIONALIZED SILICA MONOLITH 67

V.B.1. EXPECTATIONS 67

V.B.2. CHARACTERIZATION OF THE ELECTRO-OSMOTIC FLOW 68

V.B.3. TEST ANALYTE CLENBUTEROL..... 69

V.B.4. COUNTER ION INFLUENCE..... 70

V.B.5. TOTAL ELECTROLYTE CONCENTRATION 71

V.B.6. ORGANIC MODIFIER 73

V.B.7. OPTIMIZED MOBILE PHASE CONDITIONS 75

V.B.8. VAN DEEMTER CURVES..... 75

V.B.9. CONCLUSION 77

References 78

Abstract 82

Zusammenfassung 74

Appendix

Danke schön

Curriculum Vitae

Abbreviations

AB	2-aminobutanol
ABr	allylbromide
ACN	acetonitrile
AIBN	α,α' - azoisobutyro nitrile
BGE	background electrolyte
BPP	2-(4-Bromo-phenoxy) propionic acid
CDA	chiral derivatizing agent
CE	capillary electrophoresis
CEC	capillary electrophoresis
CLC	capillary liquid chromatography
CSP	chiral stationary phase
DCPP	2-(2,4-Dichloro-phenoxy) propionic acid
DEA	diethyl amine
DNB-Leu	2,4-dinitrobenzoyl leucine
EDL	triethyl amine
EDMA	ethylene dimethacrylate
EOF	electro-osmotic flow
ESI	electrospray ionisation
EtOH	ethanol
FA	formic acid
GMA	glycidyl methacrylate
HPLC	high performance liquid chromatography
ID	inner diameter
MCPP	2-(4-Chloro-2-methyl-phenoxy) propionic acid
MCR	multicomponent reaction
MeOH	methanol
MS	mass spectrometry
MW	microwave
NOP	2-(2-Napthoxy) propionic acid
OPM	organic polymer monolith
pp	2-Phenoxypropionic acid
RPLC	reversed phase liquid chromatography
RT	room temperature
SO	selector
t-BuCQN	tert-butylcarbamoylequinidine
t-BuCQN	tert-butylcarbamoylequinine

TCP	2-(2,4,5-Trichloro-phenoxy) propionic acid
TEA	triethyl amine
THF	tetrahydrofurane
TMSBr	trimethylsilyl bromide
v/v	volumetric content
w/w	mass fraction

Device

CEC Equipment

Hewlett Packard ^{3D}CE system + Chemstation Software

HPLC Equipment

Agilent 1100 Series HPLC System + Chemstation Software
Dionex Ultimate 3000 LC System + Chromeleon Software

Column dimension: 5 µm; 150 x 4 mm ID

MS Equipment

Agilent 1100 Series LC/MSD/Trap
Applied Biosystems 4000 Q TRAP® LC/MS/MS System^{*}

Other

Perkin Elmer Polarimeter 341
Bruker Tensor 27 FT-IR & OPUS Data Collection Program

^{*} employed only for the measurement in chapter III.E.3.2.

I. CHIRALITY MATTERS

The present diploma thesis deals with the synthesis and evaluation of a new chiral selector class, phosphonic acid pseudo-peptides, for enantiomer separation in capillary electrochromatography (CEC). The primary test selector was methyl 3,3-dimethyl-2-[4-allyloxy- α -(2,6-dimethylanilido)-benzylamino]-butane phosphonate (**1**), a novel zwitter-ionic compound.

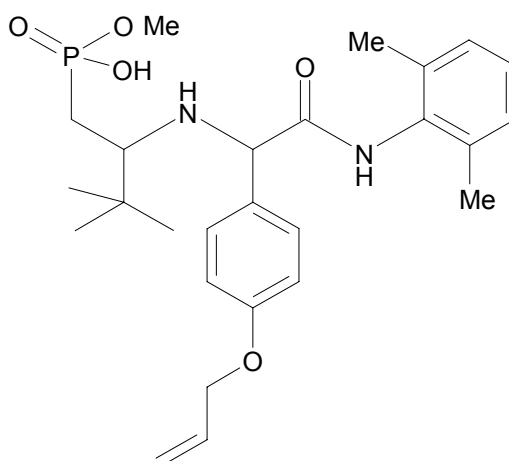


Fig. I-1: Methyl 3,3-dimethyl-2-[4-allyloxy- α -(2,6-dimethylanilido)-benzylamino]-butane phosphonate (**1**)

I.A. WHY does chirality matter?

Chirality is the pre-condition that a substance can exist as a pair of enantiomers. Louis Pasteur was the first to recognize and divide the enantiomeric forms of chiral tartrates as early as 1848 (1). Chiral recognition is a phenomenon of utmost importance in nature due to the intrinsic chirality of biological systems. E.g., receptors regulating the way the smell of a substance is sensed are chiral (2, 3). Hence, whether the odour of a perfume is appreciated or not can depend significantly on the stereo configuration and the enantiomeric excess of its main compound. This knowledge allows a well-directed manipulation of flavours. D-amino acids for example often taste sweet, whereas the L-counterparts are rather bitter (4). More serious examples are encountered in pharmacology: As the human body reacts stereoselectively, toxicokinetics and toxicodynamics may vary considerably, resulting not only in different bioavailability but entirely different effects as well. A sad but prime example are the two enantiomers of thalidomide, a sedative well known as Contergan to the public (5). As well as the human body can transform prochiral molecules into chiral ones in the course of toxicokinetics, achiral substances can be turned into chiral (toxic) species by degradation following their release into the environment. This can happen e.g. by microbes like bacteria or

fungi present in soil and water. Dopa and atenolol were tested with three aquatic organisms, indicating significant enantioselectivity in aquatic toxicity (6). Furthermore, pharmaceuticals and their metabolites can be degraded enantioselectively in sewage plants and following surroundings. The impact of agrochemicals must not be underestimated either. Approximately 25 % of pesticides exist in chiral forms in nature (7). Degradation pathways can favour the production of one enantiomer. Achiral γ -hexachlorocyclohexane for example is processed into chiral, toxic γ -pentachlorocyclohexene enantiomers (8). Chiral aryloxy-carboxylic acid herbicides like mecoprop (MCP) and dichlorprop (DCP) are applied as racemates, although the herbicidal activity is primarily due to the R-(+) enantiomers (9). Another example are pyrethroids, synthetic chiral esters, the insecticidal potential of which strongly depends upon stereochemistry. Unfortunately, the enantiomers evoking insecticidal effects seriously harm fish and bees as well (10).

As a consequence the exposure of living systems to artificially inserted inactive or even impairing enantiomers is to be minimized. Hence, enantiomeric impurities have to be detected and separated. Therefore capacious knowledge about chirality and its different types constitutes the indispensable basis.

I.B. WHAT is chirality? ¹

Chirality appears in molecules which lack symmetry elements, e.g. planes of symmetry or centres of inversion. This deficiency evokes from chiral elements, amongst which stereogenic centres (like an sp^3 -hybridized carbon with four different substituents) are particularly well-established. Further types of chirality are helical and topological chirality and chirality induced by chiral planes and axes.

As has been pointed out above, chiral substances can exist as enantiomers. These are molecules that are mirror images of each other, and therefore are not superimposable, just like two hands. Indeed the term “chirality” is derived from the Greek word for “hand”.

Thus, in enantiomers the atoms are connected in the same way, the distances between single atoms are identical, so are angles and torsions, and, consequently, energy contents. Accordingly, such molecules share almost all physical and chemical properties, like melting and boiling points, solubility, extinction coefficients or interactions with achiral molecules, what clearly impedes their distinguishability in achiral surroundings.

¹ Herein aspects of chirality will only be briefly mentioned. Readers less familiar with fundamentals like nomenclature or isomerism in general may be referred to comprehensive literature given in the references (11) .

I.C. HOW can enantiomers be separated?

The importance of the accessibility of single enantiomers has been outlined above. Since enantiomers behave differently solely with regards to the rotational direction of the plane of linearly polarized light, their distinction proves to be quite a challenge in analytical chemistry. If a substance is required enantiomerically pure, a way to circumvent laborious separation procedures is the stereoselective synthesis of the demanded enantiomer. However, enantioselective reaction pathways are despite intensive research not easy to find and need chiral starting materials, which have to be supremely pure themselves. Besides, the screening of products for enantiomeric impurities depends upon enantioselective analysis, e.g. enantioselective chromatography.

Herein, the mixture of the stereoisomers of the selector was prepared and the individual stereoisomers were subsequently isolated by means of chromatography. Generally speaking, there are two pathways leading to chiral separation, the indirect and the direct approach. Both attempts rely on the formation of diastereomeric entities, which can be distinguished and separated, because diastereomers vary in their physicochemical properties.

I.C.1. Indirect approach

In the indirect approach the racemic mixture is subjected to a chiral derivatizing agent (CDA), yielding easily detectable diastereomeric products (e.g. fluorogenic groups for fluorescence detection). The resultant diastereomers can be separated with achiral stationary phases such as RP18. As diastereomers may reveal different detector responses (e.g. due to distinct ionization efficiencies in MS techniques or varying extinction coefficients in spectral detection modes), a correction factor gained from peak area ratios should possibly be accounted for if the enantiomer ratio is directly inferred from the peak area ratio of the respective diastereomers. Generally, as prerequisite, the analyte must reveal a moiety susceptible to derivatization. The obtained diastereomers must be sufficiently chemically and stereochemically stable (so must the CDA) under utilized conditions. In order not to produce another diastereomeric pair that gives rise to two enantiomer pairs in the reaction products, the CDA has to be exceptionally enantiomerically pure. Furthermore, no racemization must occur in the course of the reaction. To prevent potential kinetic resolution, the CDA is added in significant excess, making a cheap and environmentally friendly agent desirable, and the reaction has to be allowed to proceed to completion. Due to these limitations the indirect approach is only scarcely employed today. An example of an established CDA is Mosher's reagent which is used for the conversion of amines or alcohols to amides or esters, respectively (12).

I.C.2. The direct approach

In the direct approach distinguishable diastereomeric entities are provided by the formation of associates. Two attempts have been compiled:

I.C.2.1. Chiral mobile phase mode

An additive that forms diastereomeric complexes is included in the mobile phase. These associates pass a chromatographic (achiral) or electrophoretic system with different velocities according to their distinct physicochemical properties. Since the analytes are detected as diastereomers, detector responses may differ like in the indirect approach. A main drawback is the large amount of selector waste. Cyclodextrins have proven to be useful additives in electrophoretic enantiomer separation systems (13-15).

I.C.2.2. Chiral stationary phase mode

The chiral stationary phase mode constitutes the favoured chromatographic separation procedure and has been employed herein. The field of established chiral stationary phases (CSPs) covers natural, semi-synthetic and synthetic polymer selectors as well as brush-type CSPs which are supports modified with chiral selectors (16). The chiral adsorbent interacts stereoselectively with the enantiomers passing the column. One of them will arrange itself more suitably towards binding sites of the chiral selector, resulting in a stronger binding constant and a longer retention time, respectively. It is evident that the chiral selector at the stationary phase must exhibit functional groups fit for specific interactions with analyte moieties, like hydroxy or amide groups for H-bondings, aryls for π - π interactions or aliphatic chains for hydrophobic interactions. **1**, a chiral ion-exchange selector, belongs to low molecular mass selectors and so do Pirkle-type (donor-acceptor) selectors and chelating agents. Another example of this selector type is tert-butylcarbamoylquinidine (*t*-BuCQD) (**2**), which is a chiral anion-exchange CSP for enantiomer separation of chiral acids.

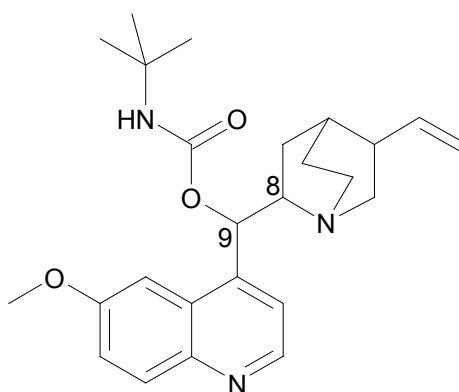


Fig. I-2: O-tert-butylcarbamoylquinidine (8R, 9S) (**2**)

Macromolecules like polysaccharides and proteins, macrocycles like cyclodextrins, macrocyclic antibiotics, or chiral crown ethers have successfully been employed as well (16).

In the detection cell where no chiral selector is present, the molecules are detected as single enantiomers, thus producing identical detector responses. The separated enantiomers in the effluent are neither covalently linked to a CDA, nor associated to another molecule, and are therefore readily available for isolation in pure form and further processing. Use of such CSPs in capillaries with electric fields as driving force for mobile phase and solute transport through the column has led to CEC, a hybrid separation technique, which combines the achievable selectivity of CSPs with high efficiencies due to the flat flow profile of the resultant electro-osmotic flow (see in detail chapter IV).

II. OBJECTIVE OF THE PRESENT WORK

The present diploma thesis aims at the development of newly functionalized monoliths for enantiomer separation in a miniaturized capillary format. Miniaturized systems are of particular interest in analytical chemistry, because less sample amounts are needed. Additionally, minimized capillary formats are environmentally friendly, as they enable drastically reduced solvent consumption.

Herein, a novel class of chiral selectors, phosphonic acid pseudo-peptides, shall be introduced. For selector synthesis, a combinatorial approach is intended to be used. The Ugi reaction, a multicomponent reaction (MCR) discussed profoundly in chapter III, is known to be suitable for the generation of compound libraries from a few variable reactants in a short time. It is to be evaluated if this reaction gives access to cyclic aminophosphonic acid pseudo-peptides as well, if a (bifunctional) aminophosphonic acid is employed as reactant.

The best selector will then be identified by means of a reciprocal screening. It is intended to attach this compound to a monolithic support and to investigate it for enantiomer separation in capillary electrochromatography. Monoliths have several advantages over particle packed supports and so has CEC over HPLC and CE. These subjects are delved into in detail in chapter IV.

However, before immobilization of the chosen selector on monolithic support, the support and/or immobilization chemistry have to be explored. Epoxy-modified silica monoliths have been provided by Merck and organic polymer monoliths (OPMs) exhibiting epoxy groups can be produced in-house. In the past, selector (SO) immobilization has been carried out *via* radical addition to thiol groups. In case of OPMs this step as well as the preceding transformation of epoxy groups into thiols have been evaluated (17). It remains to be seen if this technique is appropriate for epoxy silica monoliths as well. Therefore, preliminary experiments employing *t*-BuCQD as test selector to optimize the immobilization procedure are planned. *t*-BuCQD will be covalently attached to an OPM and to a silica monolith and subsequently the performance in CEC test runs will be compared. Tested analytes will primarily be related to environmental issues.

The best selector from the Ugi reaction will then be linked to the support exhibiting the best chromatographic properties in the preliminary experiments and the electrochromatographic properties of the capillary (electro-osmotic flow behaviour) as well as suitable mobile phase conditions will be evaluated.

III. SELECTOR SYNTHESIS

III.A. Multicomponent reactions and compound libraries

In the past, MCRs have been defined as one-pot reactions of at least three starting compounds, yielding a product that includes most of the atoms of the reactants (18-20). They exhibit several benefits compared to ordinary consecutive reaction stages, which routinely begin with the reaction of two starting materials. The achieved component is then isolated and subjected to reaction with another compound. This procedure is persecuted until the desired product is obtained. Consequently, in the course of the intermediate isolation and purification steps the yield decreases, whereas working hours and costs may tremendously increase (e.g. for laborious procedures like distillation or chromatography) at the same time. MCRs on the other hand are regularly performed simply by mixing all reactants (occasionally in a certain order) and require only one final purification step. Plenty of them rely on archetypal functional groups (alcohols, alkenes, amines, various acids, carbonyls, etc.) that are available in great variety, clearing the way for numerous accessible products in a relatively short time. This is, together with the simplicity of performance, the reason why MCRs are conveniently employed for the production of compound libraries with remarkable structural diversity and are more and more often referred to in connection with combinatorial chemistry (18, 21-23).

According to I. Ugi and A. Dömling, MCRs can be classified into three types according to the reversibility of single reaction steps (19). Mechanisms in which each process is irreversible (Type III) appear very rarely in organic synthesis, but are quite common in biological systems. Pathways containing a final irreversible stage (Type II) are particularly useful as the equilibrium is shifted towards the product side, whereas mechanisms comprising solely reversible steps (Type I) typically yield less product and, likely, a number of side products. Consequently, type II makes up the main class in organic synthesis. Isocyanides (= isonitriles) take part in a noteworthy number of these reactions (Mannich- , Passerini- , Ugi - Reaction). Indeed the use of this C^{II} species has proven to provide a valuable final irreversible reaction step, namely the exothermic oxidation of C^{II} to C^{IV} . Isocyanides belong to the very rare species that undergo nucleophilic and electrophilic reactions at the same centre. They afford intramolecular bond shiftings like intramolecular transacylation, Mumm or Smiles rearrangement (24, 25). In the following, the Ugi reaction, an MCR contributing significantly to the recognition of the value of isocyanides in organic synthesis, is discussed more thoroughly.

III.B. Adoption of an Ugi reaction for selector synthesis

III.B.1. The Ugi-reaction – retrospection and prospects

The Ugi-reaction was presented by Ivar Ugi in 1959 (26). It facilitates the design of α -aminoacidamide structures from a carbonyl, a carboxylic acid, a primary amine and an isocyanide (4-component Ugi reaction).

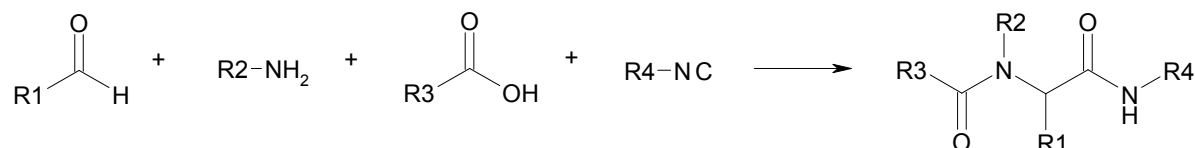


Fig. III-1: The Ugi reaction

I. Ugi early recognized the potential of the reaction for the design of compound libraries and the aligned usage in pharmaceuticals (27). Plenty of possible drugs can be obtained in a short time due to the great variety of starting compounds and convenient reaction performance. One of its first applications was the production of Xylocain, a local anaesthetic, from formaldehyde, 2,6-dimethylphenylisocyanide, diethylamine and water. Shortly afterwards a number of Xylocaine-derived structures was produced and tested for anaesthetic effects (28).

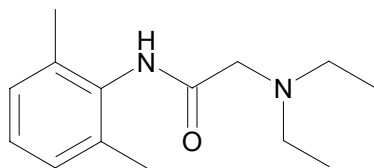


Fig. III-2: Xylocain structure

Until now the reaction has been employed primarily in pharmaceutical studies. It has been explored for a number of reactants revealing the corresponding products in many cases. As for Xylocain, the use of secondary amines affords the acylation of the former isocyanide nitrogen (instead of that of the former amine; for mechanistic details see chapter III.B.2.). Concerning the carbonyl compound, aliphatic structures commonly react more readily than their aryl counterparts and aldehydes are superior to ketones in terms of yield (19, 29, 30). Isocyanides still constitute the most restricted starting compounds, but on account of intensive research, plenty of non-commercially available isocyanides can be obtained in facile procedures (31-33). Accomplished results give rise to the assumption that aliphatic isocyanides are favourable. Miscellaneous carboxylic acids have been used. Since the Ugi reaction affords the generation of new N-C-C-N bonds, it has been adopted for the synthesis of peptidomimetics (34, 35). As bifunctional starting materials (3-component Ugi reaction) induce intramolecular cycles, the reaction has been repeatedly employed for the generation of β -lactam libraries, obtained from

β -amino acids. However, corresponding α -amino acids do not give the expected α -lactams due to the formation of stable intermediates (19, 36-38).

Aside from carboxylic acids, a number of analogously reacting compounds are accessible. Sometimes, e.g. for the synthesis of Xylocain, the solvent (water in this case) is used as acid component as well. The outcome of the Ugi reaction can barely be predicted when reactants are varied and generally depends considerably upon reaction conditions. Solvent, temperature and reactant concentration have to be optimized carefully, and so do potential additives (adjuvants like Lewis acids) and auxiliary modes (e.g. utilization of microwaves). For example, if a reaction proceeds according to Ugi or Passerini from the same start-up mix can be controlled entirely by the appropriate choice of solvent and Lewis acid (39). Although similar considerations had been made early by Ugi himself, more intensive examination has been performed only decades later. In recent research efforts of combining the Ugi reaction with other established reactions (e.g. Houben-Hoesch, Asinger, Diels Alder or Knoevenagel condensation (25, 40-42) have been undertaken, clearing the way for access to complex substances obtained in comfortable synthesis procedures. Attempts to establish stereoselective Ugi-reactions have been performed as well, but unfortunately have been of moderate success in most cases (29, 43, 44).

III.B.2. Mechanistic considerations

The reaction mechanism of the Ugi reaction has not been fully resolved yet. Uncertainties contribute to the difficulties of stereoselective synthesis. Since the reaction works well in polar solvents, an ionic mechanism seems plausible. Fig. III-3 illustrates a generally assumed, simplified possibility (19).

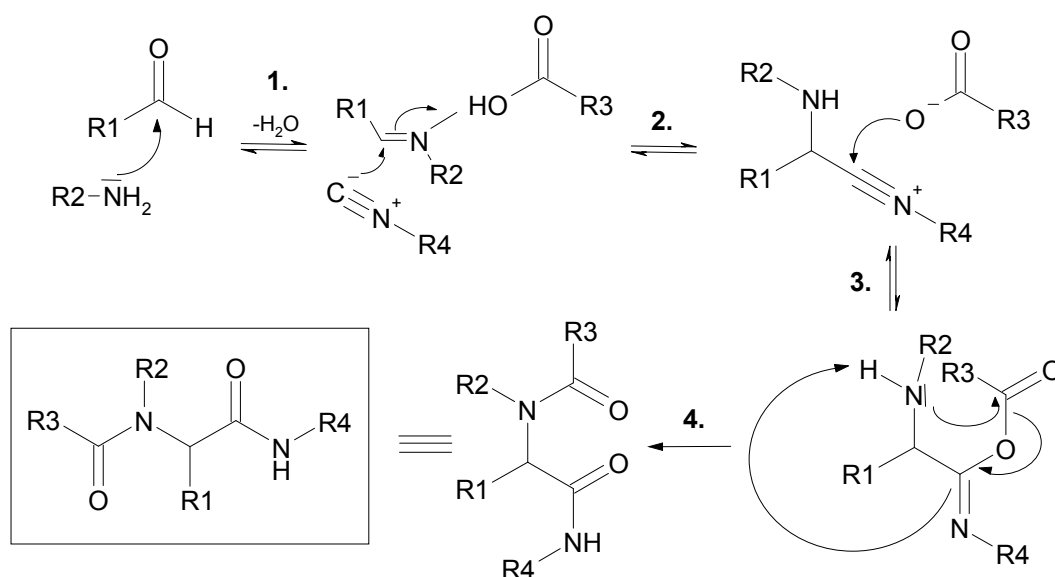


Fig. III-3 : Plausible mechanism of the Ugi reaction

The first step, the formation of the imine (Schiff base), as well as its protonation are believed to be crucial for pleasant yields. The generation of a positive charge at the nitrogen amplifies the electrophilicity of the molecule and consequently supports the nucleophilic attack of the isocyanide carbon (**2.**). The resulting species contains an electrophilic C-N triple bond susceptible to addition of the carboxylate nucleophile (**3.**). The obtained adduct undergoes a final irreversible intramolecular acylation, named after its discoverer, O. Mumm (**4.**) (45, 46). The revealed product can be described as an α -acylaminoacidamide.

The present selector synthesis originally aimed at the employment of 4-allyloxybenzaldehyde (**3**), 2,6-dimethylphenylisocyanide (**4**) and 2-amino-3,3-dimethylbutanephosphonic acid (**5**) for the generation of a cyclic dipeptidomimetic. The reaction was expected to proceed as follows:

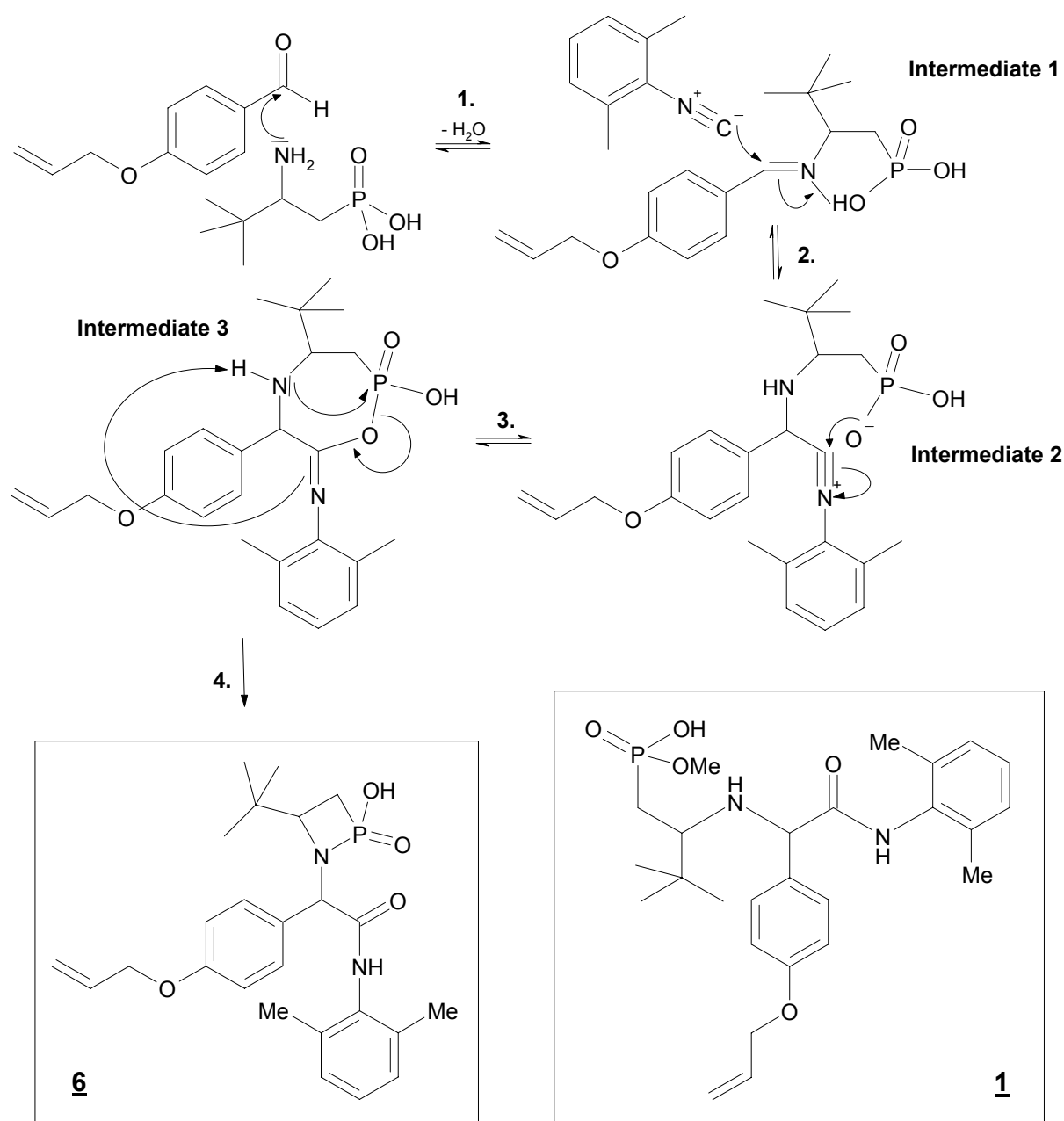


Fig. III-4: Expected course of the Ugi reaction employing phosphonic acid and obtained product, **1**.

However, product **1** depicted in Fig. III-4 was evoked. Since there is no intermediate like this, it is possible that the reaction proceeds as expected, but is followed by a cleavage of the N-P ring bonding due to a nucleophilic attack of MeOH at the positively polarized phosphorus. More likely seems stabilization of Intermediate 2 by solvolysis with MeOH (nucleophilic attack) instead of intramolecular acylation. The assumption that the aminophosphonic acid does not undergo autocatalyzed esterification is supported by experimental findings (synthesis approach I and II, exact reaction conditions given in chapter III.B.4.). In the course of synthesis approach II (stepwise reaction through stepwise reactant addition instead of simultaneous addition of all reactants in synthesis approach I) the aminophosphonic acid and the aldehyde were allowed to react for 90 minutes in absence of the isocyanide to yield the imine. Detection was carried out by means of RPLC-UV-ESI-MS.

Note: UV detection was always performed at a wavelength of 250 nm if not specified otherwise.

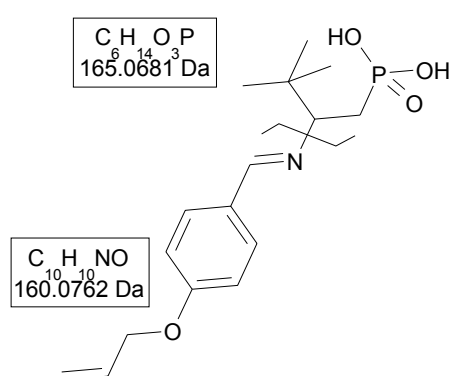


Fig. III-5: Expected imine bond cleavage

Since the molecule was detected in the positive mode, the fragment containing the nitrogen is supposed to carry the induced charge after the ionization process. Although the RP chromatogram (not shown) contains only reactant peaks, ESI-MS measurements reveal a species at an m/z ratio of 326 at 7.8 min. in the extracted ion chromatogram (Fig. III-6 (a)). This peak rapidly decreases after addition of the isocyanide to an intensity of 1×10^5 after the first microwave (MW) treatment (EIC Fig. III-6 (b)) and completely disappears after the second (EIC not shown). 326 is the m/z ratio of the expected imine with a phosphonic acid (no monoester!) residue.

As concerns reaction progress, after synthesis approach II was subjected to MW heating the same way as synthesis approach I where the isocyanide was added immediately after the carbonyl and the aminophosphonic acid, it did not proceed any faster according to RPLC-UV product peak monitoring. Consequently, experiments performed herein cannot confirm the assumption that a pre-reaction step without added isocyanide is beneficial.

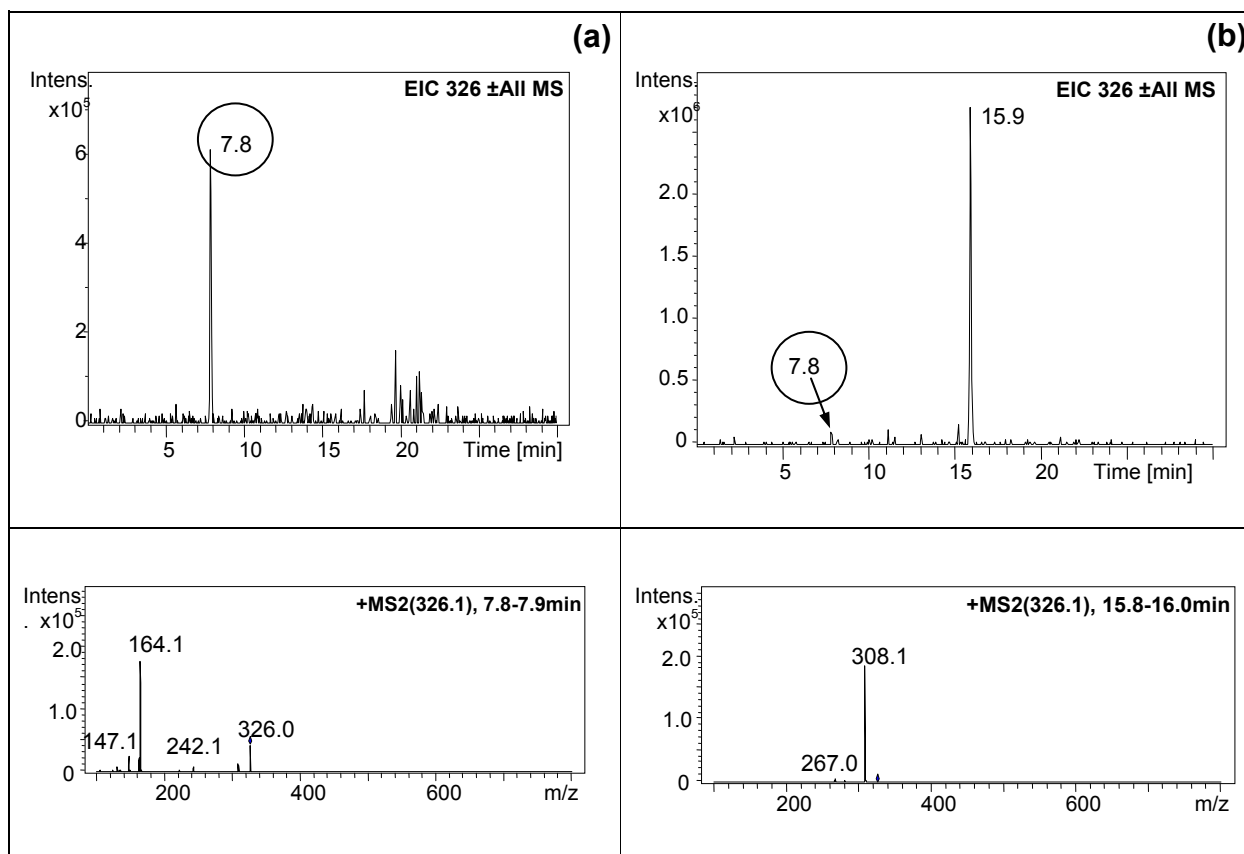


Fig. III-6: Extracted ion chromatograms and fragmentation spectra of imine (Fig. III-5) (m/z of protonated species = 326) before (a) and after (b) addition of isocyanide. RPLC Gradient: 10 to 100% B in 20 min. A: $\text{H}_2\text{O} + 0.1\%$ FA, B: ACN + 0.1% FA. Flow rate: 1ml/min.

III.B.3. Experimental conditions

Reaction conditions were explored in order to gain a pure product in a high yield. Herein experiments concerning microwave irradiation, reactant concentration, solvent and temperature have been carried out.

III.B.3.1. Microwave irradiation

The first report of microwave employment in chemical analysis was published in 1975 (47). From then on microwave techniques forced their way into various fields of chemical applications: Nowadays they are utilized in physical chemistry (to explore molecular properties), in organic synthesis (as they constitute a well-controlled energy source) and analytical chemistry (primarily in sample preparation steps). The focus herein shall be laid on organic synthesis, although microwave irradiation has gained remarkable importance in chemical analysis as well. Environmental sample preparation and digestion steps can easily be handled by microwave employment (48, 49).

In organic synthesis microwaves make up a relatively new class of energy supply compared to continuous heating, sonic, photochemical and high-pressure methodologies. They basically act

through the dielectric heating effect, meaning the transformation of electromagnetic energy into heat. An applied electric field enforces the alignment of dipoles present in the subjected material. If the frequency of the field is low compared to the ability of the dipoles to arrange themselves within the field, the molecules rotate (provided that they are free to move like in liquids) according to their polarization. Therefore they absorb energy of the field which is subsequently transformed into this rotation movement. If the applied field changes more quickly, precisely faster than the response time of the dipoles, the latter do not move at all and no heating occurs. So, the field oscillation has to be in the range of the response time of the dipoles. It has to be so fast that the resulting polarisation always lags slightly behind. Consequently, the dipoles are continuously forced to change their rotating direction before they have realigned with the field. The induced movement is a kind of vibration, evoking the dielectric heating effect. Reasonably, dipoles have to be present in the material to be heated. Hence, polar liquids are first choice solvents.

Controversial opinions came up when comparing the impact of dielectric heating to conventional heating methods. By now, microwave techniques have been used in a number of common organic reaction types like hydrolysis, heterocyclic ring formation, dehydration, esterification, (Diels-Alder) cycloaddition and etherification (50-56). Numerous studies focussing on rate acceleration effects of microwaves have been performed. However, sceptics argue that microwave employment could bring about further changes in experimental conditions difficult to control, e.g. temperature gradients (57, 58). Still, of relevance for the present study, Ugi reaction rates have been sped up by microwave irradiation (59-61). Since applied temperature values can exceed solvent boiling points, a related effect might probably gain influence: The Ugi reaction belongs to MCRs exhibiting a negative activation volume, because several molecules accumulate to give one intermediate/product. Consequently, high pressure can speed up such processes (30, 62). This effect may have added to the beneficial rate-accelerating influence of microwave irradiation in the following experiments.

Experimental

Reactants: 4-allyloxybenzaldehyde (**3**), 2,6-dimethylphenylisocyanide (**4**), 2-amino-3,3-dimethylbutanephosphonic acid (**5**)

Two approaches of 0.34 M solutions (200 μ mol of each reactant (equimolar amounts) in 586.5 μ L solvent) were prepared in MeOH. One was allowed to react for a week at room temperature (RT), whereas the other one was subjected to microwave irradiation. In the first case, a protocol described by Brahmachary et al was followed (63): phosphonic acid and carbonyl were suspended in solvent at 0 °C before the isocyanide was added. In the microwave

approach the vial was loaded in the order phosphonic acid, aldehyde, isocyanide at RT. Reaction progress was observed by means of RPLC-UV.

Note: For analyzation, a defined volume (e.g. 5 μL) was taken out of the reaction suspension, evaporated with nitrogen and subsequently dissolved in a defined volume of solvent (e.g. 500 μL MeOH). This was the same for all experiments described in this diploma thesis. The pure suspension was never used as a sample in any experiment!

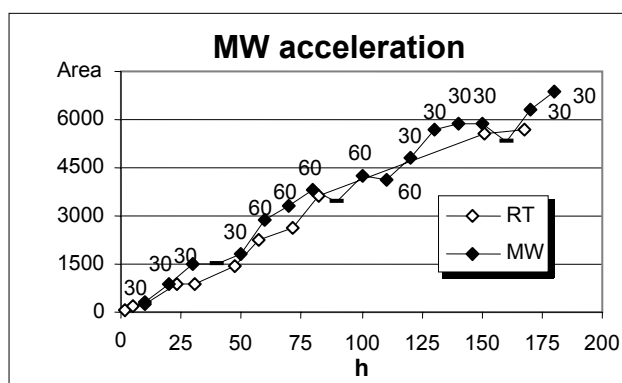
Reaction conditions in the microwave approach:

Temperature (constant):	100 °C
P _{max} :	18 bar
Power _{max} :	100 W
Run time:	30/60 min.

Prior to these comparative experiments preliminary studies on microwave settings were performed. Distinct irradiation powers, constant temperatures and run times were tested. Exact conditions are given in Table III-1 in the “*Results and Discussion*” section. Product peak monitoring was carried out on a chiral tert-butylcarbamoylequinidine (*t*-BuCQN) column. Maximum allowed pressure was kept constant at 18 bar. Most often experiments were run in the standard mode, this means the temperature was kept constant by variation of power. Test runs marked with an asterisk were run in a different mode: A constant power was applied until the upper temperature limit was reached.

Finally, since subjection to harsh microwave conditions might induce side reactions not including the acid/amine function, one “blank” approach containing only aldehyde and isocyanide (0.62 M, equimolar, 200 μmol of each in 325 μL) was examined as well. A drop of 0.1 M HCl, representing the acidic impact of **5**, was added to the reaction mixture. The approach was at first left to proceed at RT and subsequently subjected to irradiation. Temperature was kept constant during each run. Exact conditions are given in Table III-2.

Results and Discussion

Comparison of microwave treatment and reaction progress at RT

X-Axes:

“30” (“60”) indicates that the run time was 30 (60) minutes. – indicates that the reaction solution was stirred over night at RT before MW irradiation experiments were continued on the next day.

X-axes labelling refers solely to the reaction performed at RT.

Fig. III-7: Microwave acceleration of an Ugi reaction determined by RPLC-UV monitoring. Gradient: 10 to 100% B in 20 min. A: H₂O + 0.1% FA, B: ACN + 0.1% FA. Flow rate: 1ml/min

Microwave irradiation could significantly increase reaction rate. After three times of 30 minutes of microwave treatment the reaction had proceeded as far as after two days at RT. As assumed from regulation experiments (see below), an increase in run time did not necessarily translate into faster progress.

Preliminary experiments on microwave regulation

Power and temperature were amplified repeatedly to get an insight into microwave impact. Table III-1 depicts applied conditions. The same reaction mix was used throughout the experiment, meaning after the treatment described for Nr. 1, the same reaction mix was subjected to conditions given in Nr. 2 and so on.

From Fig. III-8 and Table III-1 several conclusions can be drawn. First of all, at constant temperature, an increase in run time from 30 to 60 minutes does, quite strikingly, not seem to have any impact concerning reaction progress. As expected for enantiomers, peak area curves of P11/P12 and P21/P22 show exactly the same course. Diastereomer behaviour is revealing analogies as well.

From test runs 1 to 7 it was evaluated that repeated irradiation at 100 °C does not cause degradation of the formed products. Test runs 8 to 13 investigated temperatures above 100 °C. The impact of temperature in this range is uncertain, as measured peak areas dropped from 7 to 8 and from 12 to 13 (suggesting product degradation), but rose between 8 to 12. Augmented power (runs 14 and 15) could not contribute to a reformation of product, maybe because T_{\max} was raised as well. (Nevertheless this does not mean that 200 °C were applied all the time. This value just marks the upper temperature limit.) It was concluded that temperature should

be kept at a maximum of 100 °C as its influence above this limit is not predictable from the experiments described above.

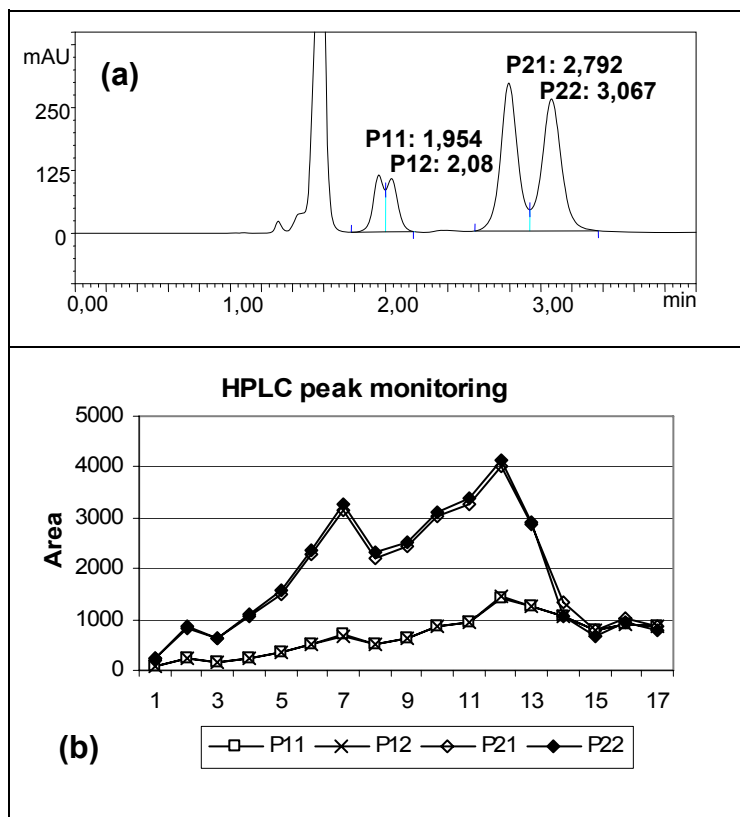


Fig. III-8 (a): HPLC chromatogram on *t*-BuCQN. Mobile phase: MeOH/AcOH/NH₄Ac (99.5/0.5/0.125; v/v/w). Flow rate: 1 ml/min. (b): HPLC peak monitoring on *t*-BuCQN.

Table III-1: MW adjustment

Nr.	T _(max) [°C]	P _(max) [W]	Time [min]
1	100	100	30
2	100	100	30
3*	100	50	0.5
4	100	100	60
5	100	100	30
6	stirring for 14 hours at RT		
7	100	100	30
8	150	100	5
9	140	100	30
10*	144	100	10
11	stirring for 14 hours at RT		
12	140	100	60
13	140	100	60
14*	200	150	15
15*	200	150	15
16	stirring for 72 hours at RT		
17*	200	150	15

Obtained products were monitored via RPLC-UV-ESI-MS measurements in different stages:

Note: The peak shown at 22-23 min. is a system peak appearing in all -UV chromatograms herein.

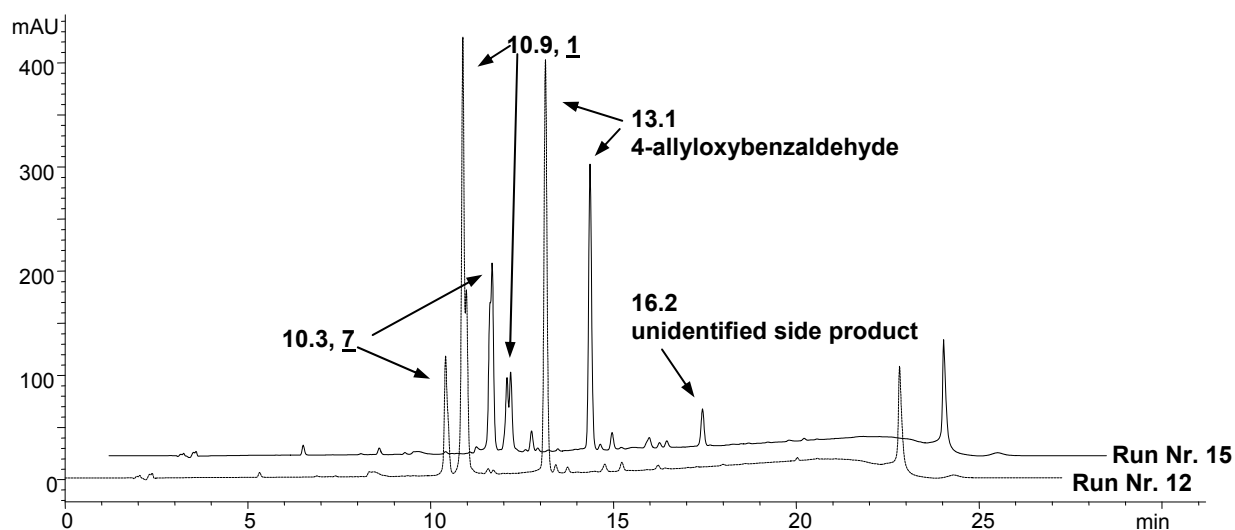


Fig. III-9: Overlaid RPLC runs of Tests 12 and 15. Gradient: 10 to 100% B in 20 min. A: H₂O + 0.1% FA, B: ACN + 0.1% FA. Flow rate: 1ml/min.

The generated product **1** elutes at 10.9 min., its free acid analogue, 3,3-dimethyl-2-[4-allyloxy- α -(2,6-dimethylanilido)-benzylamino]-butane phosphonic acid (**7**), at 10.3 min. (see “Primary test compound characterization”, chapter III.C.) Harsh microwave conditions seem to produce the free acid from the monoester, but also some unidentified side products and are therefore not suitable for the synthesis of **7**. The employment of ESI-MS detected the Ugi-ring product (**6**) m/z ratio (= 457) at 11.9 and 17.0 min. (total ion chromatogram, not shown herein). Unfortunately, no peaks appear in the RP chromatogram at these times.

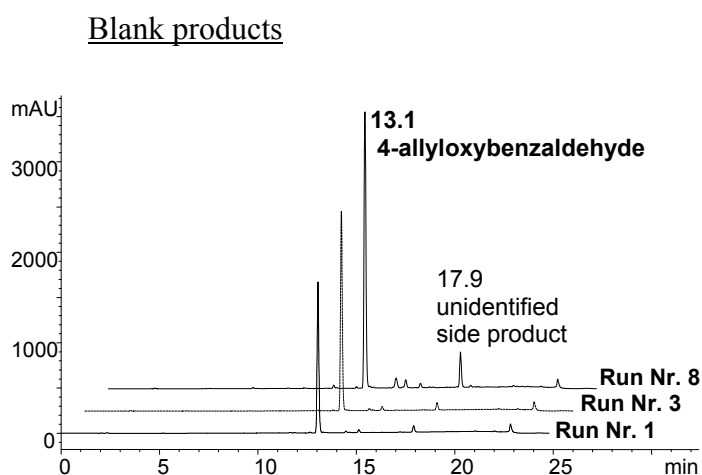


Fig. III-10: RPLC-UV chromatograms of test runs 1, 3 and 8. Gradient: 10 to 100% B in 20 min. A: H₂O + 0.1% FA, B: ACN + 0.1% FA. Flow rate: 1 ml/min.

Table III-2: MW adjustment for blank test runs without aminophosphonic acid

Nr.	T [°C]	P _(max) [W]	Time [min]
1	stirring for 2 weeks at RT		
2	100	100	30
3	100	100	30
4	140	100	30
5	stirring for 14 hours at RT		
6	140	100	60
7	200	150	15
8	200	150	15

Fig. III-10 depicts RPLC-UV chromatograms of a batch containing only carbonyl compound **3** and isocyanide **4** without aminophosphonic acid **5**. It illustrates that at RT very few (unidentified) side products arising from carbonyl/isocyanide reactions occur in a low extent. Drastic irradiation conditions generate a rise of these side products, especially of the species eluting at 17.9 minutes.

III.B.3.2. Reactant concentration

It has been found that the Ugi reaction proceeds well in a range of 0.5 M to 2 M (19). In experiments performed by Bradley et al the amount of product precipitate decreased dramatically below a concentration of 0.2 M (64). Several studies exploring the molar ratios of reactants indicate that an excess of one compound, most often the isocyanide, can be beneficial (25, 63, 64). The following tests were performed in MeOH at equimolar conditions of the individual components in the low concentration range. Since MW irradiation could obviously speed up reaction kinetics at 0.34 M starting material (chapter III.B.3.1.), it was of particular interest if it was possible to perform the reaction at an even lower concentration. Three approaches were compared to each other.

Experimental

Concentration approach I:	1.18 M	(2 mmol in 1.7 ml)
Concentration approach II:	0.34 M	(200 μ mol in 586.5 μ L)
Concentration approach III:	0.09 M	(20 μ mol in 220 μ L)

Reactants: **3**, **4**, **5**

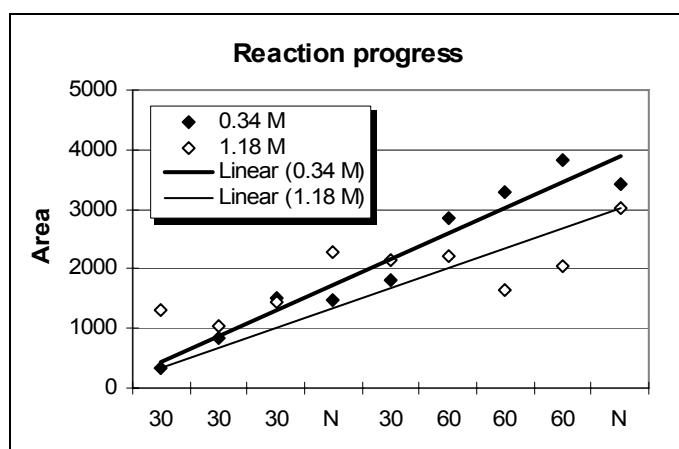
In concentration approach III the carbonyl **3** was replaced by 4-allyloxy-3,5-dibromobenzaldehyde, **8**. The aminophosphonic acid was suspended in the according volume of MeOH in a microwave vial. Next the aldehyde compound was added and ultimately the isocyanide. The vial was sealed and subjected to irradiation:

Temperature (constant):	100 °C
P _{max} :	18 bar
Power _{max} :	100 W
Run time:	30/60 min.

Reaction progress was monitored by means of RPLC-UV.

Results and Discussion

The RP chromatograms of concentration approach III showed no product peak after two times of MW irradiation (30 min. each). The reaction was left to continue at RT for two weeks, but even then no product could be detected chromatographically. Still, MS measurements indicated that the expected analogue of **1** had been formed (MS spectra shown in III.E.3.2.). Hence, MW irradiation could obviously not make up the impediment of a low starting material concentration. Fig. III-11 depicts the reaction progress curves of concentration approach I and II. Chromatographic injection volumes were the same for both approaches.



X-Axes:

“30” (“60”) indicates that the run time was 30 (60) minutes. “N” means that the reaction solution was stirred over night at RT before MW irradiation experiments were continued on the next day.

Fig. III-11: Reaction monitoring on RPLC of Concentration approach I (1.18 M) and II (0.34 M). Gradient: 10 to 100% B in 20 min. A: H₂O + 0.1% FA, B: ACN + 0.1% FA. Flow rate: 1ml/min.

The area values of concentration approach II in Fig. III-11 were multiplied by 3.45 ($=1.18/0.34$) to make them comparable to the values of concentration approach I. According to previous studies (without MW irradiation) (19), it was expected that the higher concentration approach would yield significantly more product. Quite strikingly, this was not confirmed experimentally. The yield increases in both approaches more or less continuously. It is yet unclear, why the yield seems to diminish after some experiments. This could be due to improvable standardization of sample handling.

III.B.3.3. Solvent

The Ugi reaction is usually carried out in a polar protic solvent. Although MeOH is most common and most appropriate for first trials, literature provides plenty of other examples, even aprotic ones. However, if an aprotic solvent is chosen, it must be born in mind that a competing reaction pathway according to Passerini (Fig. III-12) could be followed.

The Passerini reaction needs the same reactants with exception of the amine compound (65). Dai et al performed experiments where they showed that the Passerini or Ugi product could be obtained from the same starting mix depending on the solvent (and Lewis acid catalysis) (39). Amongst others, EtOH, ACN, THF and water have been successfully employed (19, 23, 62, 64) as Ugi reaction solvents and so have solvent mixtures (66-68). Since the solubility of the isocyanide in MeOH is very poor and that of the phosphonic acid is even worse, other solvents as well as solvent mixtures were tested. Due to a shortage of **5**, 2-aminoethanephosphonic acid (**9**) was used instead. Unfortunately, comparative studies showed that the reaction yield was significantly lower with this substitute.

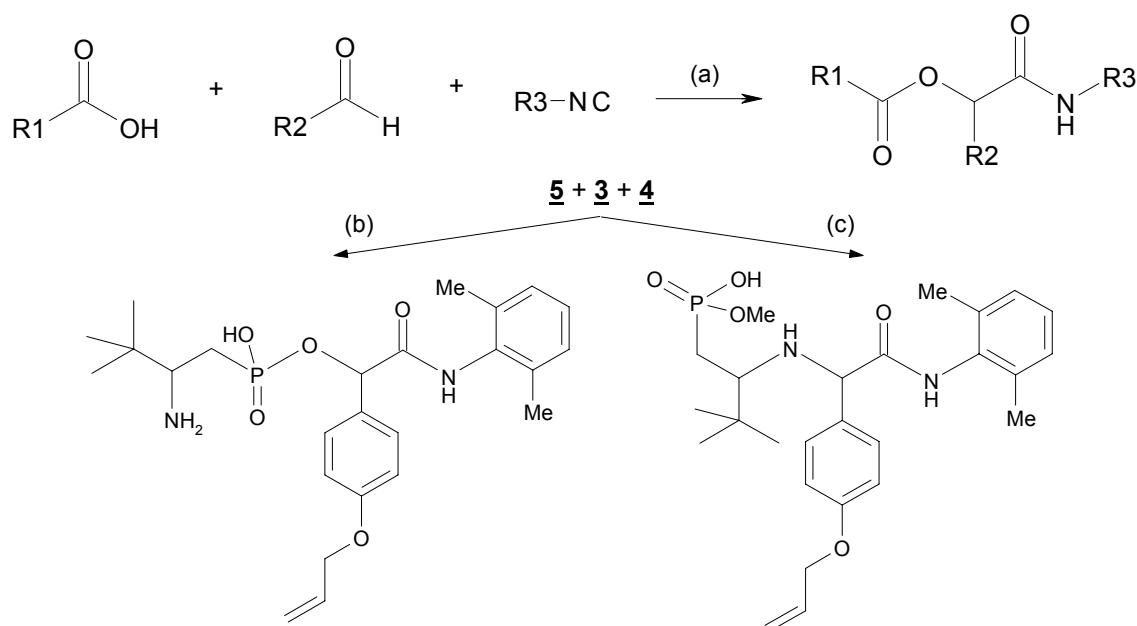


Fig. III-12: General Passerini reaction scheme (a), product according to Passerini (b) and obtained Ugi product (c) from reactants **3**, **4**, **5** (b).

Experimental

Reactant set A: **3**, **4**, **5**, equimolar mounts

Solvent approach I:	0.34 M	(200 μ mol in 586.5 μ L)	in MeOH
Solvent approach II:	0.34 M	(200 μ mol in 586.5 μ L)	in DMF
Microwave irradiation:	Temperature (constant):	100 $^{\circ}$ C	
	P _{max} :	18 bar	
	Power _{max} :	100 W	
	Run time:	30 min.	

Reactant set B: **3**, **4**, **9**, equimolar amounts

Solvent approach III:	0.41 M	(200 μ mol in 486.5 μ L)	in MeOH
Solvent approach IV:	0.41 M	(200 μ mol in 486.5 μ L)	in DMF
Microwave irradiation:	Temperature (constant):	100 $^{\circ}$ C	
	P _{max} :	18 bar	
	Power _{max} :	100 W	
	Run time:	30 min.	

The samples of approach III and IV were irradiated four times for 30 minutes and then left to proceed at RT for 11 days.

Solvent approach V:	0.34 M	(200 μ mol in 586.5 μ L)	in H ₂ O/MeOH
Solvent approach VI:	0.34 M	(200 μ mol in 586.5 μ L)	in H ₂ O/DMF
Solvent approach VII:	0.34 M	(200 μ mol in 586.5 μ L)	in H ₂ O/DCM
Microwave irradiation:	Temperature (constant):	100 $^{\circ}$ C	
	P _{max} :	18 bar	
	Power _{max} :	100 W	
	Run time:	30 min.	

The samples of approach V, VI and VII were irradiated twice and then left to stir at RT over night. Subsequently they were subjected to irradiation once again for 30 minutes and again allowed to proceed until the next day on which RP measurements were performed.

MW vials were loaded as usual in the order aminophosphonic acid, carbonyl, isocyanide. In case of biphasic solvent mixtures, the acid component was sonicated in 230 μ L water before addition of the other reactants in 325 μ L of the second solvent.

Results and Discussion

Concerning reactant set A, the reaction could obviously not be sped up by the employment of DMF. Fig. III-13 depicts RP chromatograms of solvent approach I and II after three times of MW irradiation. It is seen that no significant amount of product was formed with DMF, indicating the strong solvent dependence of the reaction.

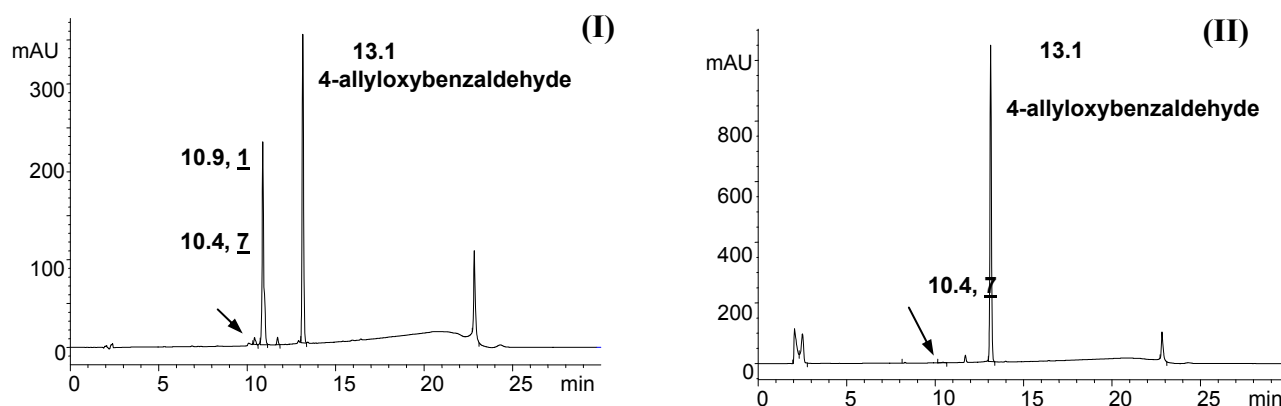


Fig. III-13: RPLC-UV monitoring of solvent approach I and II after three times of microwave treatment. Gradient: 10 to 100% B in 20 min. A: H₂O + 0.1% FA, B: ACN + 0.1% FA. Flow rate: 1 ml/min.

Solvent approaches III and IV gave the following RP-chromatograms after defined treatment:

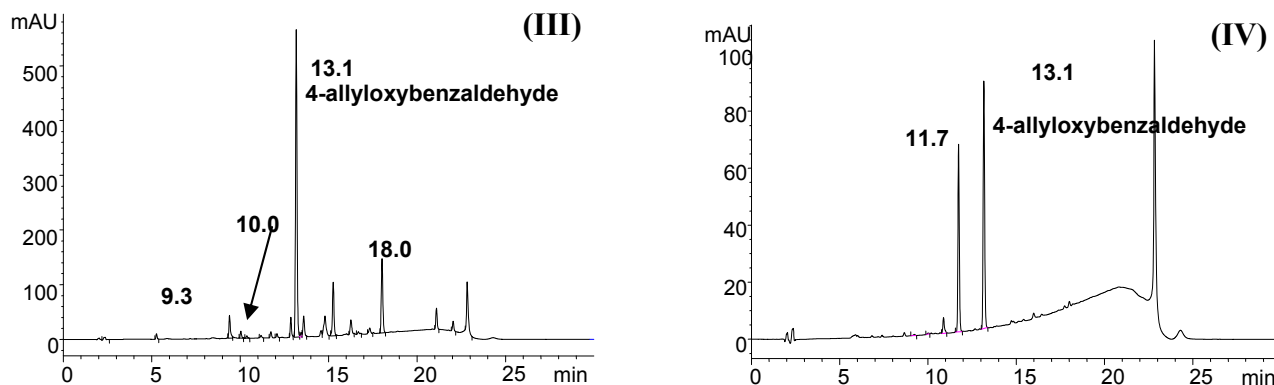


Fig. III-14: RPLC-UV monitoring of solvent approach III and IV after three times of microwave treatment. Gradient: 10 to 100% B in 20 min. A: H₂O + 0.1% FA, B: ACN + 0.1% FA. Flow rate: 1 ml/min.

The reaction mixtures were also analyzed by RPLC-UV-ESI-MS. MS Data were searched for all kinds of possible products (methyl 2-[4-allyloxy- α -(2,6-dimethylanilido)-benzylamino]-ethane phosphonate (= **1** –analogue) (**11**) and its free acid (**12**), bis-ester (**13**) and ring-closed Ugi product (**10**)). In approach III mono- and bis-ester were found (9.3 and 10.0 min.), fragmentation spectra of which are depicted below. Approach IV did not yield any known product according to extracted ion chromatograms (not shown). The species generating the RPLC-peak at 11.7 min. could not be ionized by ESI-MS. RPLC-UV chromatograms of pure **3** suggest that it could be an enriched contamination in reactant **3** (Fig. III-16).

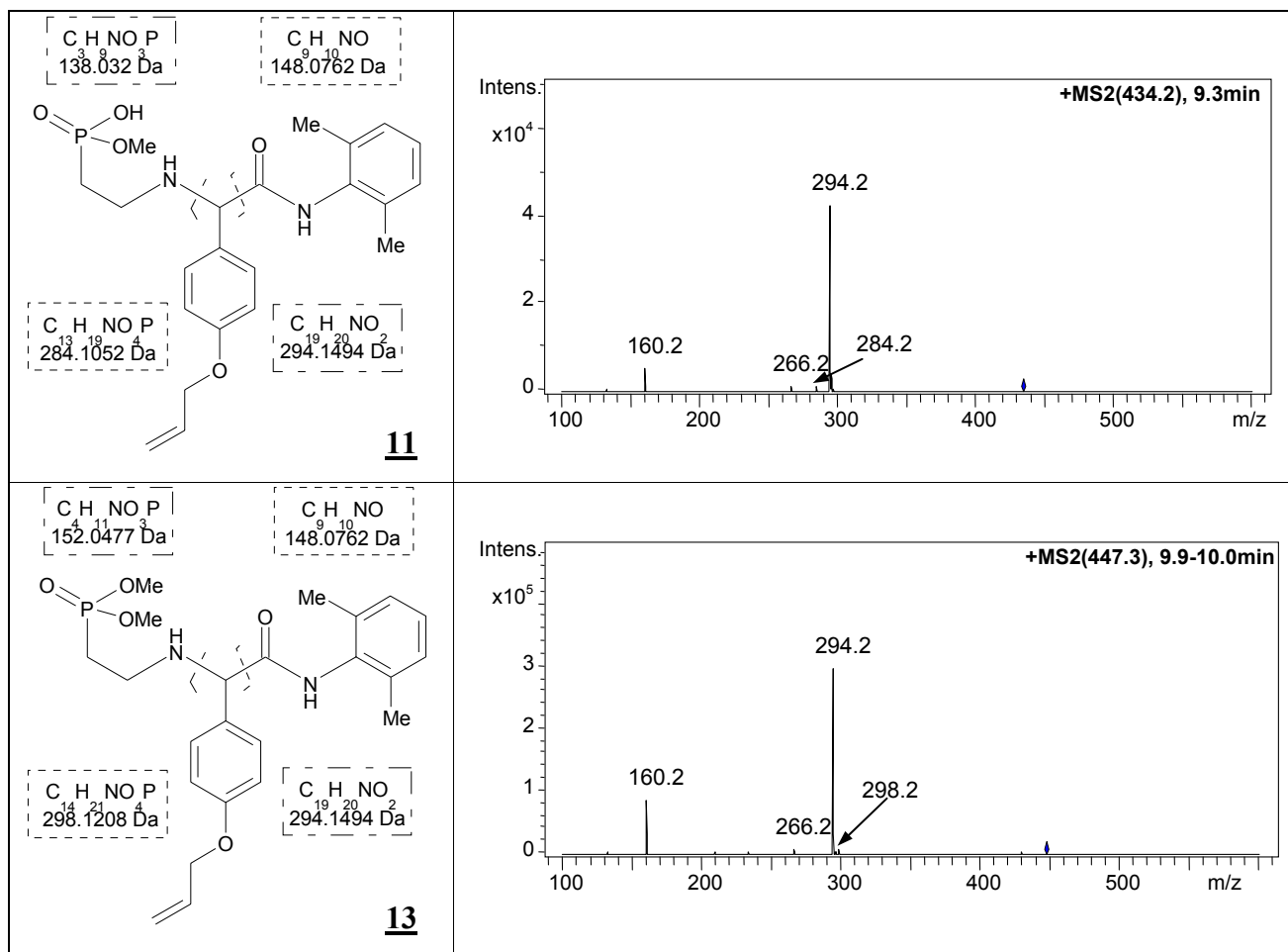


Fig. III-15: Expected bond cleavages and fragmentation spectra of reaction products **11** (9.3 min.) and **13** (10.0 min.) of reactions with Reactant Set B.

As Fig. III-14 shows, the yields were very poor for the achiral aminophosphonic acid substrate, **9**, even in MeOH, which is surprising. Therefore, the substitution of **5** by **9** is regarded as an impediment. The absence of the *t*-Bu residue probably reduces the acid solubility in solvent, leading to lower yields.

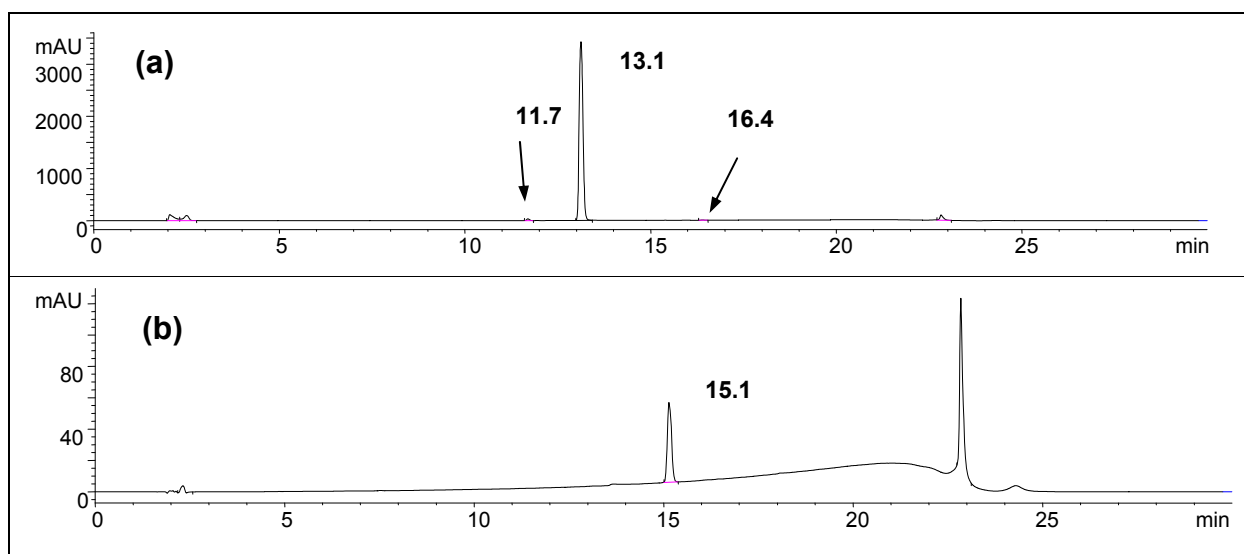


Fig. III-16: RPLC-UV chromatograms of aldehyde **3** (a) and isocyanide **4** (b). Gradient: 10 to 100% B in 20 min. A: H₂O + 0.1% FA, B: ACN + 0.1% FA. Flow rate: 1 ml/min.

However, biphasic approaches in which the acid was suspended in water did not enhance yield either. Fig. III-17 comprises RP-chromatograms of solvent approach V, VI and VII after microwave treatment.

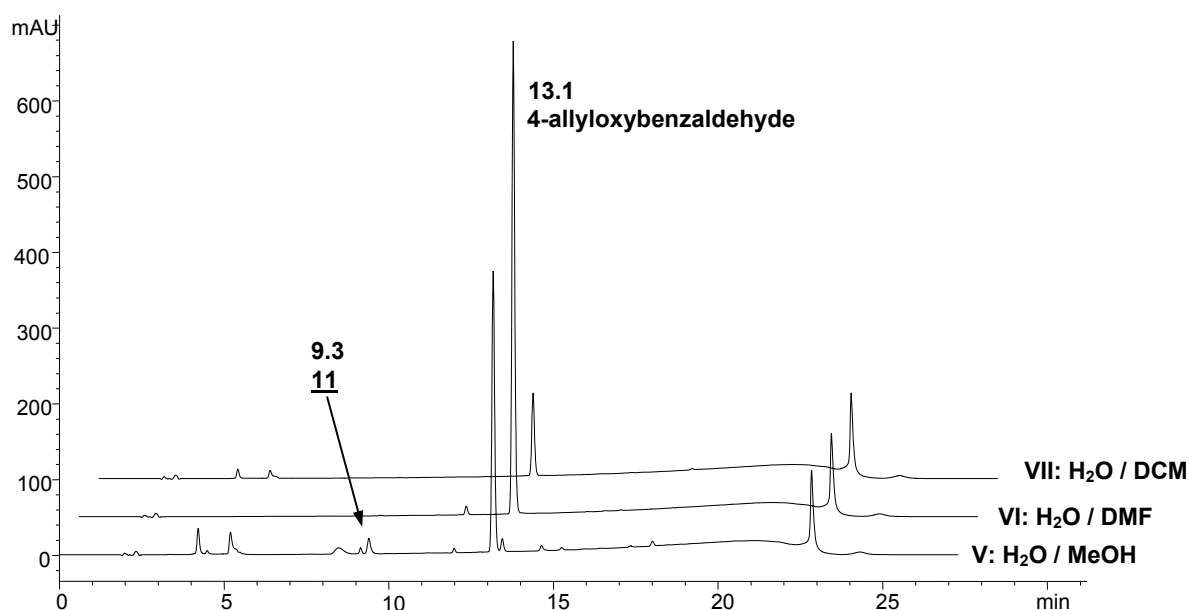


Fig. III-17: RPLC-UV chromatograms of Solvent approach V, VI and VII after microwave treatment. Gradient: 10 to 100% B in 20 min. A: H₂O + 0.1% FA, B: ACN + 0.1% FA. Flow rate: 1 ml/min.

Fragmentation spectra of approach V (not shown), almost identical with those in Fig. III-15 confirm the presence of mono- and bis-ester products at 9.3 and 10.0 min. Again, yields are absolutely poor, in approach VI and VII no RPLC-UV product peak is generated at all.

III.B.3.4. Temperature

So far most Ugi reactions generated the best results at RT or below (19). Still, there are some exceptions where heating turned out to be supportive (29). In the present work a protocol described by Brahmachary et al was followed: A mixture of the aminophosphonic acid and the carbonyl compound in MeOH was cooled to 0 °C before the isocyanide was added. This order is often observed, because of the preformation of imine. The reaction was then allowed to continue at RT.

In order to find out if constant heating could improve the reaction with **2**, one approach (0.45 M; equimolar, 400 µmol of each reactant in 895 µL MeOH) was stirred at 40 °C (water bath) instead of RT. However, no product peak could be identified by RPLC-UV. Microwave heating is consequently considered as superior, as it yielded at least detectable product amounts.

III.B.4. Synthesis protocol of the primary test compound (1)

Reactant set: 3, 4, 5

Two 1.18 M batches (Synthesis approach I (simultaneous reactant addition) and II (stepwise reactant addition), 2 mmol of each reactant in 1.7 ml MeOH/approach) were prepared. The MW vials were loaded with starting material in the order described in chapter III.B.3. The vials were sealed and subjected to MW irradiation for 3 x 30 min. each (alternating; that means, that while vial I was allowed to cool down outside the microwave, vial II was subjected to irradiation for 30 minutes). Approach II was allowed to form the imine in absence of the isocyanide before the first irradiation step for 90 minutes at RT (results discussed in chapter III.B.2.). Over night and during MW irradiation pauses the reaction mixtures were stirred at RT. Due to the findings in III.B.3.1. the temperature maximum was set at 100 °C and the highest applied power was 100 W. High pressure limit was set at 18 bar.

On the second day the vials were again subjected to microwaves: at first again once for 30 minutes and then three times for 60 minutes each. Subsequently the reaction was left to proceed at RT for one week before the vials were again irradiated twice for 60 minutes. Afterwards they were stirred at RT until the product mix was separated on a preparative RP18 five days later (III.C.1.). Single enantiomers were obtained after preparative separation on a chiral stationary phase based on cinchona alkaloid-derived selector 2 (Fig. I-2) (chapter III.C.2.).

The final yield after RPCL (RP18, 10 µm, 100 x 20.21 mm ID; mobile phase: H₂O/MeOH (45/55, v/v) + 0.1 % TFA) purification was 34 %. A plausible explanation for this moderate result could be the volatility of the isocyanide 4. After MW irradiation the vials were allowed to cool down to 40 °C inside the MW (sealed). Then they were taken out and left to stir at RT. Since the vials are not totally tight, substances in the gas phase could have leaked. This holds for the isocyanide as well as for MeOH. Standard operation procedure should be optimized by letting the vial cool down to RT inside the closed microwave oven.

III.C. Primary test compound characterization

The obtained product was identified by means of RPLC-UV-ESI-MS, NMR and IR spectroscopy (appendix). The molecule contains two stereogenic centres, one provided by reactant 5 and one newly formed in the course of the reaction. According to HPLC runs on chiral CSPs, all four possible stereoisomers were produced (III.C.2.), as expected.

III.C.1. RPLC-UV-ESI-MS

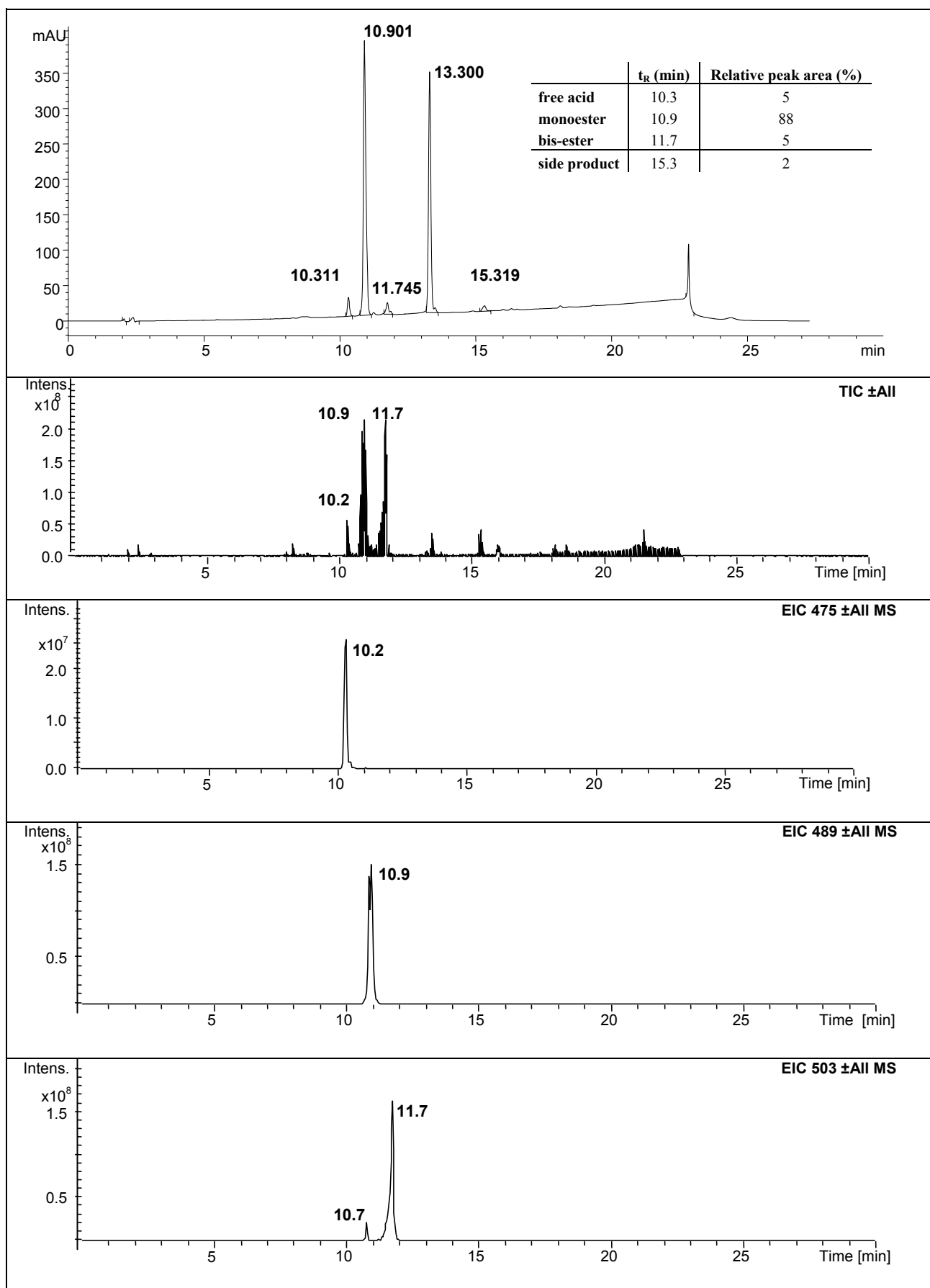


Fig. III-18: RPLC-UV chromatogram, corresponding total ion chromatogram and extracted ion chromatograms of $m/z = 475$ (free acid), 489 (monoester), 503 (bis-ester). Gradient: 10 - 100% B in 20 min. A: H₂O + 0.1% FA, B: ACN + 0.1% FA. Flow rate: 1 ml/min

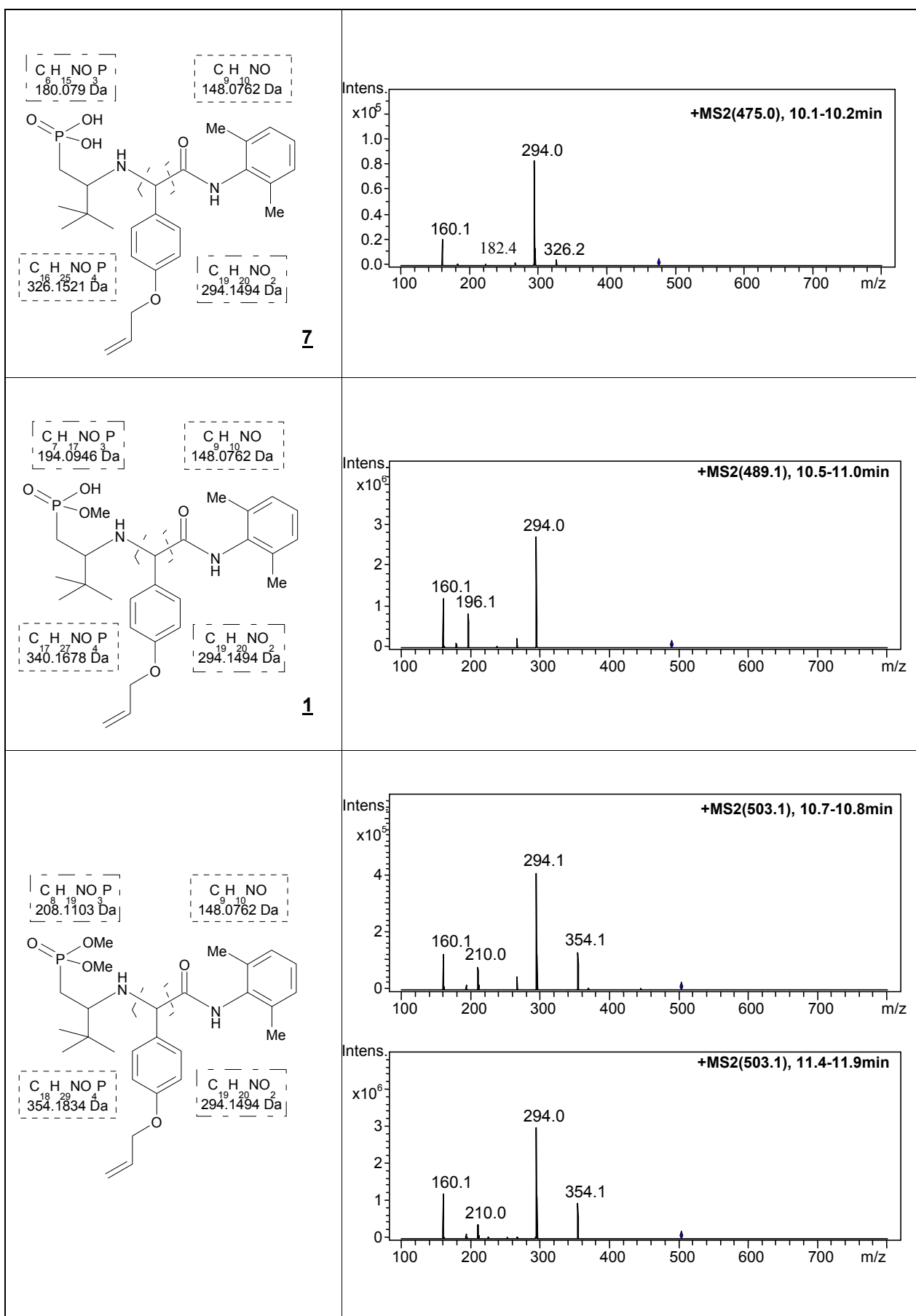


Fig. III-19: Expected bond cleavages and fragmentation spectra of obtained Ugi products.

Detection was carried out via RPLC-UV-ESI-MS. As the extracted ion chromatogram of $m/z = 489$ in Fig. III-18 demonstrates, the diastereomeric pairs eluted, as expected, close to each other in the employed gradient mode. Bis-ester stereoisomers revealed a better selectivity (peaks at 10.7 and 11.7 min., verified by +MS2 spectra, Fig III-19), whereas free acid diastereoisomers were not separated at all. Ugi-ring product (**6**) m/z ratio was found at 9.6 and 17.3 min. in an extracted ion chromatogram of 457 (Fig. III-20). Still, no visible peaks elute there in the RPLC-UV chromatogram (Fig. III-18), indicating a negligible yield. 10.2 is not likely to be the retention time of **6**, since it is not expected to elute at the same time as **7**.

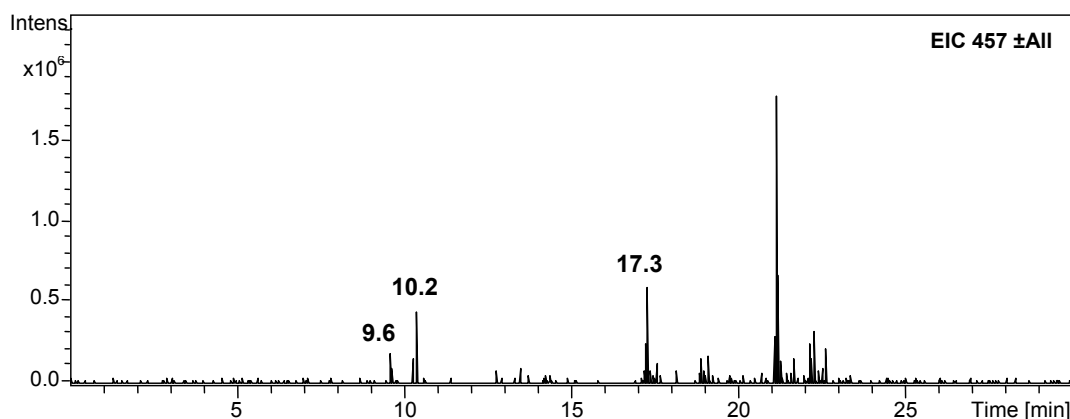


Fig. III-20: Extracted ion chromatogram of Ugi product **6** m/z ratio.

II.C.2. Enantiomer separation

In order to find the best column for stereomer separation, three chiral supports were tested.

Table III-3: Selectivity values of obtained product on distinct chiral supports. Flow rate: 1 ml/min

Support	MeOH + 0.25% AcOH						MeOH/ACN (50/50) + 0.25% AcOH					
	α (pair 1)	k_{P11}	k_{P12}	α (pair 2)	k_{P21}	k_{P22}	α (pair 1)	k_{P11}	k_{P12}	α (pair 2)	k_{P21}	k_{P22}
<i>t</i> -BuCQN	1.08	2.53	2.74	1.14	5.80	6.63	1.07	6.35	6.78	1.17	16.90	19.84
<i>t</i> -BuCQD	1.07	2.50	2.68	1.08	5.47	5.93	1.11	5.76	6.39	1.07	15.82	16.88
O-9-tert-Butylcarbamoyl-[6'- (1-adamantyl)methoxy]- cinchonidine	1.00	1.82	1.82	1.07	3.69	3.93	1.00	4.36	4.36	1.08	10.85	11.71

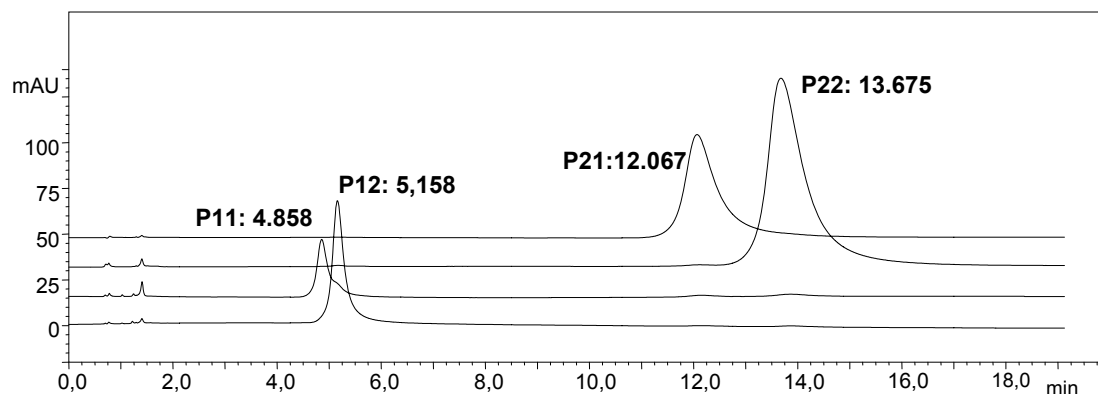


Fig. III-21: Quality control of enantiomers of **1** on *t*-BuCQN after preparative separation on *t*-BuCQD (5 μ m; 150 x 4 mm ID). Mobile phase: MeOH/ACN (50/50; v/v) + 0.25% AcOH. Flow rate: 1 ml/min.

III.C.3. Stereochemistry

III.C.3.1. Absolute configuration determination of the aminophosphonic acid building block

The most facile way to determine the configuration of the stereogenic centre of the aminophosphonic acid building block would have been to repeat the reaction with enantiomerically pure **5**. As such an enantiomer was not available, an analogue exhibiting an isopropyl residue instead of the *tert*-butyl group was chosen.

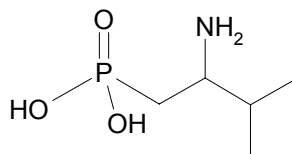


Fig.III-22: 2-amino-3-methylbutane phosphonic acid (**14**)

Experimental

The reaction was performed with a racemate and the R-enantiomer of **14**. Due to a shortage of these compounds, very low reactant concentrations (equimolar amounts) were employed:

R-enantiomer: 0.03 M (3 μ mol in 90 μ L) in MeOH

Racemate: 0.07 M (12 μ mol in 180 μ L) in MeOH

Both reaction mixtures were irradiated with microwaves three times:

Temperature (constant): 100 $^{\circ}$ C

P_{max} : 18 bar

Power $_{\text{max}}$: 100 W

Run time: 30 min.

The resulting reaction mixtures were directly injected on a *t*-BuCQN-CSP without any preceding purification steps. The chromatograms are shown in Fig. III-23.

Results and Discussion

Fortunately, the reaction yields were sufficient for analytical purposes, revealing peaks well above the detection limit, although the reactant concentration was in a critically low range. As can be inferred from Fig. III-23, the S-enantiomer of the second eluted pair of enantiomers elutes first, while the R-enantiomer shows stronger affinity to the selector. For the first eluted enantiomer pair the elution order is unclear due to a co-eluting system peak and insufficient retention and/or enantioselectivity.

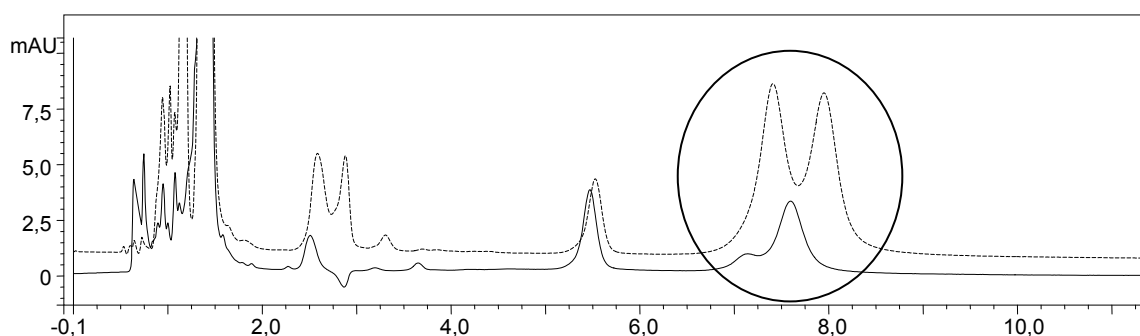


Fig. III-23: HPLC chromatograms of the Ugi products obtained with the R-enantiomer (—) and racemate (--) of **14** on *t*-BuCQN. Mobile phase: MeOH/ACN (50/50; v/v) + 0.25% AcOH. Flow rate: 1 ml/min.

III.C.3.2. Optical rotation of the stereoisomers of Ugi product **1**

The enantiomers of the second eluted peak pair of **1**, encoded as P21 and P22, were intended to be used as chiral selectors. The absolute configuration of the stereogenic centre of the aminophosphonic acid building block was unequivocally assigned chromatographically as described above, with the S-enantiomer eluting before the R-enantiomer (replacement of *t*-Bu by *i*Pr has no influence on the elution order). Unfortunately, the absolute configuration assignment of the newly created stereogenic centre, decoded in the structure of Table III-4 with ×, is less straightforward. It is planned to assign this configuration by circular dichroism and comparison of experimental spectra with spectra calculated by quantum chemistry methods (currently ongoing project). Agreement between calculated and experimental spectra would be an indication for the correct assignment of the absolute configuration (69). To pinpoint the identity in the meanwhile, signs of optical rotation were measured for the two enantiomers eluting as the second pair.

Results and Discussion

Values were calculated according to

$$[\alpha]_d^T = \frac{\alpha}{d \cdot c} \cdot 100.$$

α ... measured optical rotation

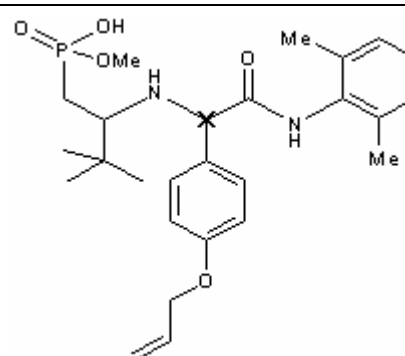
d ... path length [dm]

c ... concentration [g/100 ml]

Table III-4: Rotational direction results

P21 (2S,×)-(-) c = 0.51 d = 1 T = 20°C			P22 (2R,×)-(+) c = 0.71 d = 1 T = 20°C		
λ	α	α_{spez}	λ	α	α_{spez}
589	-0.49	-95	589	0.55	78
578	-0.48	-94	578	0.59	83
546	-0.57	-111	546	0.69	98
436	-1.03	-201	436	1.35	191
365	-1.85	-360	365	2.48	351

A cuvette was filled with a methanolic enantiomer solution and the optical rotation was measured at distinct wavelenths with a polarimeter.



III.C.4. Stability

Since the new compound **1** was intended to be used as chiral selector, its stability was tested in three different media; in a common HPLC solvent composition (MeOH/AcOH/NH₄Ac = Solvent test I)), the same solvent without acetic acid (Solvent test II) and a 1 M NH₄Ac solution (Solvent test III) (exact compositions given in Fig. III-24). Sensibility to heating was also examined.

Experimental

0.13 mg of **1** were dissolved in solvent tests I and II, and 0.1 mg in solvent test III. HPLC runs were performed on *t*-BuCQN after 1, 2, 3, 6, 10 and 23 days of stirring at RT. The vials were then kept at 35 °C over night (in an oven, without stirring) and subsequently put into a water bath at 45 °C for 48 hours.

Results and Discussion

Fig. III-24 comprises the chromatograms before the stability test (Start), after 23 days (23 d) of stirring at RT and after the heating process (H). All enantiomers turned out to be stable in all solvents and even after heating. Thus, it seems that there are no restrictions on the use of **1** as chiral selector from viewpoint of its stability.

Note: The loss in resolution of the first eluted enantiomer pair in Fig. III-24 (I) is due to overloading.

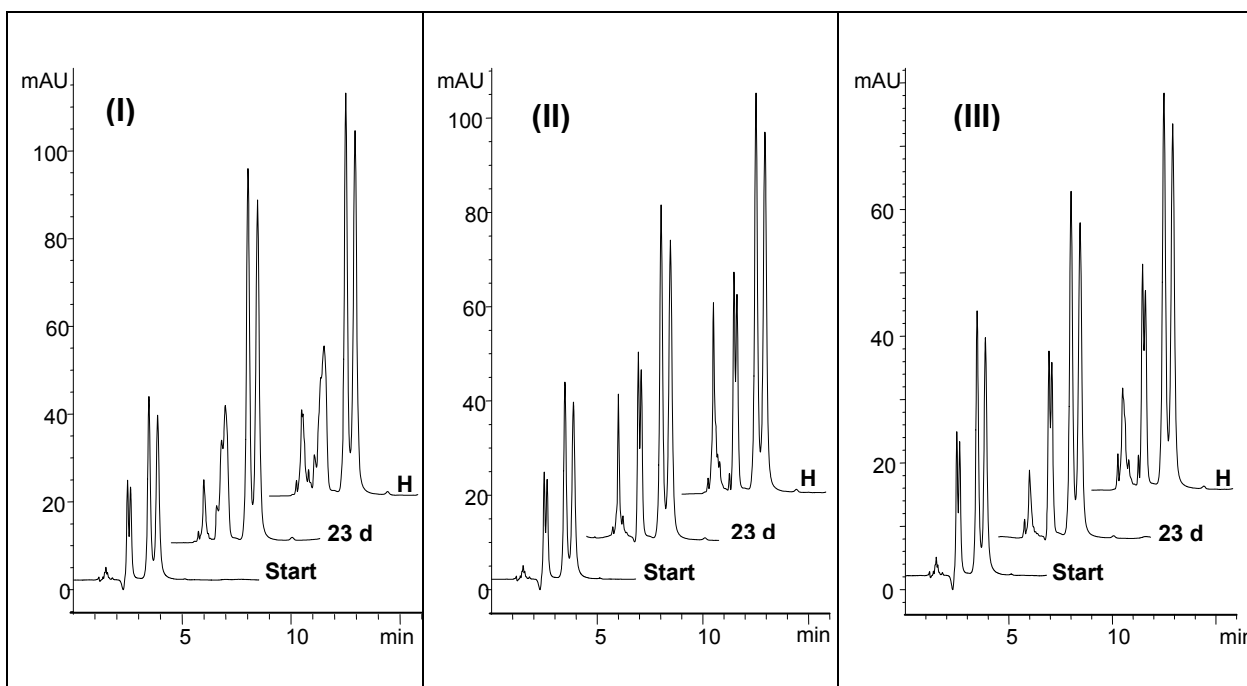


Fig. III-24: Stability tests of **1 in different chromatographic media. Chromatograms on *t*-BuCQN in different test stages. Solvent test I: MeOH/AcOH/NH₄Ac (98/2/0.5; v/v/w). Solvent test II: MeOH/NH₄Ac (100/0.5; v/w). Solvent test III: 0.1 M NH₄Ac in MeOH, acetic acid ad pH = 7.5.**

III.D. Monoester cleavage

In order to enhance chromatographic performance, a stronger anionic surface resulting in a more stable electro-osmotic flow and more distinct molecular interactions could be favourable. Hence, the susceptibility of the phosphonic acid monoester to hydrolysis yielding the free acid, **7**, was explored. Phosphonic acid monoesters are commonly transformed into the corresponding acids by subjection to acidic (but also basic) media, like aqueous HCl (or NaOH) (70, 71). However, in the present case such a reaction was supposed not to be suitable as it would have provoked cleavage of the amide bond as well. Thus, other pathways had to be found.

Amongst those provided by literature, reports employing Trimethylsilylbromide (TMSBr) seemed the most promising ones. The potential of this agent has already been noted in the 1960ies (72, 73). More recently, TMSBr was utilized in the course of the synthesis of potential drugs (70, 74-76), also containing amide bondings. It is well worth mentioning that TMSBr specifically cleaves phosphonic acid esters besides carboxylic acid esters, because the latter functional group was not present in the selector molecule. With regard to a minimized number of reaction and tedious (chromatographic) purification steps, it would be of high value if a way to hydrolyze both, phosphonic acid mono and bis-esters in one step, could be found. According to literature TMSBr fulfills such demands. Unfortunately, TMSBr is also known for its ability to cleave ether groups (77). This has to be taken into consideration as the selector molecule contains an allylether moiety.

In the past, approaches for a basic cleavage of phosphonic esters by employment of KOH, NaOH and their carbonates have also been carried out (78, 79), revealing satisfying results as well. Furthermore, HBr was successfully used in a similar case (80), despite its potential to affect the amide bond.

Herein, all reactants mentioned above were taken into account for monoester cleavage.

III.D.1. Experimental

III.D.1.1. Ester cleavage with TMSBr

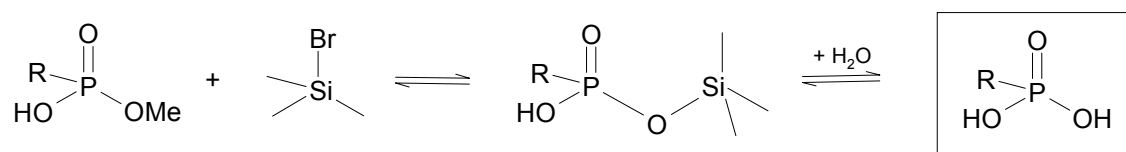


Fig. Fig. III-25: Monoester hydrolysis by TMSBr

i) 1 mg of the monoester was suspended in 70 μL DCM containing 1.4 μL TEA (slightly modified literature procedure (81)). A white residue precipitated as soon as 5.25 μL TMSBr were added. Another 135 μL DCM were filled into the reaction vial, which was then put onto a shaker for thirty minutes. The reaction mixture was analyzed chromatographically: It is seen in Fig. III-26 that only 1.8 % monoester had remained and no side reaction, especially no ether cleavage had taken place.

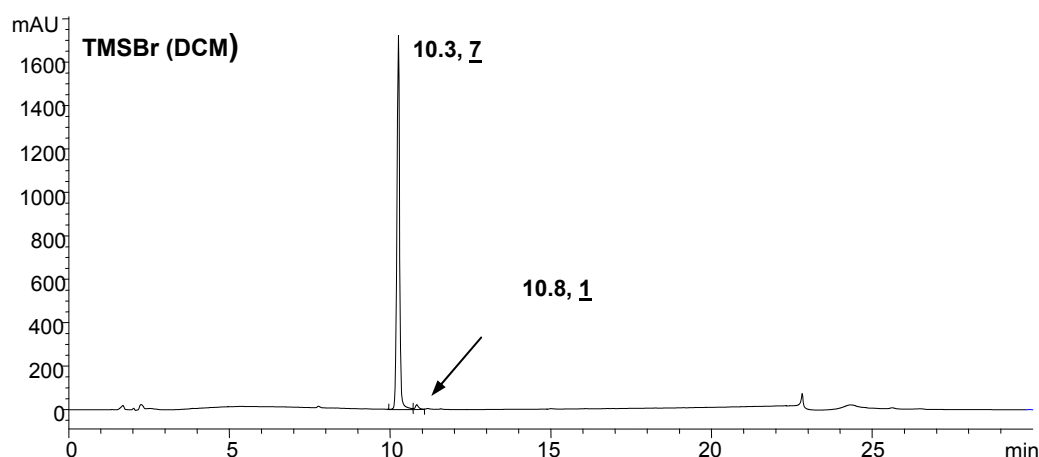


Fig. III-26: RPLC-UV chromatogram of **1** after treatment with TMSBr in DCM. Gradient: 10 to 100% B in 20 min. A: H_2O + 0.1% FA, B: ACN + 0.1% FA. Flow rate: 1 ml/min.

ii) 1 mg **1** was dissolved (sonicated) in 90 μL DMF. Subsequently 5.25 μL TMSBr (75) were added and the mixture was put onto a shaker at RT. After three hours the solvent was evaporated with nitrogen, leaving an oily brown residue, the colour of which changed immediately to white when brought into contact with water (250 μL). This suspension was sonicated and shaken for three hours and subsequently analyzed by means of RPLC-UV. The released acid eluted at 10.2 minutes, followed by hardly any reactant (1.8 %) and 5.3 % of an unidentified side reaction product at 12.3 minutes.

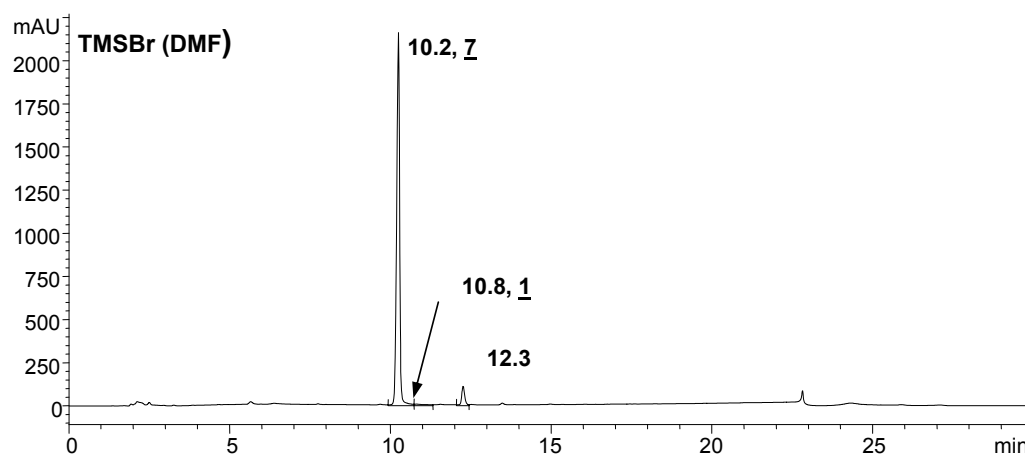


Fig. III-27: RPLC-UV chromatogram of **1** after treatment with TMSBr in DMF. Gradient: 10 to 100% B in 20 min. A: H_2O + 0.1% FA, B: ACN + 0.1% FA. Flow rate: 1 ml/min.

III.D.1.2. Hydrolysis with HBr (80)

1 mg of **1** was dissolved in 450 μ L glacial acetic acid containing 33 % HBr. This mixture was shaken for 6.5 h, yielding an oily brown substance when blown off with nitrogen. Addition of 250 μ L H₂O caused the already described change in colour to white. Chromatographic analysis revealed that the generated mixture consisted of only 13.5 % acid and two side products (7.7 min/2.4 %; 8.2 min/12.8 %) only a small amount of monoester had been transformed into the acid and furthermore about as much of a side product had been produced (probably the corresponding compounds with cleaved ether groups).

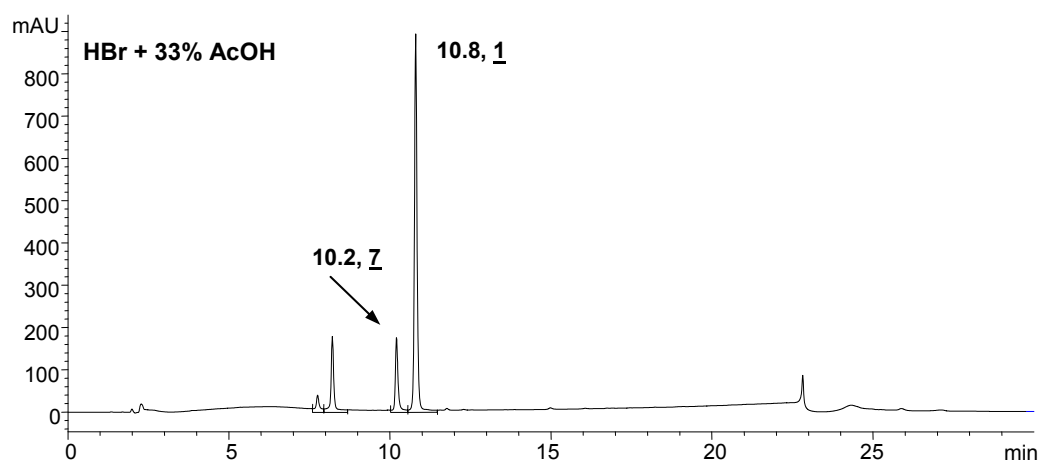


Fig. III-28: RPLC-UV chromatogram of **1** after treatment with HBr in glacial acetic acid. Gradient: 10 to 100% B in 20 min. A: H₂O + 0.1% FA, B: ACN + 0.1% FA. Flow rate: 1 ml/min.

III.D.1.3. Hydrolysis with NaOH, KOH, NaHCO₃, KHCO₃

These reagents have also been employed to prepare phosphonic acid monoesters and acids from a bis-ester starting material (**79**). In the present study 8 mg monoester were dissolved in 4 ml MeOH and another 8 mg in 4 ml water. These solutions were divided and filled into eight vials, one vial containing 2 mg monoester in 1 ml MeOH or water, respectively. Subsequently 0.5 M solutions were prepared by adding the necessary amount of NaOH, KOH, NaHCO₃ and KHCO₃. The eight mixtures were shaken and allowed to react for about 20 h at RT. Following RPLC-UV analysis exhibited no signs of a hydrolysis. So the solutions were split: one half (500 μ L each) was shaken again over night (at 40 °C), the other half was subjected to MW irradiation ($T_{\text{const.}} = 100$ °C, $P_{\text{max}} = 18$ bar, $\text{Power}_{\text{max}} = 100$ W, $t = 15$ min.). Concerning the water samples, MW irradiation obviously caused a stronger degradation (Fig. III-29). Still, no phosphonic acid was formed in any case.

So, TMSBr has been recognized as the most efficient way to produce **7** from **1**.

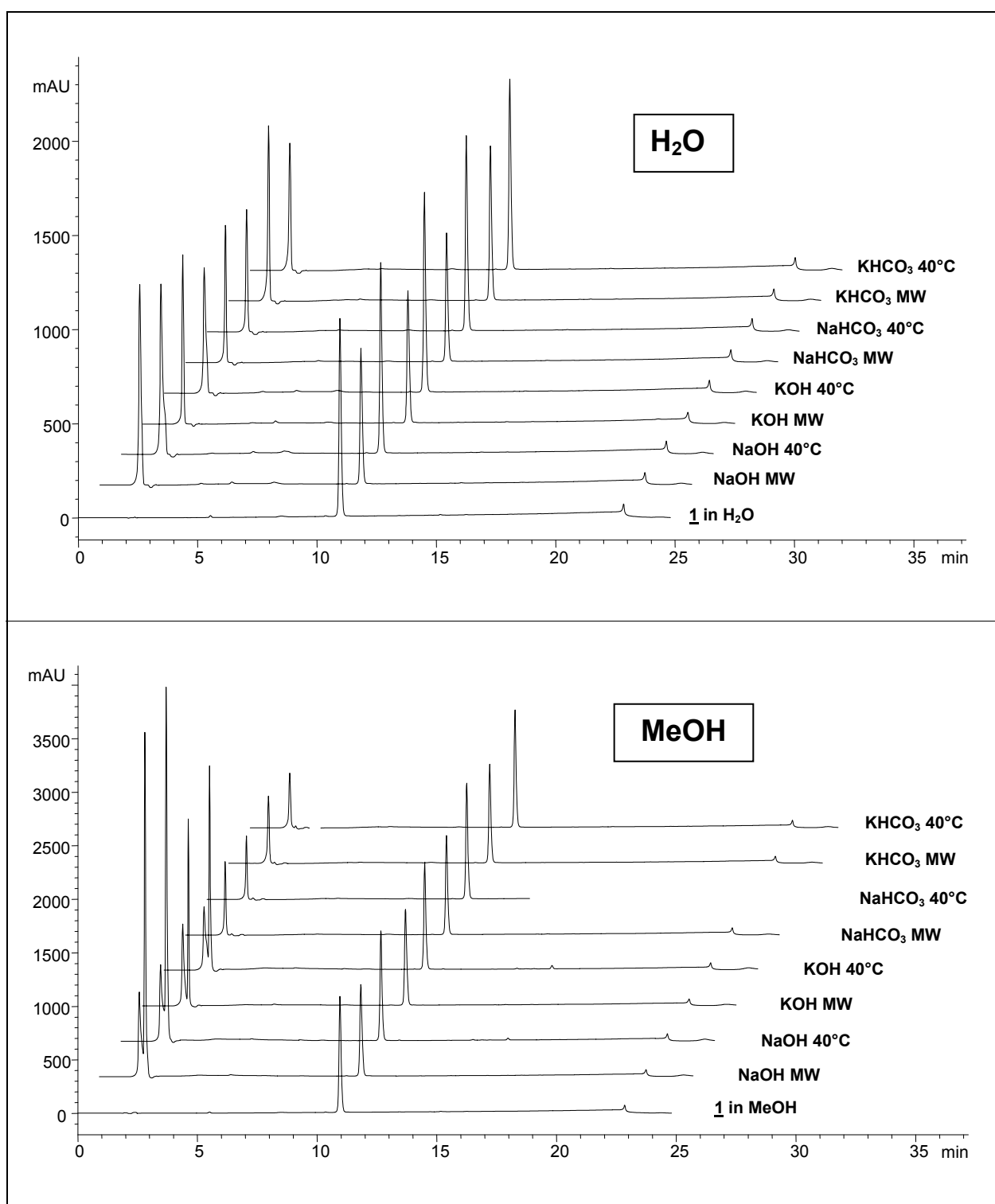


Fig. III-29: RPLC-UV chromatograms of **1 after treatment with NaOH/KOH/NaHCO₃/KHCO₃ at distinct conditions. Gradient: 10 to 100% B in 20 min. A: H₂O + 0.1% FA, B: ACN + 0.1% FA. Flow rate: 1 ml/min.**

III.E. Design of selectors for CEC usage

III.E.1. Outline

As has been mentioned in the objective, the creation of a library of potential selectors by the Ugi reaction has been envisaged herein. While all compounds may be varied, in the first place 2,6-dimethylphenylisocyanide (**4**) was the employed isocyanide. The remaining building blocks (Fig. III-31) consisted of three different aldehydes, two of which were produced in-house (**8**, 4-allyloxy-3,5-dimethoxybenzaldehyde (**15**), synthesis described in chapter III.E.3.1.) and three bifunctional amino acids. Due to a shortage of acid components, not all possible combinations were accomplished. Research on sulfonic acid based selectors has been performed previously in our group (82-85), consequently laying the focus on phosphonic acid derivatives. Precisely, selector **1**, which exhibits a *t*-Bu residue enabling further van der Waals interactions compared to **11** (Fig. III-31), was aimed at. An Ugi reaction with β -phenylalanine (**16**) was intended as a control experiment to assure that the reaction proceeded as usual with a carboxylic acid under applied conditions. Indeed, the reaction performed well with **16** (leading to **17**), but produced a non-cyclic methanol monoester (**1**) in case of **5**, as described above (chapter III.B./C.). The performance of the selector was expected to be influenced by the introduction of electron-withdrawing or electron-donating species at the former aldehyde moiety. Hence, bromo- and methoxygroups were chosen as substituents.

The original concept envisaged a reciprocal screening of the three resulting products (Fig. III-30): A target molecule was to be immobilized on a (monolithic) support (e.g. *t*-BuCQN) and tested for the separation of the selectors in CEC or HPLC runs. One enantiomer of the product with the highest α -value would have been covalently linked to a silica monolith and employed for CEC separations.

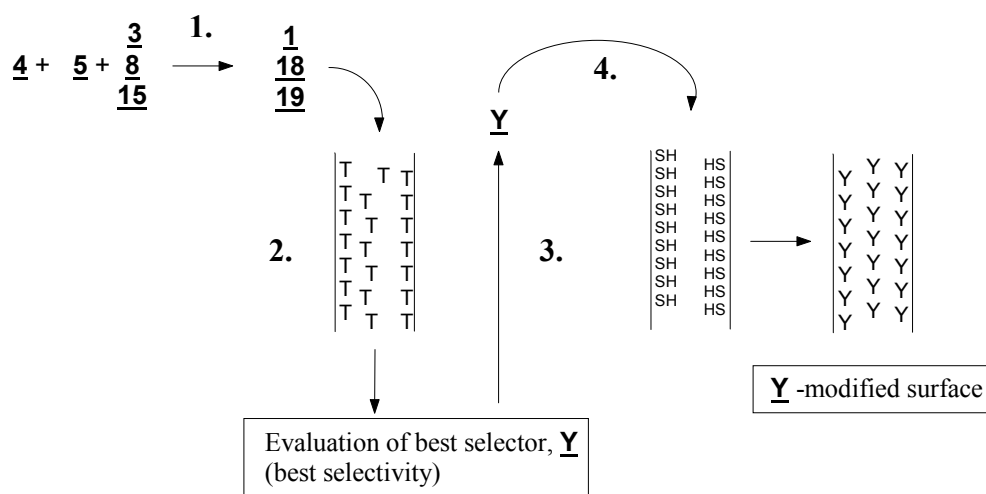


Fig. III-30: Concept of reciprocal screening

1. Production of possible selectors, **1**, **18**, **19** 2. CEC test run on target (T) modified support to evaluate selectivity of racemic product mixtures 3. Preparation of enantiopure **Y** 4. Immobilization of **Y**

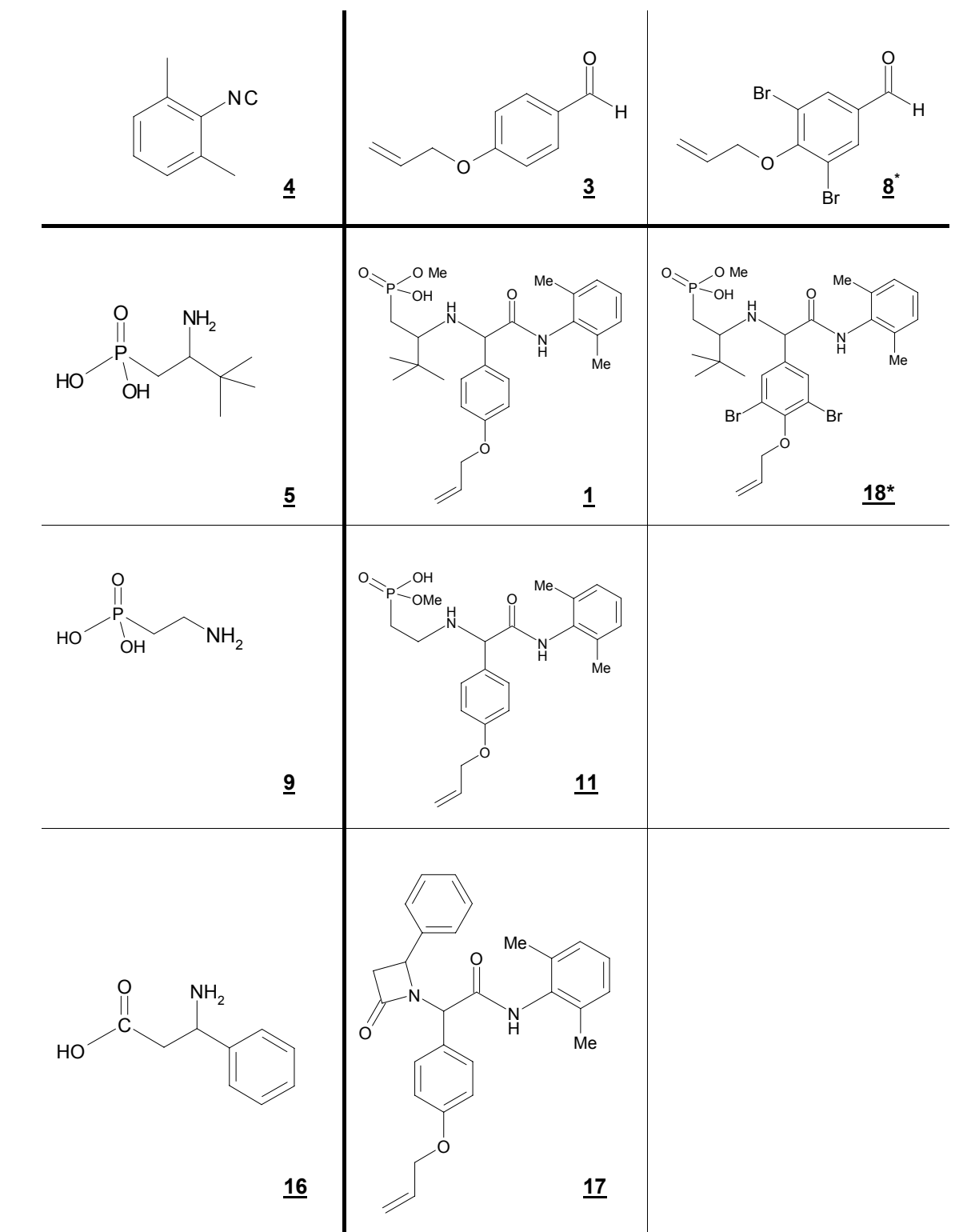


Fig. III-31: Library of selectors. *: 15, 19: -OMe instead of -Br

Since our “library” consisted of only three phosphonic acid derived selectors, another way to investigate their performance would have been to immobilize each of them on OPMs. Silica-based monoliths which have generally turned out to be superior (especially in terms of efficiency, as described in detail in chapter IV) were available only in a restricted number. As selectivity issues were to be examined in this case, OPMs seemed a reasonable alternative for

the exploration of the best selector which would finally have been attached to a silica monolith.

III.E.2. Variation of the acid component

The acid compound is probably the most versatile of the reactants. Since the reaction has been established with carboxylic acids, miscellaneous analogues have been tried and tested. Cyanates and thiocyanates, salts of secondary amines, hydrogen selenide and water are named next to sulfonic and phosphonic acids and phenols (19).

Herein, the investigation of a bifunctional β -amino carboxylic acid seemed particularly interesting, because carboxylic acids most often yield the desired products; the four membered ring in this case. Additionally, the molecule should also carry a bulky residue at the β -position. β -Phenylalanine which has a phenyl group (instead of *t*-Bu in **5**) was considered expedient and was available in enantiomeric forms as well. Two approaches, with and without MW irradiation, were carried out.

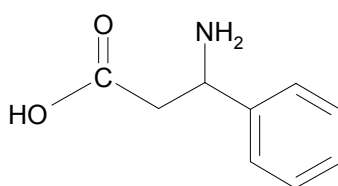
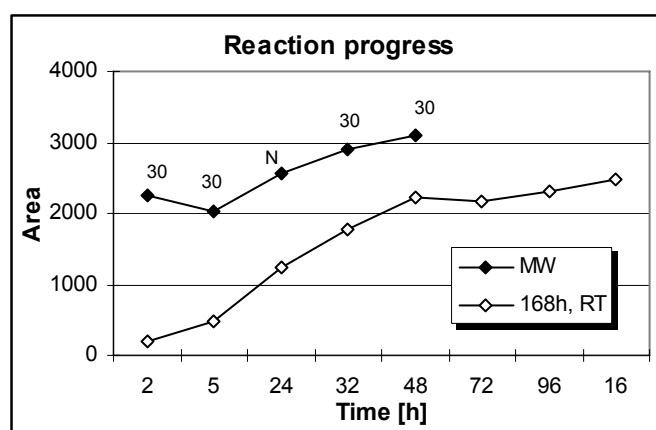


Fig. III-32: β -Phenylalanine (**16**)

Experimental

Two 0.34 M approaches were prepared: 200 μ mol of β -phenylalanine were suspended in 555 μ L MeOH before addition of an equimolar amount of carbonyl (at 0° C for the approach that was allowed to react at RT subsequently). At last 200 μ M isocyanide were added. One approach was allowed to react at RT, while the other was subjected to MW irradiation and stirred at RT in irradiation pauses and over night (exact conditions given in Fig. III-33).

Results and Discussion



MW lettering:

“30” indicates that the run time was 30 minutes. “N” means that the reaction solution was stirred over night at RT before MW irradiation experiments were continued on the next day.

X-axes labelling refers solely to the reaction performed at RT.

Temperature (constant): 100 °C

P_{max}: 18 bar

Power_{max}: 100 W

Fig. III-33: Reaction progress monitoring by means of RPLC-UV of an Ugi reaction employing β -phenylalanine. Gradient: 10 to 100% B in 20 min. A: H₂O + 0.1% FA, B: ACN + 0.1% FA. Flow rate: 1 ml/min.

Fig. III-33 illustrates that the microwaves augmented the reaction rate drastically.

After 30 minutes of MW heating the reaction proceeded as far as after 48 h at RT according to RPLC-UV peak areas. In both cases the product peak grew rather slowly, but more or less continuously. The plainly visible aldehyde peak (Fig. III-34) proves that the reaction did not go to completion then. This could be due to a sub-optimal concentration of 0.34 M.

It is noteworthy that repeated MW irradiation does obviously not produce more side products.

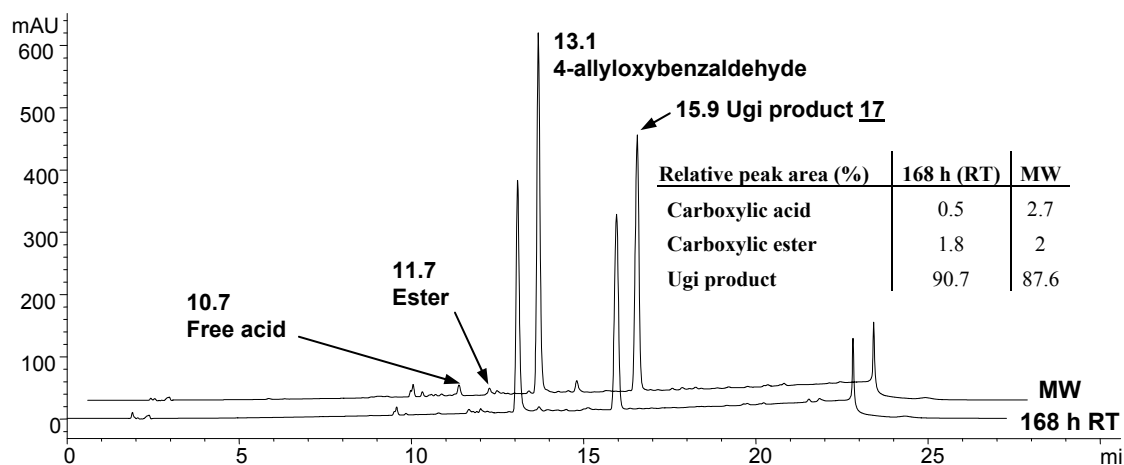


Fig. III-34: RPLC-UV chromatograms of an Ugi reaction with β -phenylalanine as acid compound. Gradient: 10 to 100% B in 20 min. A: H₂O + 0.1% FA, B: ACN + 0.1% FA. Flow rate: 1 ml/min.

MS spectra illustrate that the peak at 15.9 really arises from the expected Ugi product (Fig. III-36). Besides, traces of carboxylic ester and free acid **1**-analogues could be found: At 10.7 min. (Fig. III-37) there probably elutes the carboxylic acid and at 11.7 min. its monoester (Fig. III-38).

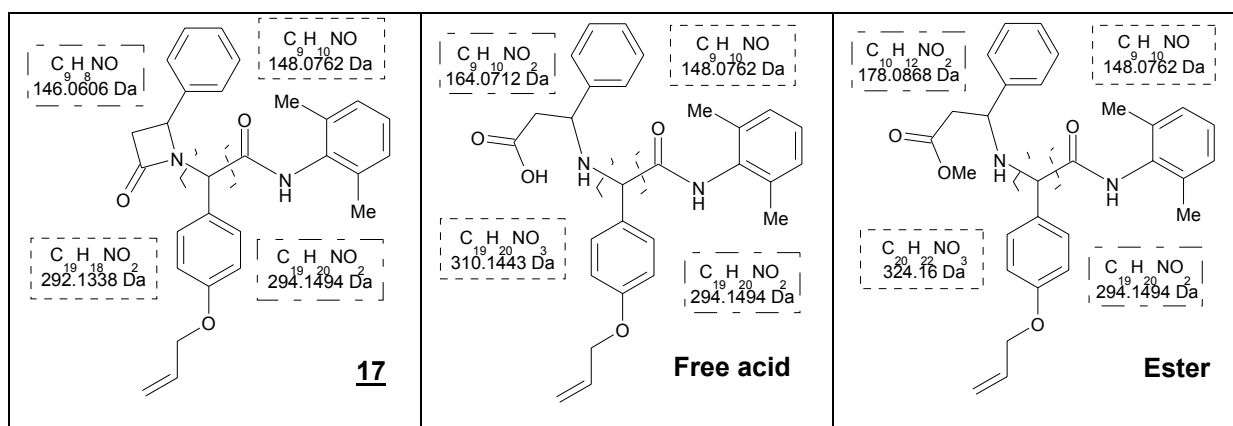
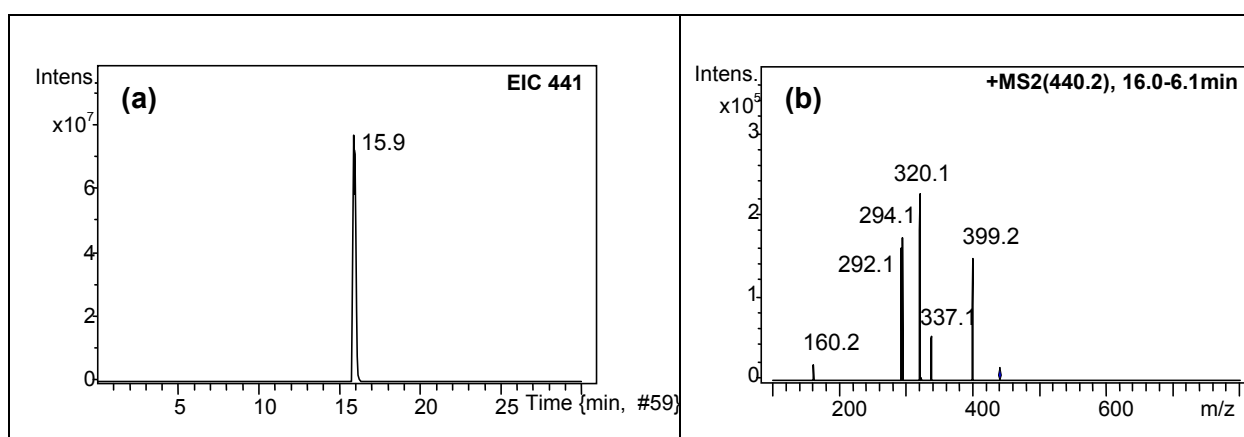
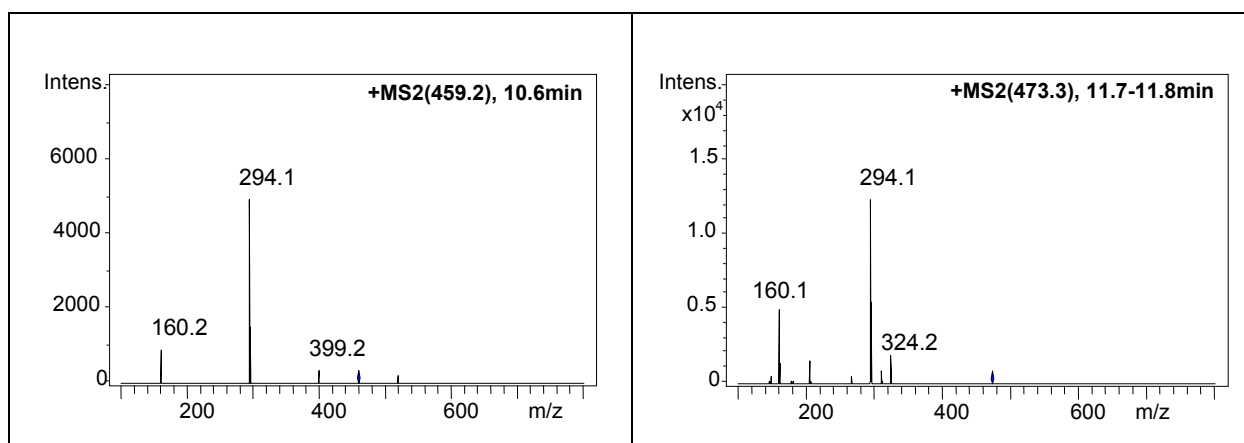
Fig. III-35: Expected bond cleavages of β -phenylalanine Ugi productsFig. III-36: Extracted ion chromatogram ($m/z = 441$) (a) and fragmentation spectrum (b) of the Ugi product, **17**. Gradient: 10 to 100% B in 20 min. A: $H_2O + 0.1\%$ FA, B: ACN + 0.1% FA. Flow rate: 1 ml/min.Fig. III-37: Fragmentation spectrum of carboxylic acid m/z ratio.

Fig. III-38: Fragmentation spectrum of the ester at 11.7 min.

III.E.3. Variation of the aldehyde component

III.E.3.1. Synthesis of 4-allyloxy-3,5-dibromobenzaldehyde and 4-allyloxy-3,5-dimethoxybenzaldehyde

In order to amplify the performance of the selector in the future, the carbonyl component was varied. Precisely, aldehydes with electron-withdrawing (bromo) and electron-donating (methoxy) substituents were produced.



Fig. III-39: 2,5-dibromo-4-hydroxybenzaldehyde (**20**) and 4-hydroxy-2,5-dimethoxybenzaldehyde (**21**)

These compounds had to be modified in a way permitting linkage to a stationary phase. Thus, the introduction of an allylresidue *via* etherification was adopted for linkage to thiol-modified supports by a radical addition reaction. Etherification according to Williamson needs an alcohol or phenol as starting compound. The hydroxygroup is deprotonated by a strong base (typically KOH (86, 87)), rendering an anionic species able to perform a nucleophilic attack at the positively polarized carbon of a halogenated alkane (or another species expressing an X-C bond at one residue). Herein the aldehydes shown above were subjected to reaction with allylbromide in MeOH. Several possible side reactions were taken into account. At first, MeOH might provide the hydroxygroup instead of the aldehydes. Secondly, a strong base could support the formation of the hemiacetal from the aldehyde. Generally, the usage of mild basic conditions is favourable. A weak base should be effective as phenols are more acidic than alcohols due to mesomerism. Literature provides the successful synthesis of phenylethers with K_2CO_3 in MeOH (88). Besides, this approach is also employing the beneficial effects of MW irradiation affording the products in less than one hour.

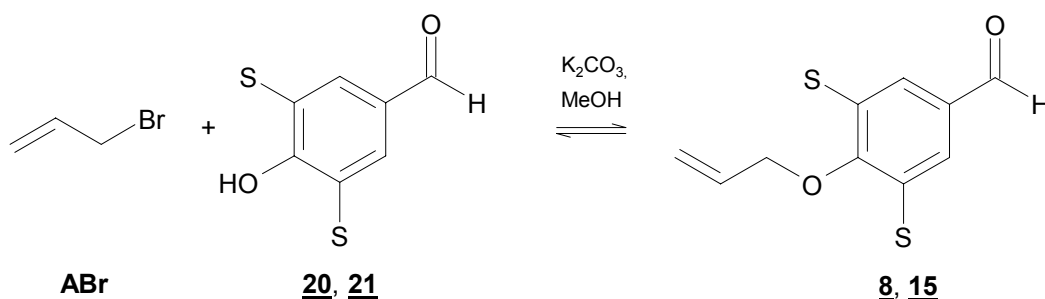


Fig. III-40: Williamson etherification. S = substituent (**20**, **8**: -Br **21**, **15**: -OMe)

Experimental

The aldehyde (2 mM **20**, 1 mM **21**) was put into a microwave vial with an equimolar amount of K_2CO_3 . 1 ml MeOH and a stirring bar were added, followed by a 1.2 molar excess of allylbromide (ABr). The vial was sealed and the reaction mixture subjected to MW irradiation. The temperature was kept constant at 100 °C for 15 minutes. The highest tolerated pressure was 18 bar and the upper power limit was 300 W. After irradiation the composition was allowed to cool down. Remaining solvent was evaporated with nitrogen and the residue extracted with several ml of hexane three times. The combined hexane phases were extracted twice with water. Hexane was evaporated and the ethers obtained as solids. **8** was light brown, whereas **15** was rather of a white (slightly yellowish) matter.

Results and Discussion

The obtained ethers were identified by means of NMR. Additionally, in the course of the MS analysis of the according Ugi reaction the expected m/z ratio and fragmentation spectrum was found for **8** (chapter III.E.3.2.). Fig. III-41/42 comprise the RPLC-UV chromatograms of the starting aldehydes and ABr and the chromatograms of the products, illustrating the completed progress since no reactants are left. Both products were generated in high purity, 94 % for **8** and 92.5 % for **15**.

RPLC-UV chromatograms

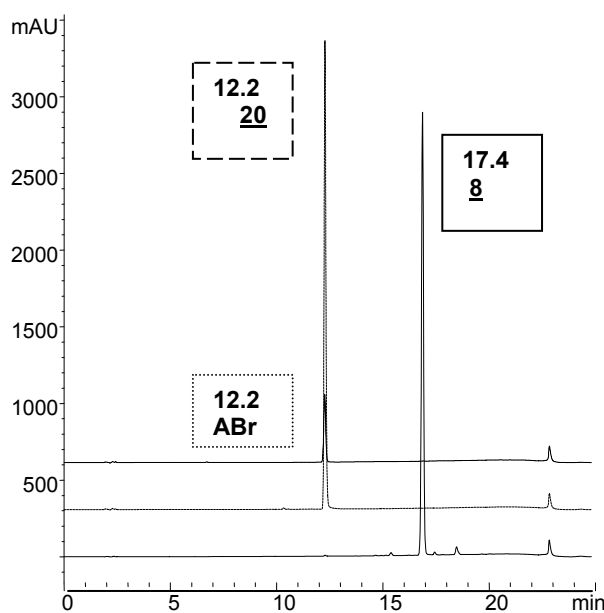


Fig. III-41: RPLC-UV chromatograms of ABr, **8**, and **20**. Gradient: 10 to 100% B in 20 min. A: $H_2O + 0.1\%$ FA, B: ACN + 0.1% FA. Flow rate: 1 ml/min. Purity: 94% **8** + 0.2% ABr + 3.4% side product at 18.5 min.

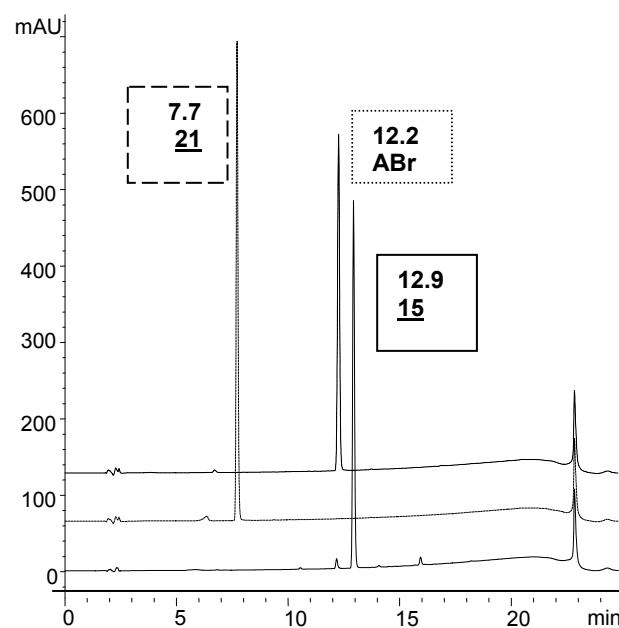
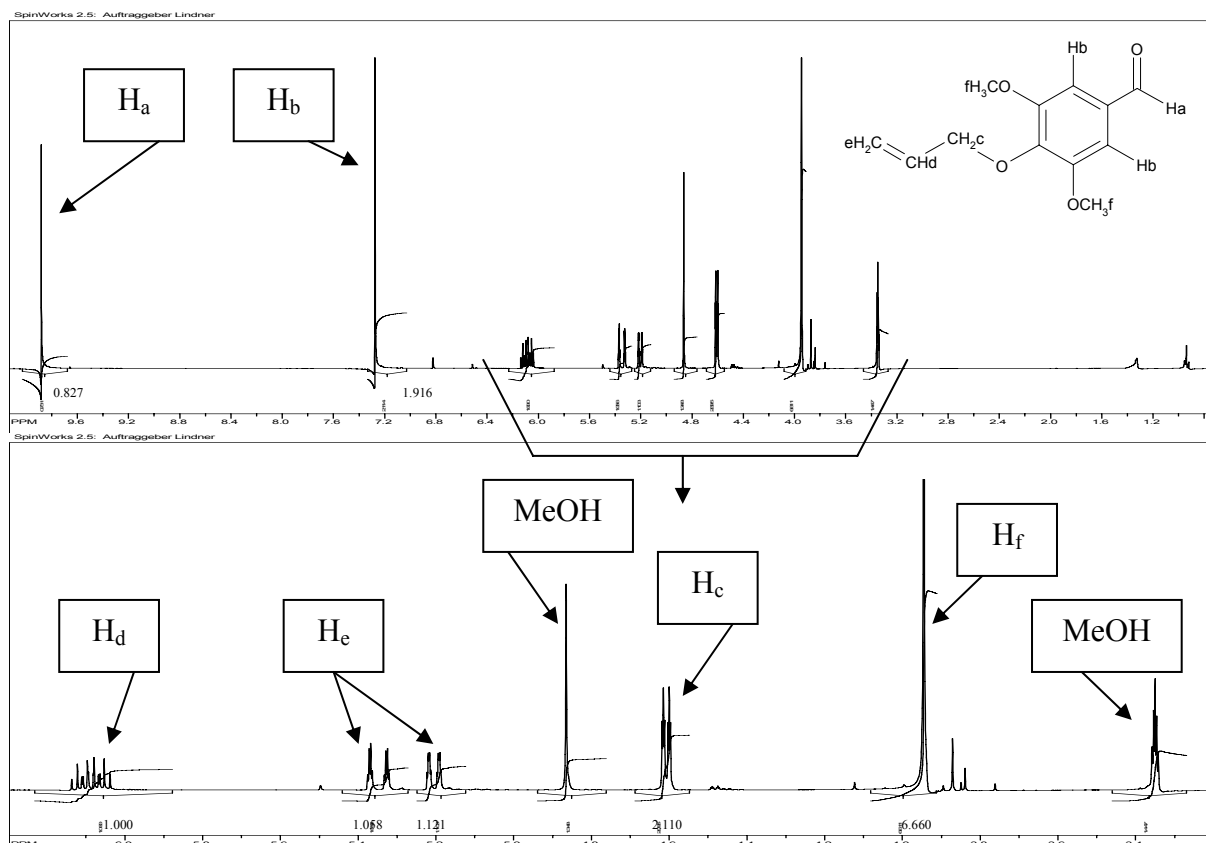
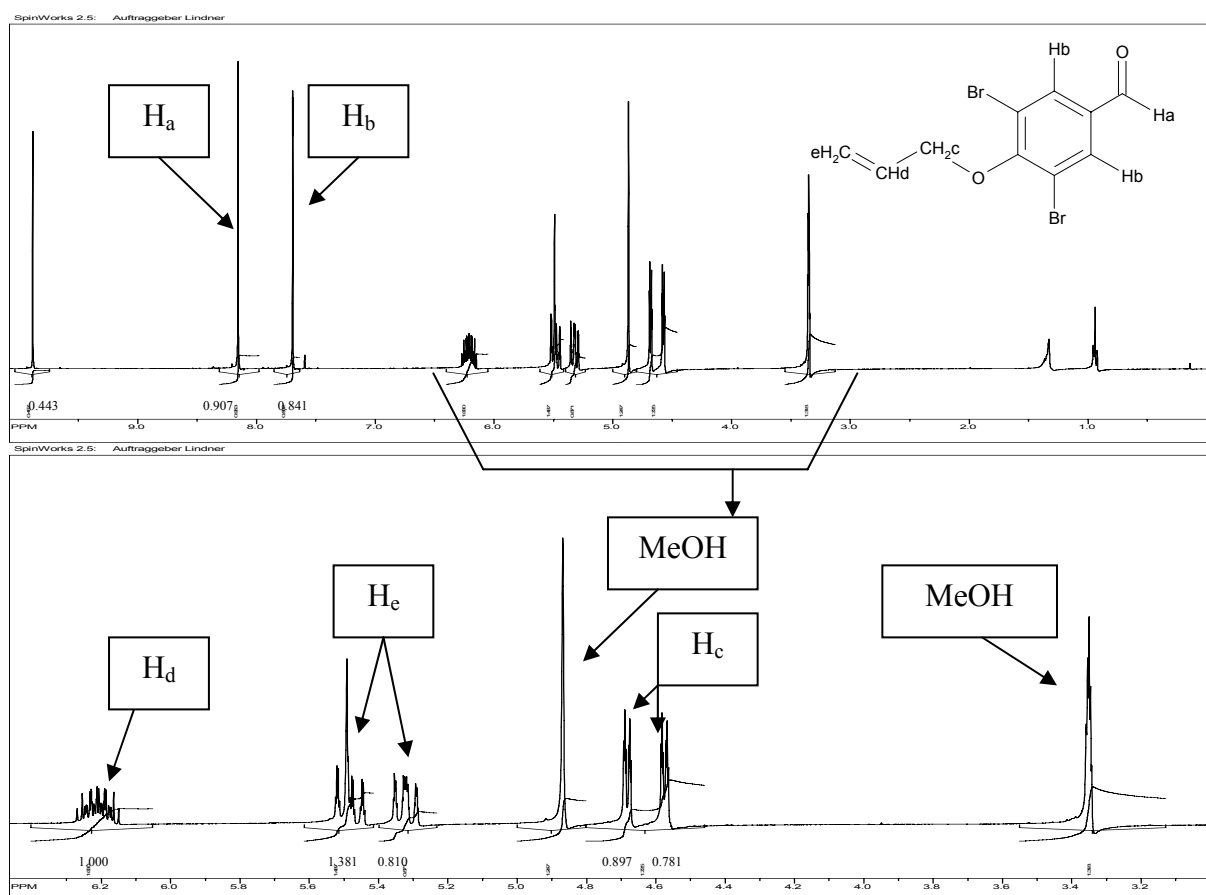


Fig. III-42: RPLC-UV chromatograms of ABr, **15**, and **21**. Gradient: 10 to 100% B in 20 min. A: $H_2O + 0.1\%$ FA, B: ACN + 0.1% FA. Flow rate: 1 ml/min. Purity: 92.5% **15** + 2.5% ABr + 5% side product at 16.0 min.

H-NMR spectra

Fig. III-43: H-NMR spectrum of 4-allyloxy-3,5-dimethoxybenzaldehyde (**8**)Fig. III-44: H-NMR spectrum of 4-allyloxy-3,5-dibromobenzaldehyde (**15**)

III.E.3.2. Ugi reaction with 4-allyloxy-3,5-dibromobenzaldehyde, 8, and aminophosphonic acid, 5

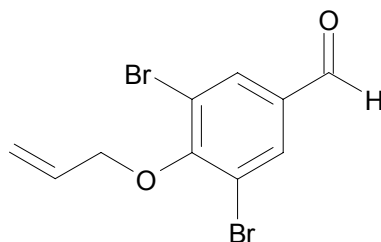


Fig. III-45: 4-Allyloxy-3,5-dibromobenzaldehyde (8)

This modified aldehyde was employed with regard to altering enantioselectivity of the obtained product as potential selector in CEC.

Experimental

Synthesis given in III.B.3.2.

Results and Discussion

Unfortunately, as discussed in chapter III.B.3.2., no reaction progress could be observed *via* RPLC-UV monitoring. Still, the employment of mass spectrometry proved that some amount of 18 (Fig. III-31) had been formed:

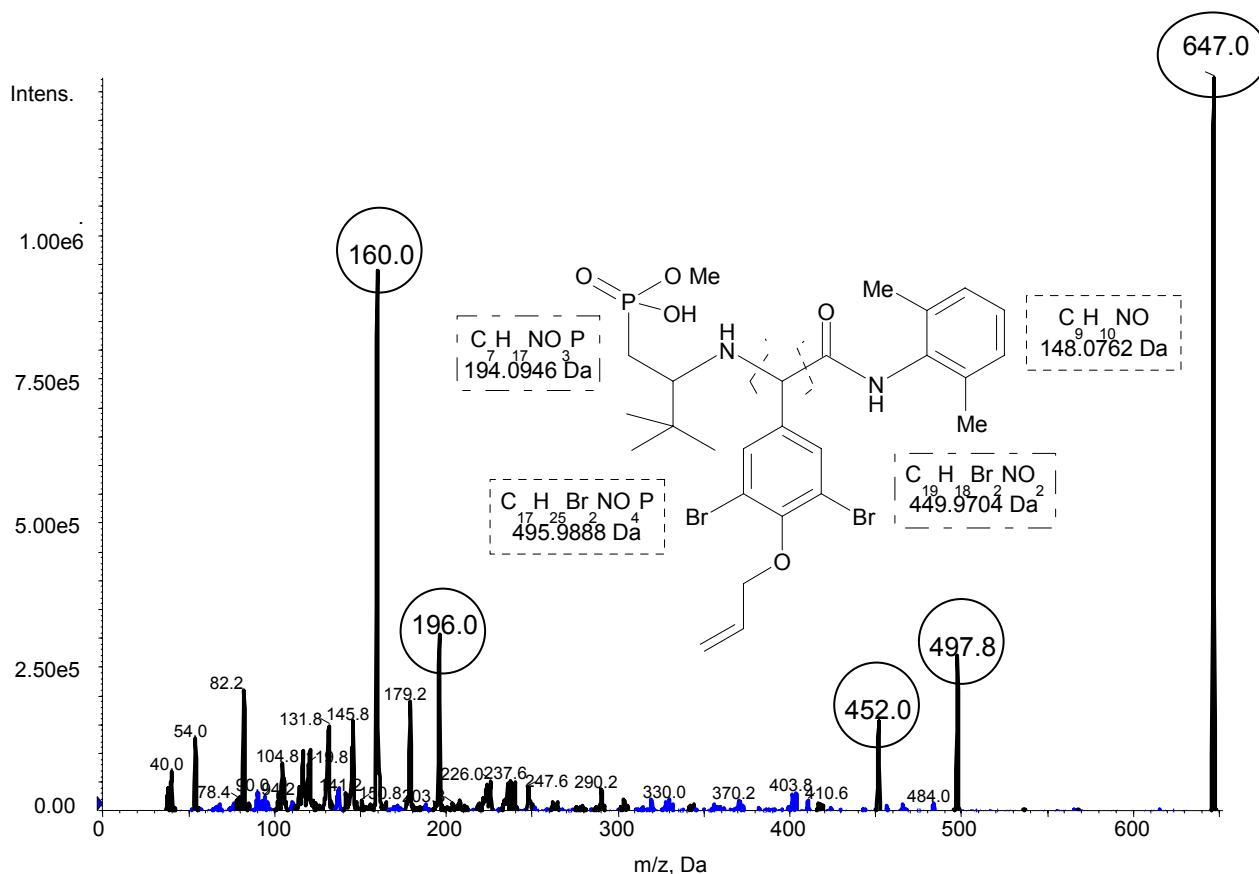


Fig. III-46: Expected bond cleavages and fragmentation spectrum of 18.

III.F. Conclusion

These preliminary experiments clearly show that the Ugi reaction is capable to provide compound libraries that may serve as source for new chiral selectors. It could be verified that this reaction yields phosphonic acid pseudopeptides (peptide mimetics) when amino phosphonic acids are employed as bifunctional amine/acid compounds in a 3-component Ugi reaction. The yields of the reaction are improvable. Excess of isocyanide should be investigated in future studies.

IV. IMMOBILIZATION CHEMISTRY

IV.A. Introduction to HPLC, CE and CEC

In the previous chapter the synthesis of a novel chiral phosphonic acid derived selector has been described. The next logical step was the immobilization of this moiety on a suitable support followed by a comprehensive study of its chromatographic and electrokinetic properties. So, first the best support had to be identified as has been mentioned in the objective.

The method employed was CEC. CEC is a hybrid technology of High Performance Liquid Chromatography, HPLC, and Capillary Electrophoresis, CE. Hence, the distinguishing principles of these two approaches shall briefly be described:

IV.A.1. High Performance Liquid Chromatography

HPLC is a separation technique in which the solutes are distributed between a liquid mobile phase and a stationary phase that is typically made of particles.

Due to molecular interactions between an analyte and moieties of the stationary phase, the former is retarded according to the strength of these forces. The type of interaction is sometimes eponymous, e.g. ion-exchange chromatography.

Chromatographic parameters

Compounds commonly elute in a Gaussian peak shape from the column:

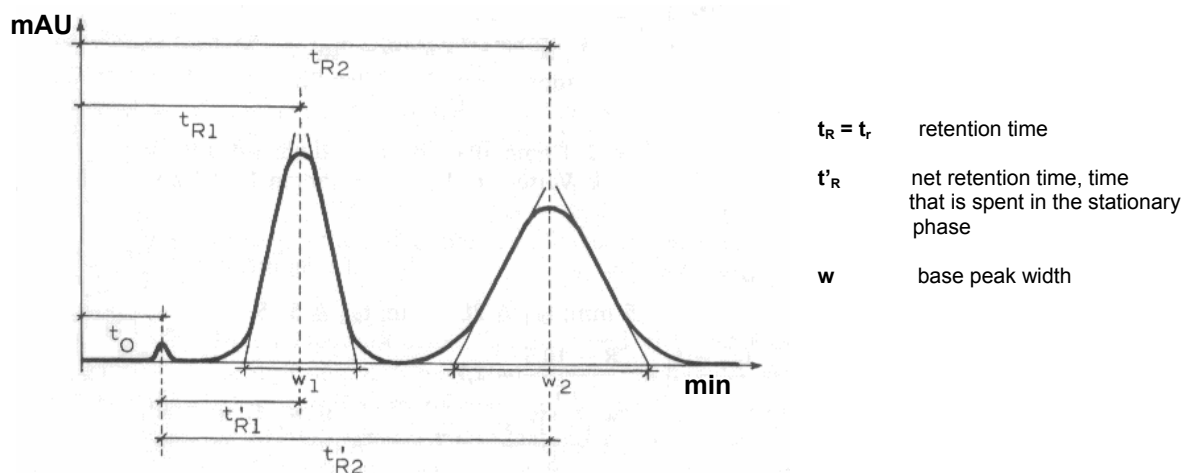


Fig. IV-1: Characteristics of a chromatogram (89)

The time when the bulk of the substance has reached the detector is referred to as retention time, t_r . From the retention time and the dead time, t_0 , which is the time that a non-retarded compound needs to pass the column, the retention factor, k_r , can be calculated:

$$k_r = \frac{t_r - t_0}{t_0} \quad (1)$$

The peak dispersion is indicated by the plate number, N :

$$N = \left(\frac{t_r}{\sigma} \right)^2 \quad (2) \quad \sigma \dots \text{standard deviation}$$

The height equivalent to a theoretical plate, *HETP*, or simply plate height, H , is defined by the column length, L , divided by the plate number:

$$H = \frac{L}{N} \quad (3)$$

In 1956 the following dependency of the plate height on the flow velocity, u , was published by J. J. van Deemter (90):

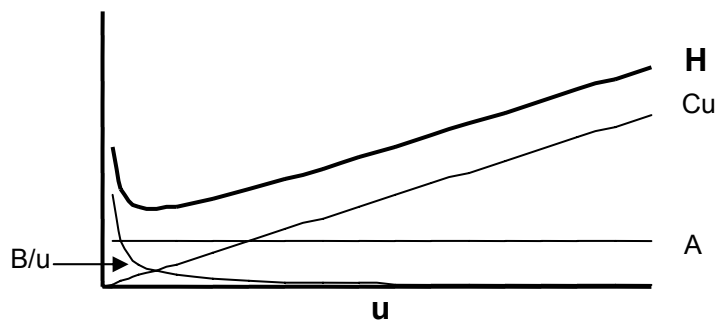


Fig. IV-2: Van Deemter plot

$$H = A + \frac{B}{u} + C \cdot u \quad (4)$$

where A is the contribution of convection emerging from irregularities of the flow velocity (eddy diffusion), B represents the diffusion of the solute in the longitudinal direction and C measures the influence of mass transfer resistance. These three terms further depend on:

$$A = 2\lambda d_p \quad (4a) \quad d_p \dots \text{particle diameter} \quad \lambda \dots \text{packing factor}$$

$$B = 2\gamma D_m \quad (4b) \quad \gamma \dots \text{factor accounting for obstruction to diffusion}$$

$D_m \dots$ diffusion coefficient in the mobile phase

$$C = \frac{k d_p^2}{D_s (1 + k)^2} \quad (4c) \quad D_s \dots \text{diffusion coefficient in the stationary phase}$$

Since the plate height is obviously significantly influenced by the particle diameter, particles of smaller and smaller sizes have been used to improve efficiency. However, this approach is restricted by an ever growing back-pressure.

The pressure-driven movement of the mobile phase through the stationary phase generally induces the characteristic parabolic profile of a laminary flow in a cylindrical tube, which itself increases the plate height, more precisely the A-term.

For a homogenously packed column the minimum plate height, H_{min} , is approximately twice the particle diameter, the latter being frequently three to five micrometers in standard HPLC.

Hence, efficiency is quite a challenge in HPLC and values only between 40 000 and 60 000 *per meter* are regularly achieved (column length: 10-30 cm; ID: 2-5 μm ; particle size: 3-10 μm) (91).

Besides, another parameter, *viz* selectivity, α , is crucial for the performance of a column:

$$\alpha = \frac{k_{n+1}}{k_n} \quad (5)$$

and must *per definitionem* be greater than 1. If it is equal to 1, there is no separation. As selectivity illustrates, the ability of a chromatographic system to separate two successively eluting compounds can conveniently be augmented by altering the chemical composition of the chemical adsorbent. Nowadays a broad variety of stationary phases have been developed and are commercially available. For this reason selectivity is a less critical point in HPLC than efficiency.

The chromatographic resolution, R , is closely related to selectivity:

$$R = \frac{t_{r(n+1)} - t_{r(n)}}{4\sigma} \quad (6a) \quad \text{or alternatively}$$

$$R = \frac{1}{4}(\alpha - 1) \left(\frac{k}{1+k} \right) \sqrt{N} \quad (6b)$$

IV.A.2. Capillary Electrophoresis

In contrast to chromatography there is no specific stationary phase in CE. The separation unit of a classic CE system consists of a plain fused silica capillary filled with background electrolyte (BGE), which is composed of a solvent or solvent mixture containing electrolytes. The movement of the BGE through the capillary is afforded by electro-osmosis. At a pH higher than the pK_a of the silanol functions of the fused silica wall the latter are deprotonated and the inner capillary wall negatively charged, respectively. Next to this surface charge layer a fixed and adjacent to it a diffuse charge layer of excess counter-ions (cations) is formed, yielding an electrical double layer (EDL). The (negative) potential at the shear boundary between fixed and diffuse layer is called ζ -potential. If voltage is applied to the capillary, the cations start migrating towards the negative pole, carrying along adjacent species and thus generating an overall movement directed towards the cathode, the electro-osmotic flow (EOF).

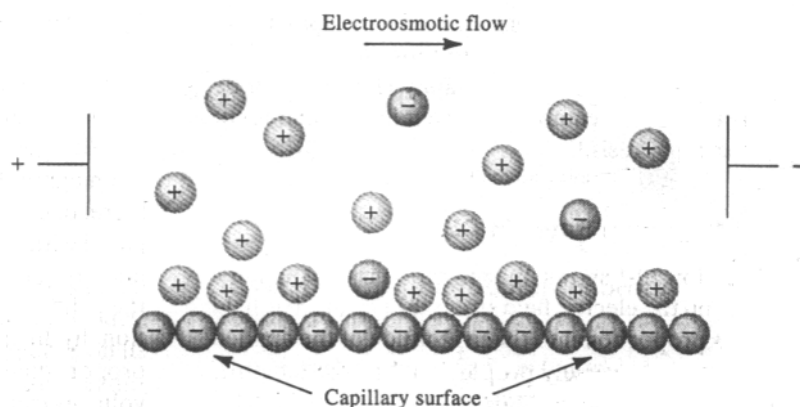


Fig. IV-3: EOF formation (92)

Likewise analytes are transported under the influence of an electric field according to their size, shape and charge. Subject to their polarity they can co-migrate with or move in the opposite direction of the EOF. Most often the impact of the EOF prevails, subsequently enabling the detection of anions in the normal (positive polarity) mode with the cathode at the capillary outlet as well.

In general, the solutes are exposed to an accelerating and a decelerating force, namely the force created by the electric field, F_E and the frictional force, F_R , for spherical species:

$$F_E = z_i e E \quad (7) \quad z_i \dots \text{charge number of the solute}$$

$e \dots$ unit charge

$E \dots$ applied field strength

$$F_R = 6\pi\eta r_i u_i \quad (8) \quad \eta \dots \text{dynamic viscosity of the solvent}$$

$r_i \dots$ hydrodynamic radius of the solute

$u_i \dots$ velocity of the solute

Since $F_E = -F_R$ holds for equilibrated conditions (the negative sign indicating the opposing effect), the velocity u_i can then be expressed as

$$u_i = \frac{z_i e E}{6\pi\eta r_i} \quad (9)$$

A commonly employed parameter independent of the applied field strength is the electrophoretic mobility, μ_i :

$$\mu_i = \frac{u_i}{E} = \frac{z_i e}{6\pi\eta r_i} \quad (10)$$

It is essential to realize the impact of the degree of dissociation, α , which is logically especially significant for weak electrolytes. Therefore the effective mobility, μ_{eff} , is presented as

$$\mu_{eff} = \alpha \cdot \mu_i \quad (11)$$

M. von Smoluchowski was the first to derive an equation linking the mobility of the EOF to the ζ -potential: (93)

$$\mu_{eo} = \frac{\varepsilon_r \varepsilon_0 \zeta}{\eta} \quad (12) \quad \varepsilon_r \dots \text{reduced permittivity}$$

$\varepsilon_0 \dots$ vacuum permittivity

Additionally the ζ -potential is depicted by

$$\zeta = \frac{\sigma_0}{\kappa \varepsilon_0 \varepsilon_r} \quad (13) \quad \sigma_0 \dots \text{surface charge}$$

$\kappa \dots$ Debye-Hückel parameter

The Debye-Hückel parameter is the reciprocal thickness of the EDL, δ (the distance at which the potential has dropped to 1/e of its value at the surface), and further

$$\kappa = \frac{1}{\delta} = \sqrt{\frac{2F^2 I}{RT \varepsilon_0 \varepsilon_r}} \quad (14) \quad F \dots \text{Faraday constant}$$

$R \dots$ gas constant

$T \dots$ temperature

$I \dots$ ionic strength

$$I = \frac{1}{2} \sum c_i z_i^2 \quad (15) \quad c_i \dots \text{concentration of the solute}$$

From these equations a few decisive conclusions can be drawn. The mobility of the EOF is directly proportional to the value of the ζ -potential, which in turn depends on the thickness of the electric double layer. As can be derived from Eq. (14), the latter is inversely proportional to the square root of the ionic strength. Thus, the electrolyte concentration of the BGE represents the most important tool, besides the pH, to adjust the strength of the EOF. Furthermore, the electro-osmotic flow mobility linearly depends on the surface charge which will play a momentous role in CEC.

The lack of a stationary phase exhibits several benefits compared to HPLC, especially in terms of efficiency. Since there are no particles, Eddy diffusion contributions practically disappear as well as mass transfer resistance. Moreover, the electrokinetically generated EOF exhibits a plug-like profile, causing a minimized zone dispersion.

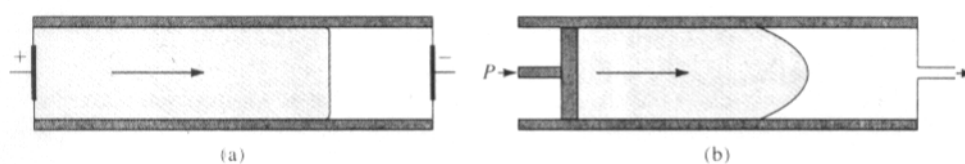


Fig. IV-4: Plug-like mobile phase front in CE (a) and laminary flow profile in HPLC (b) (92)

Hence, the van Deemter equation can virtually be reduced to

$$H = Bu. \quad (16)$$

This combined with the facts that due to the absence of pressure, longer capillaries can be utilized and voltages up to 30 kV can be applied with usual CE equipment, leads to excellent plate numbers in the magnitude of a million (94).

On the other hand side a plain fused silica capillary reveals a tremendous lack of selectivity as no other moieties for interaction on a molecular level than the negatively charged silanols can be provided. The classic way to circumvent this drawback, e.g. if chiral solutes shall be separated, is the usage of additives with the ability to form diastereomeric complexes like cyclodextrines (13-15). Yet the inclusion of auxiliaries might be unfavourable, for example if the pure solute is to be further processed after the separation or in case of hyphenation to MS.

IV.A.3. Capillary Electrochromatography

As the name indicates, thin capillaries with a diameter of approximately 10 to 100 μm are employed in CEC (95). This miniaturization maintains several conveniences like the reduced need for solvents and the possibility to analyze limited sample amounts.

Furthermore, CEC aims at combining the advantages of both, HPLC and CE, *viz* selectivity and efficiency. As in chromatography, the stationary phase consists of a material providing sites for molecular interactions like, most important for this diploma thesis, chiral recognition. The main difference to liquid chromatography is that the flow of the solvent is achieved by electro-osmosis. Hence, the flow profile is plug-like as in CE, resulting in a declined zone dispersion and flatter H/u curves. Additionally, there are no back-pressure limitations. However, electro-osmosis requires the adoption of an ionizable support. CEC measurements can therefore be performed with HPCE equipment where a capillary packed with a stationary phase is used instead of a plain fused silica capillary (Fig. IV-5).

The stationary phase fulfills a double function: It has to provide molecular interaction sites guaranteeing sufficient selectivity and secondly, it reveals chargeable entities for the generation of the electro-osmotic flow. Accordingly, the EOF is pH-dependent, concerning its strength as well as its direction. If the pH is above the pK_a of the acidic ligand, the surface will be negatively charged and the EOF directed towards the cathode. Still, in opposition to common CE, anodic EOF can be afforded as well if the pH is lower than the pK_a of a basic ionizable moiety and the latter henceforth protonated. For zwitter-ionic surfaces EOF changes from anodic to cathodic at the pI .

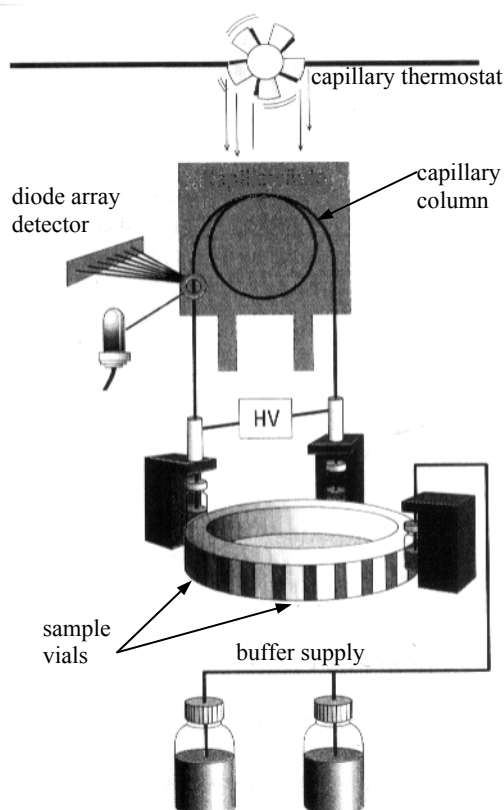


Fig. IV-5: CE(C) equipment (96)

The velocity, u_{CEC} , of a charged compound in such a system is expressed by

$$u_{CEC} = \frac{u_{eo} + u_{ep}}{1 + k} \quad (16)$$

and the mobility consequently by

$$\mu_{CEC} = \frac{\mu_{eo} + \mu_{ep}}{1 + k} \quad (17)$$

As for CE, the degree of dissociation has to be considered and the von Smoluchowski equation (Eq. 12) can be applied to depict the dependency of the EOF on the reduced permittivity, the dynamic viscosity of the solvent and the ζ -potential. Still, deviations from Eq. (12) may arise as in CEC the voltage does not drop linearly due to the different conductivities in the packed and the open segment.

Practically, electrophoretic mobilities can be calculated from experimental data by the following relations:

$$\mu_{eo} = \frac{L_{eff} L_{tot}}{t_0 V} \quad (18)$$

L_{eff} ... effective capillary length, viz the length of the packed segment

L_{tot} ... total length of the capillary

t_0 ... time that a non-retarded neutral solute needs to pass the column

V ... applied voltage

$$\mu_{CEC} = \frac{L_{eff} L_{tot}}{t_r V} \quad (19) \quad t_r \dots \text{retention time of a charged solute}$$

As in CE, solutes in CEC can migrate faster than non-retarded molecules and therefore elute before t_0 . Consequently, if the chromatographic selectivity definition (Eq. 5) is employed, negative selectivity values might be brought about. Thus, another approach to determine α is chosen:

$$\alpha = \frac{\mu_n}{\mu_{n+1}} \quad (20)$$

If the flow was solely generated by pressure, the electrophoretic impact would be lost and the resulting technology would be capillary liquid chromatography, CLC.

However, the term “CEC” does not totally exclude the usage of pressure. In case of a weak EOF additional pressure-assistance may lead to a more robust system. This method is referred to as pressure-assisted CEC, pCEC.

Hence, Eqs. (16) and (17) have to be complemented to

$$u_{CEC} = \frac{u_{eo} + u_{ep} + u_{press}}{1 + k} \quad (21) \quad \text{and} \quad \mu_{CEC} = \frac{\mu_{eo} + \mu_{ep} + \mu_{press}}{1 + k} \quad (22)$$

$$\text{with } u_{press} = -\frac{k\Delta P}{\eta L} \quad (23) \quad u_{press} \dots \text{pressure-related linear flow velocity}$$

according to Darcy's Law.

ΔP ... applied pressure drop

k ... permeability of the porous bed

Still, an amplified EOF, sparing additional pressure, is desirable as in pCEC the flat flow profile is lost and thus efficiency is decreased. Yet, selectivity is though better than in CLC.

Besides, a strong EOF is beneficial to gain a stable system and reproducible results. Therefore the ratio permittivity/dynamic viscosity of the mobile phase should typically be high. Mixtures of ACN/MeOH have accomplished this demand well (97, 98). Compared to solvents containing water, polar organic mixtures are favourable as less Joule heating appears and thus higher voltages, still resulting in satisfactorily low currents (below 15 μA), can be applied. Additionally, hydrophilic (and electrostatic, respectively) interactions are weakened in aqueous liquids. From that point of view the employment of normal-phase mobile phases seems preferable. Nonetheless such lipophilic media are not eligible for dissolving the required electrolytes and furthermore exhibit a low permittivity, yielding an unstable EOF. Consequently, polar organic solvents seem to be the ideal solution.

IV.B. Monolithic capillary columns as chromatographic support

So far little attention has been paid to the chemical support, a powerful tool to alter the chromatographic performance. Generally, three different types, namely open-tubular capillary columns, particle-packed capillary columns and monolithic capillary columns can be employed. The present work will focus on the latter.

The word “monolith” is derived from the Greek language. The literal translation is “single stone”. The first separation material labelled “monolith” was a single piece of functionalized cellulose sponge in 1993 (99).

The evolution of new materials was driven by the discontentedness with the limitations of common bead based media, e.g. slow mass transfer resulting in low efficiencies. In principle, a typical monolith consists of a single piece of porous material, providing macropores in the low micrometer range (2-8 μm) for the mass transfer of the mobile phase and mesopores (2-50 nm), yielding a large surface area for chiral recognition, or, more generally, molecular interaction. Nowadays monoliths can be classified into three different types by their composition and their preparation, respectively. These are OPMs, inorganic silica-based monoliths and hybrid monoliths. A comparative review of the former two is presented below.

IV.B.1. Organic polymer monoliths

In the 1990ies pioneering work was carried out by Svec, Frechet and co-workers in the field of preparing OPMs (100-102).

Basically a monomer, occasionally also a comonomer, a crosslinker and an initiator are allowed to react in a porogen (mixture) in an unstirred mold. The initiation is triggered according to the properties of the starter thermally or by UV radiation. The radicals formed build polymer chains including the crosslinker and finally yield a macroporous polymer after the solvent has been washed out. The chromatographic performance of the resulting monolith depends largely on the pore structure which can be controlled by variation of temperature, porogen composition and crosslinker. Polystyrenes, polyacrylamides and poly(meth)acrylates are commonly employed. However, the first are avoided in enantiomer separation, due to their intrinsic susceptibility to non-specific aromatic interactions.

The polymerization starts from solution and the porogens completely fill the porous space at the end of the polymerization. Since the usage of CEC demands the creation of an electro-osmotic flow, an ionizable function must be introduced at the surface. This can be achieved by two different methodologies:

Copolymerization of a functional monomer

In this case the favoured selector for the molecular interaction is directly applied as a comonomer, provided the availability of polymerizable functions. This approach is highly flexible as the properties of the resulting monolith, *viz* porosity and surface structure, can be tailored according to the analytical task. However, the tradeoff for variability is plenty of time that is consumed for optimizing conditions when employing a new functional monomer. Hence, another way of surface modification was chosen in the course of the present work.

Postmodification

If a reactive moiety is introduced into the polymer backbone, the surface chemistry can be varied after the polymerization step. E.g. a hydrophilic surface can be generated on a hydrophobic support *via* linkage of polar molecules. Likewise thiol functions can be derived from epoxy groups and further be subjected to radical addition of a chiral selector. The pivotal benefit of the postmodification approach is that the polymer backbone has to be optimized only once. As a consequence, fewer chiral selector is needed, because tedious experiments modelling the support are omitted. The capital drawback on the other hand is a lower selector surface density, resulting in a declined EOF.

IV.B.2. Inorganic silica-based monoliths vs OPMs

Silica monoliths are generally produced in a sol-gel process from silica alkoxy precursors (103). The monoliths employed herein were additionally epoxy-modified.

In contrast to OPMs, where solely the average pore size can be controlled, the well explored preparation process of silica materials allows an exact tailoring of the desirable bimodal pore structure. In opposition to microglobular OPMs, silica-based monoliths typically exhibit a sponge-like morphology. As has been mentioned above, macropores are favourable to guarantee a flow through mode and thus enable the convective bulk flow of the mobile phase, whereas numerous mesopores provide a large active surface area for high adsorption capacity and, consequently, selective interaction.

The comparatively narrow pore size distribution is an outstanding benefit of silica-based monoliths. Preinerstorfer et al determined macropores of about 2 μm and mesopores of approximately 16 nm, whereas the average diameter of a macroporous polymer monolith was 1.1 μm (95). Commonly OPMs are more densely packed than their inorganic counterparts, which have a total porosity of about 90 %. Besides, the thin silica skeleton brings about shorter diffusion distances leading to an elevated mass transfer and therefore transforms into better efficiencies.

With regard to selectivity, non-specific hydrophobic interactions of the polymer backbone constitute a serious impediment. This can be alleviated by copolymerization of more hydrophilic monomers. (104). Otherwise silica-based monoliths are definitely superior in terms of selectivity.

Another benefit of silica monoliths emerges from the mechanical stability of the inorganic material, which makes them suitable for CLC applications as well. Furthermore, they are not subjected to shrinkage and swelling upon changes of mobile phase during their use like polymers.

The capital drawback of silica-based monoliths is their multi-step laborious preparation procedure limiting their availability. For the realization of this work four epoxy-modified silica monoliths of 60 cm each were provided by Merck.

IV. C. Preparation of functionalized monoliths

IV.C.1. Preparation of GMA-co-EDMA monoliths (17)

IV.C.1.1. Vinylization of the plain fused silica material

A fused silica capillary of 350 cm length and an inner diameter of 100 μm was vinylized prior to the polymerization step. A Hamilton syringe was employed for rinsing with 1 M NaOH (30 min.) , followed by 0.1 M HCl (30 min.), water (15 min.), HPLC grade Acetone (15 min.) and, finally, a 1:1 mixture of Acetone and 3-methacryloxypropyltrimethoxysilane (30 min.), the vinylization reagent. The universal flow rate was 300 $\mu\text{L/h}$. A tiny piece of teflon was wrapped around the capillary to grant the absence of leaks. Afterwards the ends of the capillary were sealed with GC septa and the reaction was allowed to proceed for 12 to 24 hours at RT.

IV.C.1.2. Preparation of GMA-co-EDMA OPMs

Next the capillary was flushed with Acetone for about 20 minutes (Flow rate: 300 $\mu\text{L/h}$) and divided into ten capillaries of approximately 35 cm each, which were put into an oven of 60 $^{\circ}\text{C}$ over night or longer.

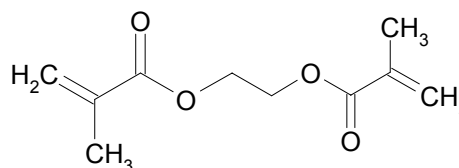
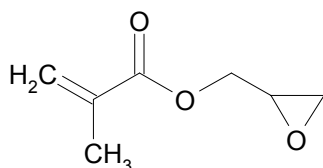
For the polymerization step a mixture of monomers and porogens was prepared (% in w/w):

30 % Dodecanol

30 % Cyclohexanol

24 % Glycidylmethacrylate

16 % Ethylenedimethacrylate



Hence, the monomer was GMA, accompanied by the comonomer EDMA. The porogen solvent consisted of dodecanol and cyclohexanol. AIBN (1 % (w/w), with regard to total monomer content) was added as initiation component. The final solution was sonicated for about 10 minutes and subsequently purged a few minutes with nitrogen to get rid of oxygen which would have disturbed the polymerization process. The capillaries were filled with the polymerization mixture to a length of roughly 26 cm with a Hamilton syringe.

It is noteworthy that AIBN is UV-sensitive. As a consequence, it is essential not to expose the final mixture to sunlight, otherwise the reaction is triggered off and a new solution has to be prepared.

The filled capillaries were enclosed with GC septa and put into a water bath of 60 °C for 20 h. Subsequently they were washed for several hours (ideally over night) with ACN. For rinsing, an HPLC pump at the minimum flow of 10 µL/min and a manifold were used, enabling the flushing of six capillaries simultaneously. In an ACN-filled state the OPMs can be stored, either by using a septum to seal them or putting two HPLC vials of ACN at their ends.

IV.C.1.3. Thiolization of the monolithic surface:

Prior to the immobilization step a moiety utilizable for a radical SO immobilization had to be introduced. Hence, the revealed epoxy groups at the surface were transformed into thiols by an S_N2 mechanism:

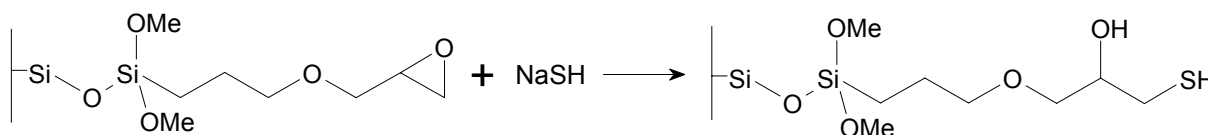


Fig. IV-6: Generation of reactive thiol groups on monolithic surface

For the following practical steps either a syringe pump with a Hamilton syringe (30 µL/h) or an HPLC pump (10 µL/min) and a manifold were used. In case of the latter up to six capillaries could be modified simultaneously. As a matter of convenience, the current working procedure henceforth describes the preparation of one capillary.

First, the monolith was preequilibrated in MeOH/H₂O (20/80; v/v). A 2 M solution of NaSH in MeOH/0.1 M aqueous NaH₂PO₄ (20/80; v/v) was freshly prepared and the pH adjusted to 8.15 with H₃PO₄. The capillary was flushed with a mixture of this solution for two hours. It was consecutively washed with MeOH/H₂O (20/80; v/v). In the meantime a 0.5 M solution of Tris-(2-carboxyethylphosphine)-hydrochloride (TCEP) in 0.4 M aqueous NaH₂PO₄ was produced. TCEP was intended to reduce potential disulfide bondings to thiols. The monolith was rinsed with MeOH/TCEP-solution (20/80; v/v) for one hour. Afterwards it was washed with MeOH/H₂O (20/80; v/v) and stored in ACN.

IV.C.1.4. Selector immobilization

100 mg (~ 0.24 mmol) of *t*-BuCQD were dissolved in 100 μ L MeOH and 10 % AIBN of the molecular SO concentration were added. This solution was sonicated and purged with nitrogen for a few minutes. For filling the capillary with the SO mixture either a Hamilton syringe and pump (flow rate: 30 μ L/h) or an HPLC pump (flow rate: 10 μ L/min) and a manifold attached to two or more capillaries were employed. After one hour of flushing the capillary was waterproofed with GC septa and put into a bath of 60 °C for 24 h. Afterwards the remaining components were washed out with MeOH utilizing an HPLC pump and the capillary eventually stored in ACN.

IV.C.2. Selector linkage to an epoxy-modified silica monolith

Since the preparation procedure described above has exclusively been evaluated for OPMs, it was of particular interest if it could be adapted for silica monoliths as well. As the monolith had already been epoxy-modified only thiolization and immobilization steps had to be done. These were performed in exactly the same way as described for the OPMs in IV.C.1.3 and IV.C.1.4.

IV.C.3. Monolith data for OPMs and silica monolith

After preparation/modification steps the monoliths were shortened to the following lengths:

Effective length:	25 cm
Total length:	33.5 cm
Inner diameter:	100 μ m

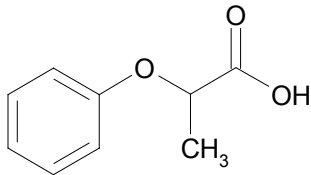
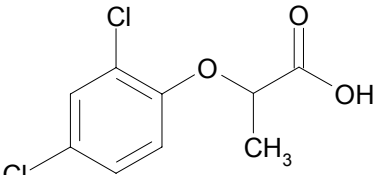
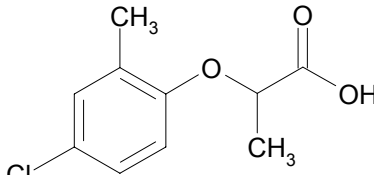
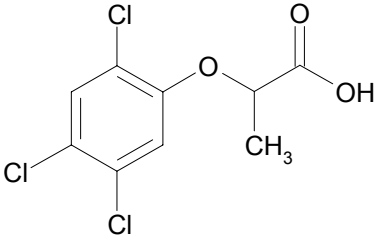
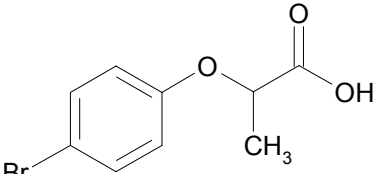
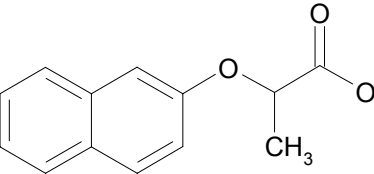
IV.D. Comparison of the silica-based and organic polymer monolith

IV.D.1. Expectations

t-BuCQD was attached to a thiol-modified epoxy silica monolith. This study served as preliminary experiments to develop and optimize the immobilization chemistry prior to usage of **1**. Additionally, *t*-BuCQD was linked to an organic polymer monolith to identify the more suitable support. Subsequently the impact of various parameters was explored for both monoliths and compared to each other. Aryloxy carboxylic acid herbicides (Table IV-1) and two amino acids were employed as test substances.

The employed selector (Fig. I-2) exhibits several moieties suitable for molecular interaction. First of all, since an EOF has to be generated, a potentially charged unit must be provided. The quinuclidine tertiary amine function has a pK_a of 8.9*. So, in neutral and acidic media an anodic EOF is expected. Residual silanols have to be considered in case of the silica monolith. Therefore, the overall CSP is supposed to be zwitter-ionic. The quinoline group is an amine as well, however it is far less basic due to its aromatic properties. It represents a π/π interaction site. Hydrophilic interactions, hydrogen bondings more precisely, are afforded by the carbamate moiety and bulky groups like the *tert*-butyl residue enable steric interactions.

Table IV-1: Propionic acid derived herbicides

 <p>2-Phenoxypropionic acid PP</p>	 <p>2-(2,4-Dichloro-phenoxy) propionic acid, DCPP</p>	 <p>2-(4-Chloro-2-methyl-phenoxy) propionic acid, MCP</p>
 <p>2-(2,4,5-Trichloro-phenoxy) propionic acid, TCPP</p>	 <p>2-(4-Bromo-phenoxy) propionic acid, BPP</p>	 <p>2-(2-Naphthoxy) propionic acid, NOP</p>

Note: The wavelength for all chromatograms depicted in chapter IV was 230 nm.

* all pK_a values calculated with ACD/Labs Software

IV.D.2. Evaluation of the total electrolyte concentration

The impact of the ionic strength of the BGE was studied. Acidic conditions were utilized to ensure the predomination of a positive surface charge for both monoliths. Since distinct solutes and conditions were employed (Analytes: DCPP in case of the silica capillary and DNB-Leu for the OPM), only qualitative reckoning comes into question.

Results and Discussion

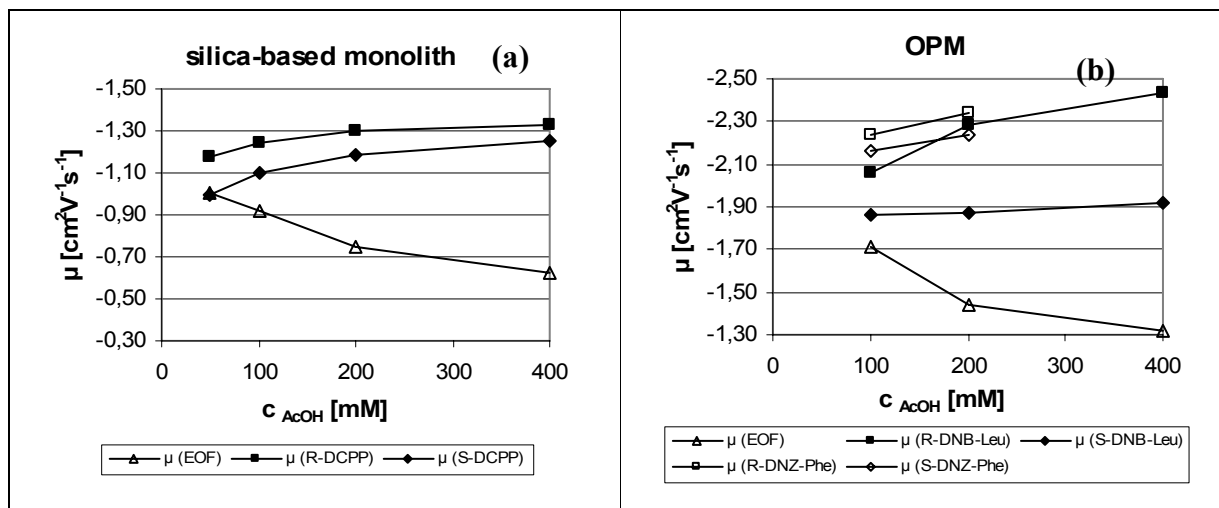


Fig. IV-7: Impact of total electrolyte concentration on mobilities on silica and organic polymer support. (a) Sample conc.: 2 mg/ml. Mobile phase: MeOH/ACN (20/80; v/v). Voltage: -13 kV. Inj. time: 5 sec. Temp.: 25°C. EOF-marker: Acetone. (b) Sample conc.: 1 mg/ml. Mobile phase: MeOH/ACN (20/80; v/v). Voltage: -10 kV. Inj. time: 10 sec. Temp.: 30 °C. EOF-marker: Acetone.

An elevated BGE concentration yields a reduced EOF in agreement with von Smoluchowski (Eq. 12). On the contrary, enantiomer mobilities are amplified when more counterions are present, as the latter shield selector adsorption sites. Congruently with former studies (105-107), a higher electrolyte composition amplifies efficiencies, also indicating that the ion exchange mechanism is operative. The higher number of counter-ions accelerates mass transfer and consequently ameliorates plate heights and peak shapes.

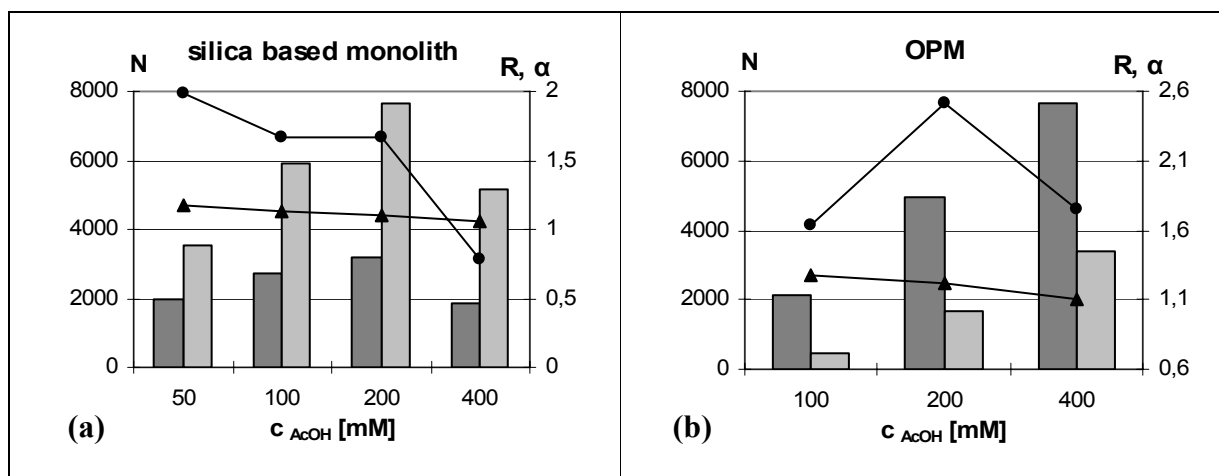


Fig. IV-8: Impact of total electrolyte concentration on plate numbers, resolution (●) and selectivity (▲) on silica and organic polymer support. Details as specified under Fig. IV-7.

The plate number drop in Fig. IV-8 (a) at 400 mM AcOH emanates from an overlap of the enantiomer peaks. Thus plate numbers cannot be identified correctly. As concerns the silica-based monolith, resolution is enhanced steadily towards the lowest AcOH-concentration. This is caused by a simultaneous increase of selectivity and the retention term of Eq. (6b), as can be derived from Fig. IV-9 (a). Although selectivity exhibits the same behaviour in the graph of the OPM, the resolution curve looks distinct. The sharp drop from 200 to 100 mM might emerge from the declined plate number supported by a rather flat ascent of retention factors.

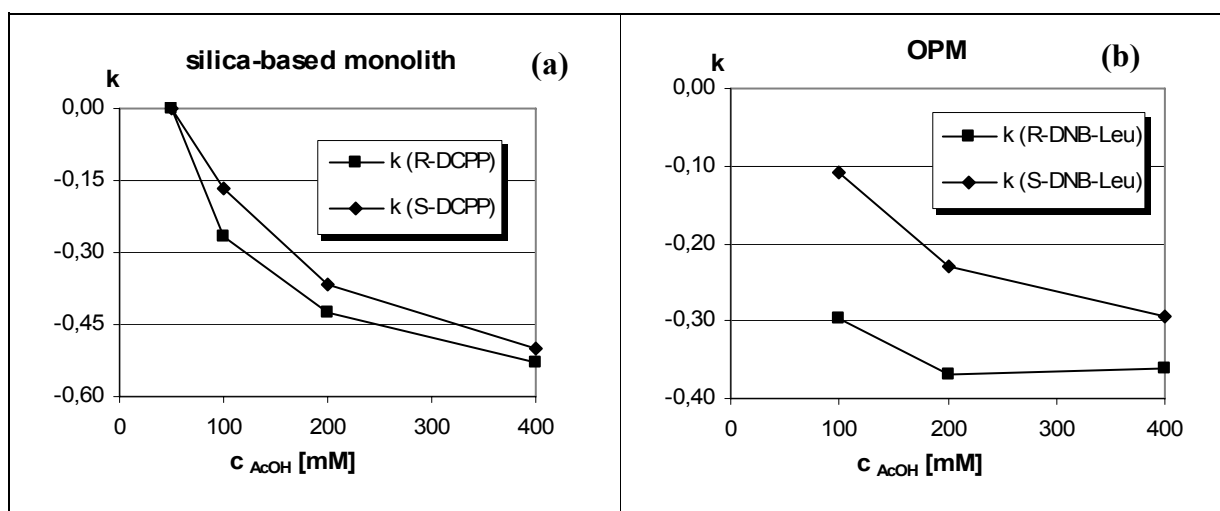


Fig. IV-9: Impact of total electrolyte concentration on retention factors on silica and organic polymer support. (a) Sample conc.: 2 mg/ml. Mobile phase: MeOH/ACN (20/80; v/v). Voltage: -13 kV. Inj. time: 5 sec. Temp.: 25°C. EOF-marker: Acetone. (b) Sample conc.: 1 mg/ml. Mobile phase: MeOH/ACN (20/80; v/v). Voltage: -10 kV. Inj. time: 10 sec. Temp.: 30 °C. EOF-marker: Acetone.

Quite interesting, the silica-based monolith exhibits higher efficiencies for the more strongly retarded enantiomer (Fig. IV-10), whereas the OPM reveals the opposite effect (Fig. IV-11). However, this could be analyte-specific, because test runs with amino acids on the silica monolith also confirmed a tendency of focussing the first eluting enantiomer (data not shown).

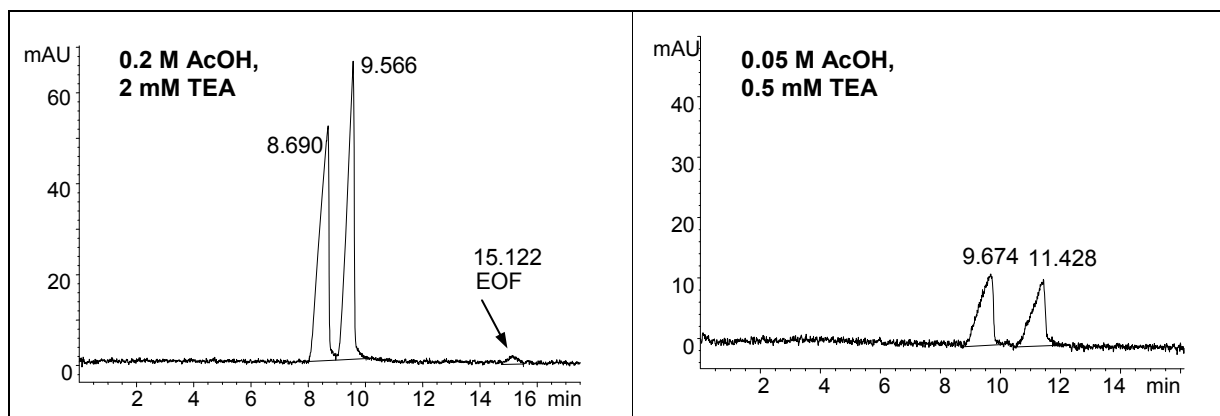


Fig. IV-10: Separation of DCPD enantiomers on silica support. Sample concentration: 1.8 mg/ml. Mobile Phase: MeOH/ACN (20/80; v/v). Voltage: -13 kV. Injection time: 5 sec. Temp.: 25°C. EOF marker: Acetone.

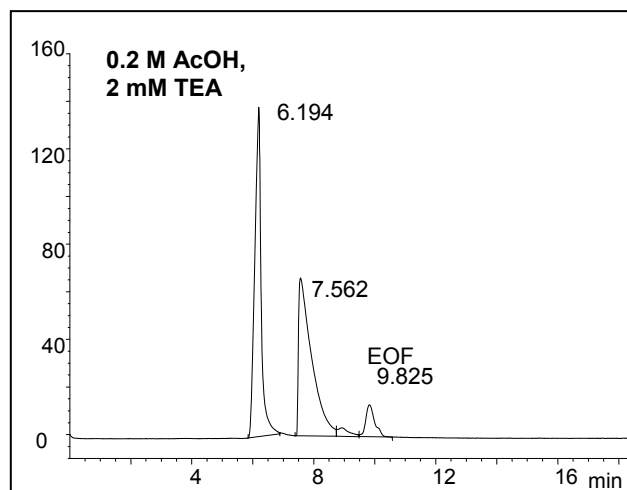


Fig. IV-11: Separation of DNB-Leu enantiomers on OPM: Sample conc.: 1 mg/ml. Mobile phase: MeOH/ACN (20/80; v/v). Voltage: -10 kV. Inj. time: 10 sec. Temp.: 30 °C. EOF-marker: Acetone.

IV.D.3. Organic Modifier

The influence of the solvent composition has been examined as well. Various MeOH percentages have been tested. The most promising parameter to predict EOF mobility is the ϵ/η ratio, which is highest in ACN-rich solvents.

Results and Discussion

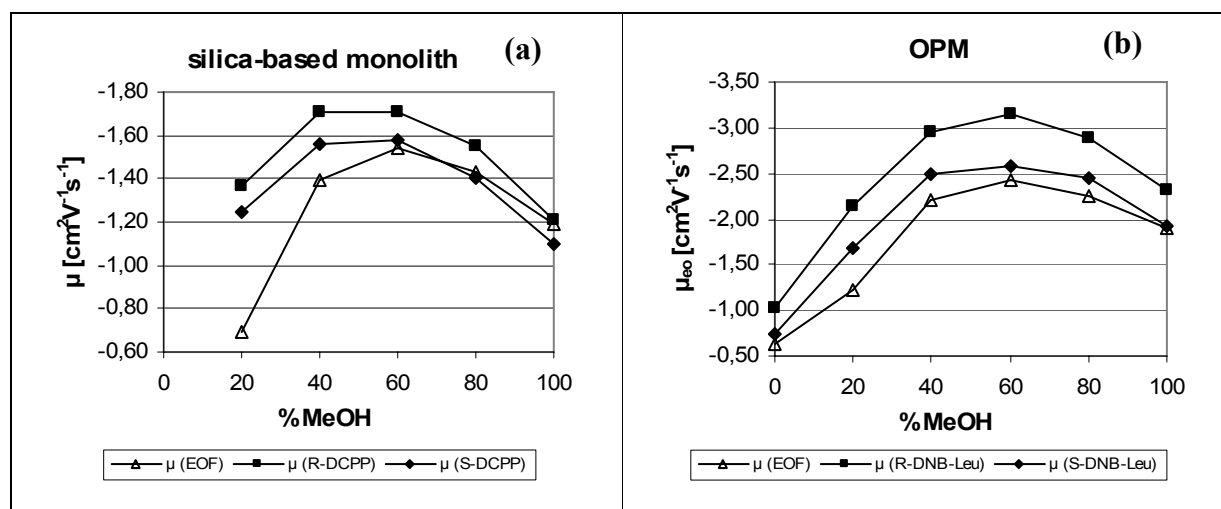


Fig. V-12: Impact of organic modifier concentration on mobilities. (a) Sample conc.: 2 mg/ml. Mobile phase: 0.2 M AcOH/2 mM TEA. Voltage: -10 kV. Inj. time: 7.5 sec. Temp.: 25°C. EOF-marker: Acetone. (b) Sample conc.: 1 mg/ml. Mobile phase: 0.2 M AcOH/2 mM TEA. Voltage: -10 kV. Inj. time: 10 sec. Temp.: 30 °C. EOF-marker: Acetone.

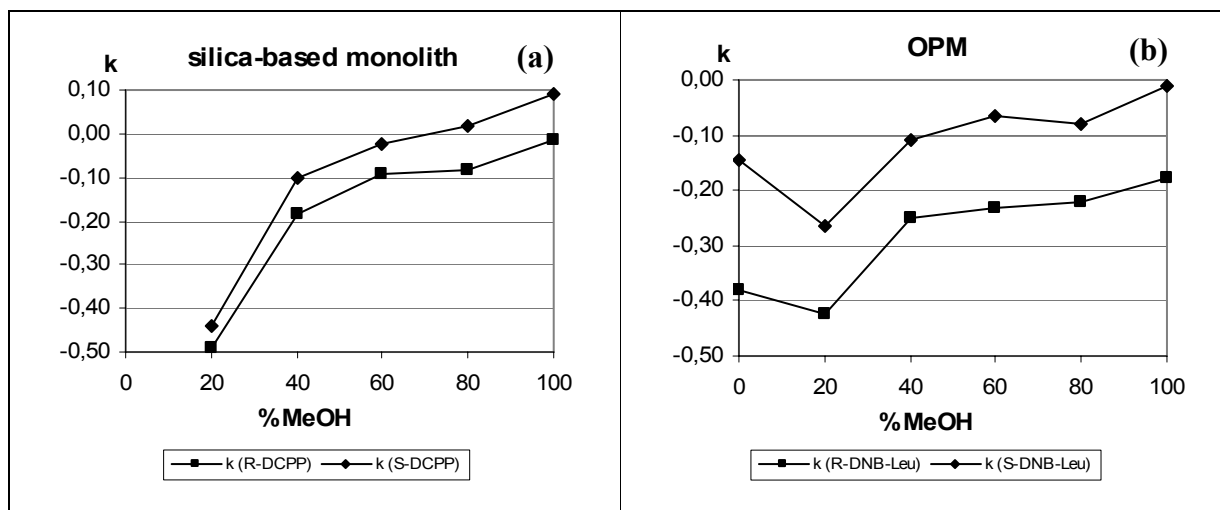


Fig. V-13: Impact of organic modifier concentration on retention factors. (a) Sample conc.: 2 mg/ml. Mobile phase: 0.2 M AcOH/2 mM TEA. Voltage: -10 kV. Inj. time: 7.5 sec. Temp.: 25°C. EOF-marker: Acetone (b) Sample conc.: 1 mg/ml. Mobile phase: 0.2 M AcOH/2 mM TEA. Voltage: -10 kV. Inj. time: 10 sec. Temp.: 30 °C. EOF-marker: Acetone.

Similar to the results obtained below (chapter V.B.6.), μ_{eo} is maximized at 60 % MeOH. This behaviour has been observed for different support materials by now (silica monolith and OPM herein, silica particle column (107)). The deviation from ϵ/η -maxima is likely to emanate from the hardly predictable influence of pH shifts in polar organic media on BGE and selector dissociation. Besides, solvent polarity affects the electric-double layer and consequently μ_{eo} . In line with results obtained earlier (chapter V.B.6, (107)), the electro-osmotic mobility definitely superimposes other contributions to μ_{CEC} in the figures depicted above. Hence, the fortification of hydrophilic interactions between selector and solute, counter-ion and selector or co-ion and solute in less polar mixtures is not decisive for the course of the mobility curves. Fig. IV-14 comprises the best separations. Surprisingly and contrary to former experiments (107), pure MeOH did not result in dramatically impaired peak shapes.

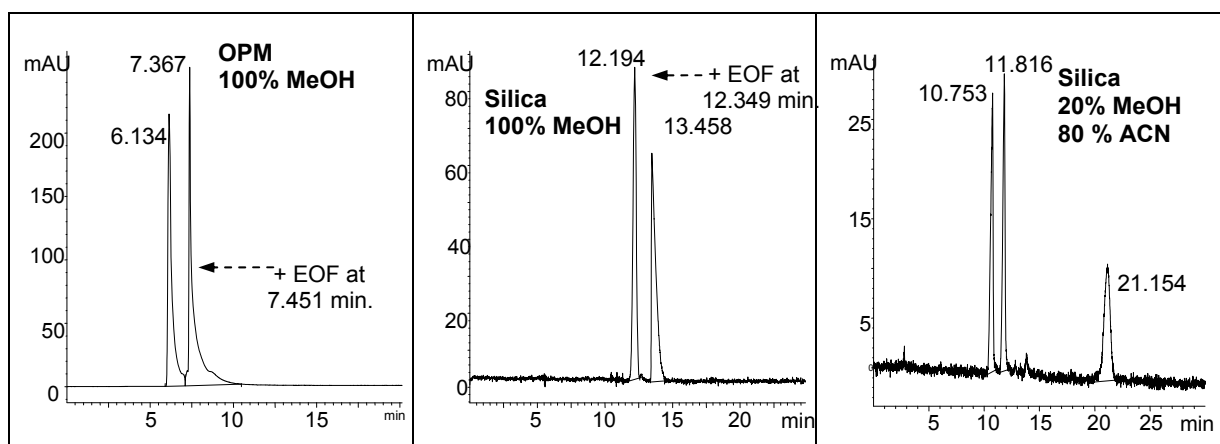


Fig. IV-14: Enantiomer separations of DNB-Leu (on OPM; sample concentration: 1 mg/ml. Mobile phase: 0.2 M AcOH/2 mM TEA. Voltage: -10 kV. Inj. time: 10 sec. Temp.: 30°C. --- EOF marker: Acetone) and DCP (on silica support; sample concentration: 1.8 mg/ml. Mobile phase: 0.2 M AcOH/2 mM TEA. Voltage: -10 kV. Inj. time: 10 sec. Temp.: 25 °C. --- EOF marker: Acetone).

IV.E. Conclusion and evaluation of the silica monolith

As the silica monolith performed generally better concerning selectivity as well as efficiency, it was concluded that **1** was to be immobilized on a silica support (chapter V). Besides, further tests with focus on enantiomer separation of aryloxy carboxylic acid herbicides were run. At the beginning injection conditions were optimized.

IV.E.1. Overloading of the silica-monolith

In the early stages of testing the silica-based *t*-BuCQD monolith the sample concentration and injection time were optimized. A solute concentration of 1.8 mg/ml injected for 10 seconds at -13 kV turned out to exceed favourable conditions. Therefore, two approaches were tested to ameliorate chromatographic performance. First, the injection time was halved twice while the sample composition was kept constant. Secondly, the solute concentration was decreased, but sample injection was always carried out for 10 seconds. The results were more or less the same, each approach yielding significantly enhanced performance.

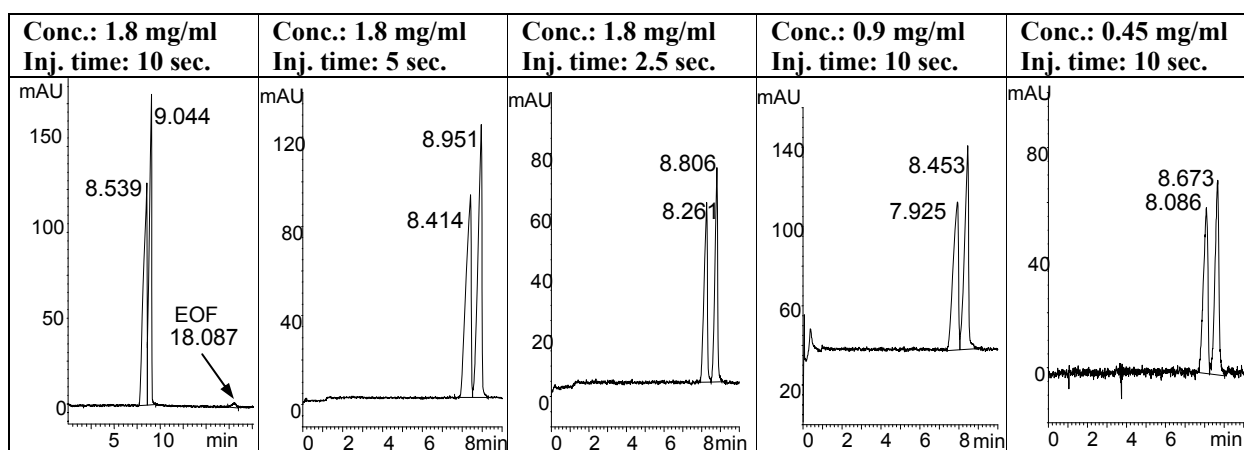


Fig. IV-15: Overloading of a *t*-BuCQD silica monolith with DCPP. Mobile phase: MeOH/ACN (20/80; v/v) + 0.4 M AcOH + 4 mM TEA. Voltage: -13 kV. Temp.: 25°C. EOF-marker: Acetone.

Henceforth samples were prepared of approximately 2 mg of analyte and injected for 5 seconds.

IV.E.2. Separation of aryloxy carboxylic acids

The first electrolyte concentration employed was that which had revealed the best efficiency for DCP, providing sufficient selectivity at the same time: 0.2 M AcOH and 2 mM TEA. The solvent composition was MeOH/ACN (20/80; v/v).

TCPP enantiomers were satisfactorily separated whereas MCPP and PP were not.

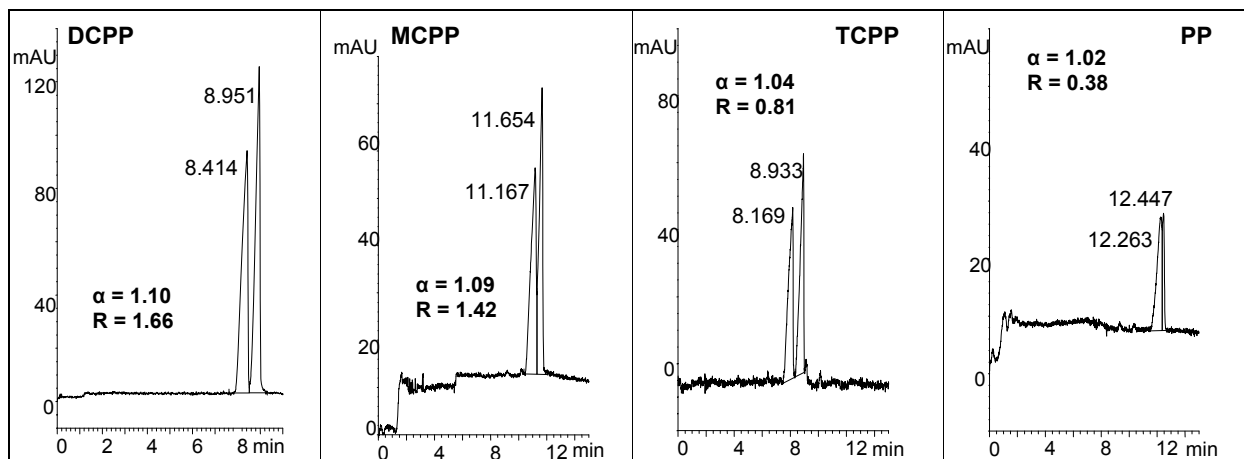


Fig. IV-16: CEC enantiomer separations of aryloxy carboxylic acid herbicides: Sample conc.: 2 mg/ml. Mobile phase: MeOH/ACN (20/80; v/v) + 0.2 M AcOH + 2 mM TEA. Voltage: -13 kV. Inj. time: 2 sec. Temp.: 25°C.

So, the total electrolyte concentration as well as acid/base ratio and solvent composition were modified and tested with mecoprop as these enantiomers exhibited better chances to be separated than those of phenoxy propionic acid. The following table depicts tested conditions and resulting selectivities and resolutions:

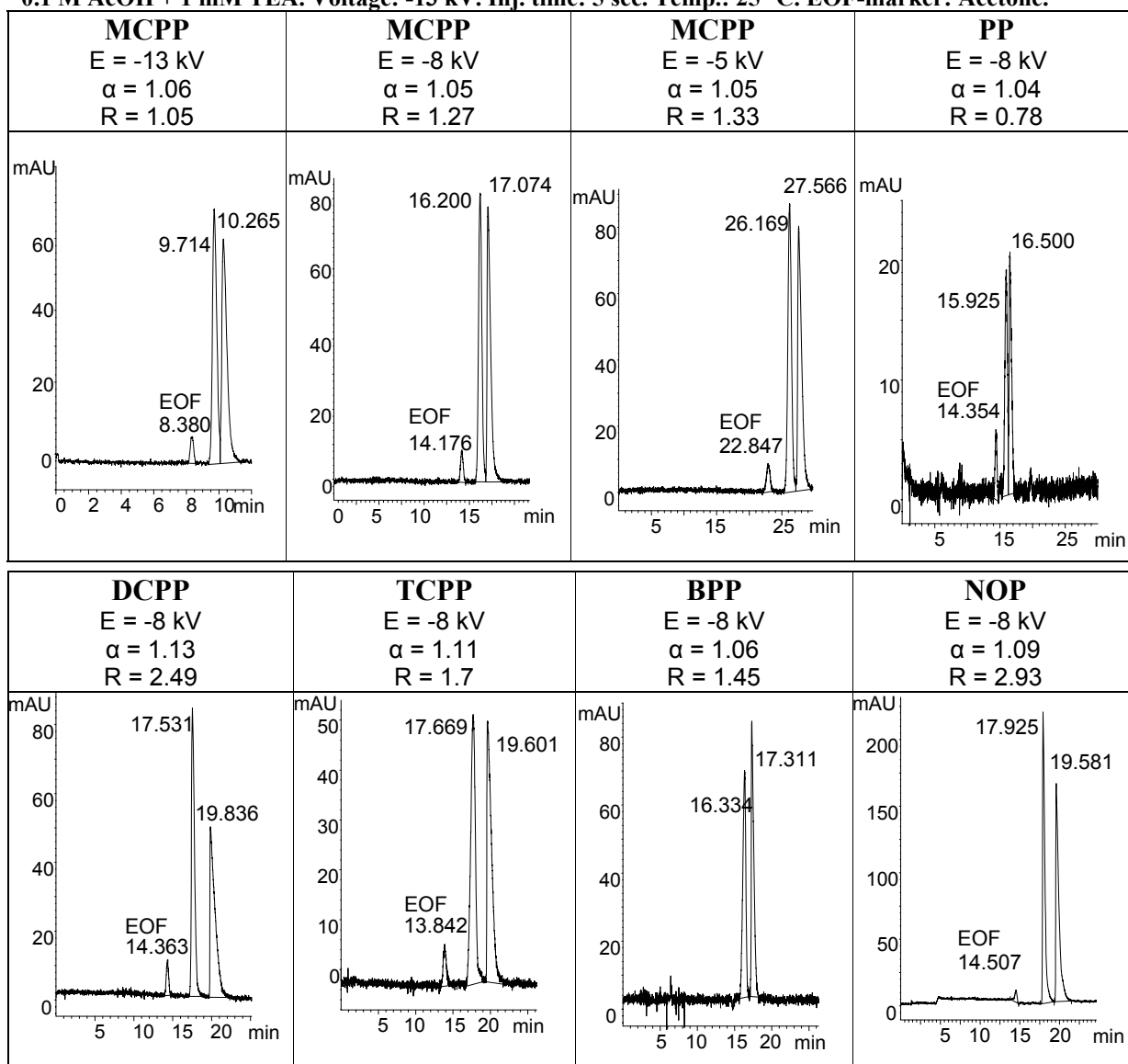
Table IV-2: Tested conditions for mecoprop enantiomers.

AcOH [M] / TEA [mM]	ACN/MeOH (v/v)	Inj. [kV, s]	E [kV]	α	R
0.1/2	80/20	-13.5	-13	1.05	0.74
0.2/2	40/60	-13.5	-13	1.04	0.78
0.1/1	40/60	-13.5	-13	1.05	0.95
0.05/0.5	40/60	-13.5	-13	1.07	1.02
0.05/2	40/60	-13.5	-13	1.06	0.55
0.1/0.2	40/60	-20.5	-20	1.05	0.54
0.1/0.2	40/60	-20.5	-13	1.06	0.77
0.1/0	40/60	-13.5	-13	1.06	0.56
0.1/1	0/100	-13.5	-13	1.16	1.05

Consequently, 0.1 M AcOH and 1 mM TEA in 100 % MeOH were selected for subsequent experiments.

It is striking that conditions depicted in Fig. IV-16 obviously induce a focussing of the S-enantiomer (2nd eluting), whereas optimized conditions in Table IV-3 show opposite tendencies (except for BPP).

Table IV-3: Separations at optimized conditions. Sample conc.: 1.8 mg/ml. Mobile phase: 100% MeOH + 0.1 M AcOH + 1 mM TEA. Voltage: -13 kV. Inj. time: 5 sec. Temp.: 25 °C. EOF-marker: Acetone.



From the data obtained from MCPP a short range H/u dependency can be established (Fig. IV-17). It can be seen that plate heights can be decreased by a factor of about two by decreasing the applied voltage from -13 kV ($u \sim 3$ cm/min) to -5 kV ($u \sim 1$ cm/min). Thus, except of PP all aryloxy carboxylic acid test compounds could be baseline separated.

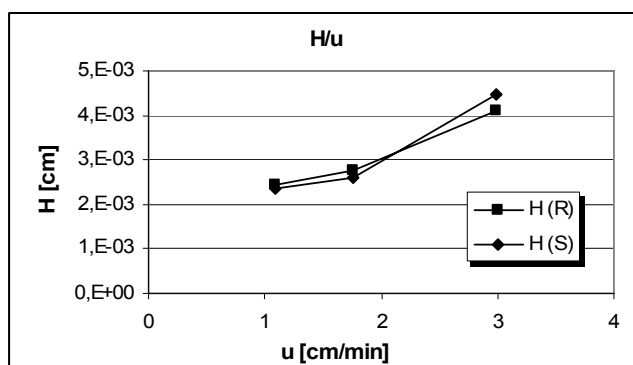


Fig. IV-17: Van Deemter plot of MCPP at optimized conditions. Sample conc.: 1.8 mg/ml. Mobile phase: 100% MeOH + 0.1 M AcOH + 1 mM TEA. Voltage: -13 kV. Inj. time: 5 sec. Temp.: 25 °C.

V. SELECTOR EVALUATION

V.A. Preparation of the chirally functionalized silica monolith

In accordance with the results presented in chapter IV, **1** was immobilized on a silica monolithic support. Except for the immobilization step, modification procedures for the monolith were those described for the *t*-BuCQD modified silica monolith in chapter IV.C.2. Thiolization and TCEP reduction were carried out twice.

V.A.1. Selector immobilization

A radical addition mechanism was employed for the attachment of **1** to the surface (Fig. V-1). 5 mg (~ 10 μ mol) of **1** were dissolved in 25 μ L 4 M V-50 in MeOH. V-50 was used instead of AIBN due to its lower decomposition temperature. The solution was exposed to ultrasound and purged with nitrogen for a few minutes, to get rid of oxygen potentially disturbing the addition. Due to uncertainties concerning the tightness of the Hamilton syringe and the little amount of purified SO on hand, a CE system was employed to fill the capillary with the reaction mixture. The monolith was put into the CE cassette and an inlet micro-vial was charged with the SO solution. The capillary was rinsed at 18 °C with a pressure of 10 bar for one hour. The liquid in the microvial outlet which had previously been filled with 100 μ L MeOH was chromatographically analyzed to make sure the SO had passed the capillary. Subsequently the capillary was waterproofed with GC septa and put into a water bath of 60 °C for 24 h.

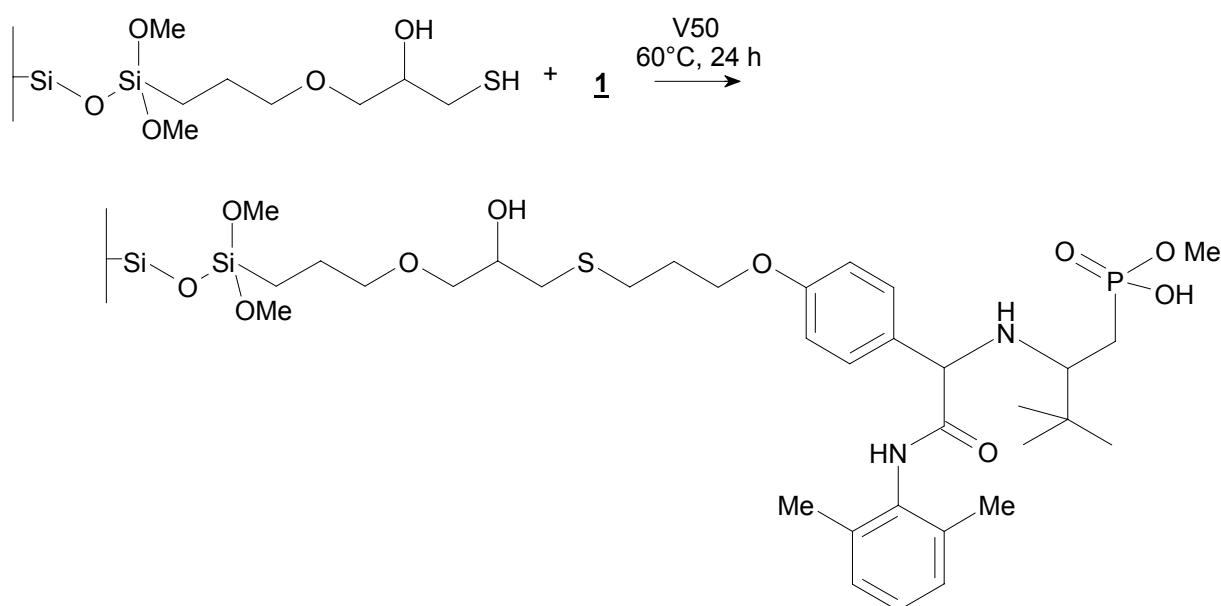


Fig. V-1: Selector modified monolithic surface

V.A.2. Monolith data

After modification procedures the monolith was cut to the following lengths:

Effective length:	25 cm
Total length:	33.5 cm
Inner diameter:	100 μm

V.B. Evaluation of the functionalized silica monolith

V.B.1. Expectations

The selector was intended to be used for the separation of enantiomers. Therefore, a variety of chiral recognition units had to be provided. In the course of this sub-chapter the principal interaction sites will shortly be presented and compared to those of the initially desired Ugi product.

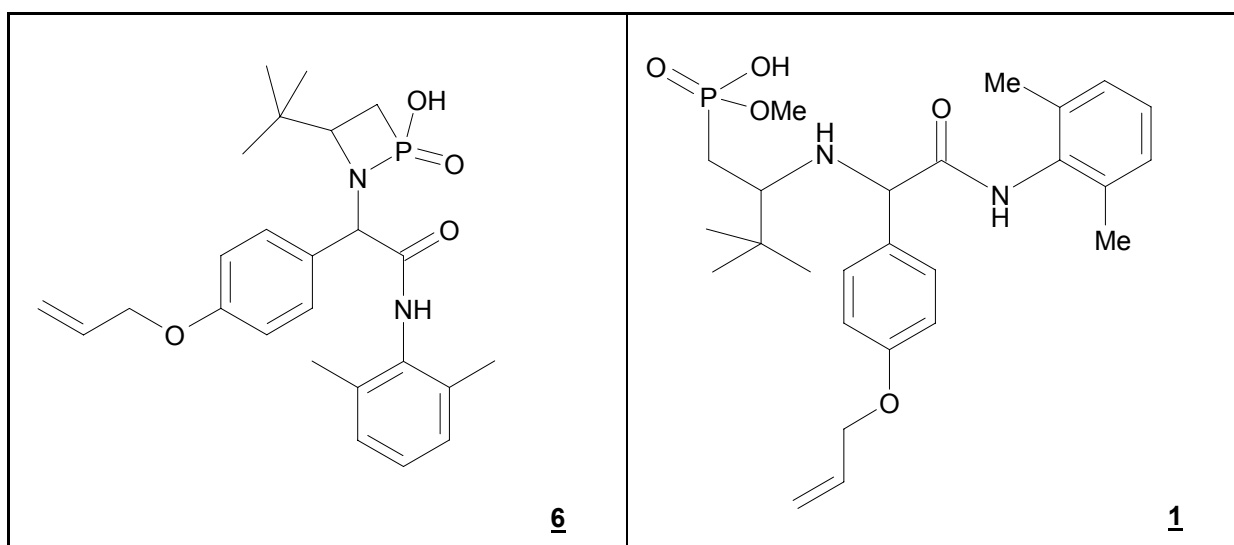


Fig. V-2: Expected selector structure, **6**, and obtained product, **1**

Basically, the remaining acid group of the former phosphonic acid in molecule **1** exhibits an anionic residue above a pH of 1.95*. Hence, long-distance electrostatic forces will attract positively charged solutes, e.g. bases. Once the molecule has reached the SO, short-range interactions will dominate the chiral recognition process. The two aromatic moieties stemming from the former aldehyde and isocyanide enable π - π interactions, whereas the peptide-like backbone enforces additional hydrogen bonding. Furthermore there is a *tert*-butyl group introducing another stereogenic centre close to an interaction site, *viz* the phosphonic acid monoester residue. This sterical hindrance might positively affect chiral separations, as one

* all pK_a values calculated with ACD/Labs Software

enantiomer structure may arrange itself more suitably around the SO. Moreover, van der Waals forces can be implemented at the *tert*-butyl group. The latter may also add to the rigidity of the selector which can be favourable concerning entropic contributions. Generally, the obtained structure, **1**, is relatively free to move compared to the originally expected Ugi product, **6**, which would have included the formation of a ring. **1** incorporates several rotatable bonds resulting in considerable flexibility, that will be significantly declined in the course of a solute complexation. Impediments due to entropic effects might be reduced upon usage of **6**. The latter might also yield more rigid binding pockets enhancing chiral recognition. Besides, the pK_a of the acid function is lower and may consequently generate a more stable electro-osmotic flow. The tradeoff would be the loss of two hydrogen bonding sites.

Considering the zwitter-ionic nature of **1**, cathodic EOF above the pI of the surface and anionic EOF below its pI should occur.

V.B.2. Characterization of the EOF

The created Ugi-derived product, **1**, reveals potentially oppositely charged moieties, resulting in its zwitter-ionic properties. The former phosphonic acid residue exposes a negative charge above a pH of 1.95, whereas a positive charge is generated on the nitrogen nearby at a pH lower than 6.74. Following these values, the pI of the selector molecule was calculated to be 4.34. Thus, at a pH above 4.34 the selector is expected to be net negatively charged, resulting in a cationic EOF, favourable for the separation of positively charged solutes. On the contrary, at more acidic conditions than 4.34, the ligand will be net positively charged and thus could yield an EOF directed towards the anode. Despite this holds true for the theory of a totally selector-loaded monolith, in practice the impact of residual silanols cannot be neglected. Since their pI is set between 5 and 6, they add to a negative net surface charge in and above this range.

To evaluate these assumptions, the pH of the mobile phase has been varied and, accordingly, the mobility of the electro-osmotic flow has been determined. Variable ratios of FA and 4-aminobutanol (AB) in MeOH/ACN were used to adjust the pH. As organic media cause pH shifts, apparent pH values (pH_a) were measured with an ordinary pH-electrode before use.

Results and Discussion:

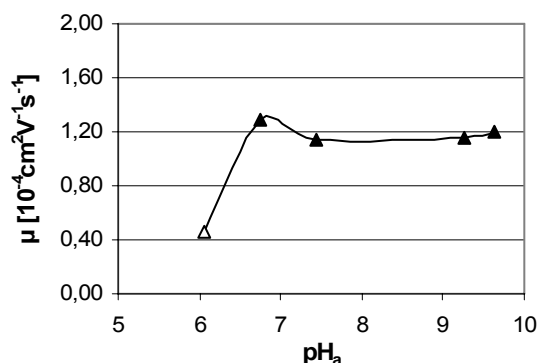


Fig. V-3: μ_{eo} as a function of pH_a . EOF-marker: Acetone. Mobile phase: MeOH/ACN (20/80; v/v). Voltage: 5 kV. Temp.: 30 °C

Table V-1: Tested pH_a values

FA [mM]	AB [mM]	pH_a
100	10	5.56
50	10	6.06
5	1	6.75
10	10	7.45
10	50	9.26
10	100	9.63

The tested pH_a ranged from 5.56 to 9.63. Since a cationic EOF was expected in that range, a positive voltage was applied. At 6.75 a distinct EOF was observed; the net charge of the surface was unambiguously negative, as had been anticipated. However, at 5.56 and 6.06 no EOF peak eluted from the capillary within one hour, neither at positive nor negative applied voltage, indicating a mobility lower than $0.47 \text{ m}^2 \text{V}^{-1} \text{s}^{-1}$ in any case. This is in line with the consideration that an increasing degree of protonation of the aminogroup nitrogen adds to a more and more net neutral surface in lower pH ranges.

The increase in mobility between 7.45 and 9.63 emerges from the slight augmentation of the pH, which causes an extensively deprotonated anionic surface. The slope is rather flat as at the same time the total electrolyte concentration is enlarged as well, consequently evoking a lower electro-osmotic mobility according to von Smoluchowski. Eq. (12) also comprises the explanation for the apparent maximum at 6.75, where the lowest total electrolyte concentration was employed. For the following experiments equimolar amounts of additives (acid/base; 10 mM each) were selected and Clenbuterol was used as test substance.

V.B.3. Test analyte Clenbuterol

Clenbuterol is a β_2 -sympathomimeticum. It is utilized as a drug for the treatment of asthma in humans, due to its bronchodilative effect. It has been applied in veterinary medicine as well. Although it is not significantly more effective in horses than similar substances (e.g. Salbutamol), it exhibits a stronger effect in dogs and is therefore sometimes favoured. Still, it is not to be used in dogs, as myocardial necroses have been observed (108). In experiments performed in guinea pigs the bronchodilator effect of the (-) enantiomer was about a thousand times stronger than that of the (+) species. It is concluded that primarily the (-) form is responsible for the pharmacological effect (109).

Furthermore, Clenbuterol supports the increase of muscle mass, making it attractive for sportsmen. Indeed, Clenbuterol has illegally been used in competitions (110) and is found on the list of forbidden anabolics of the international olympic committee (111).

A tocolytic effect of Clenbuterol has also been reported. An effect of uterine activity around estrus in sows has been detected as well. Clenbuterol diminished frequency and amplitude of contractions (112). It has also led to muscle relaxation in coney urinary bladder (109).

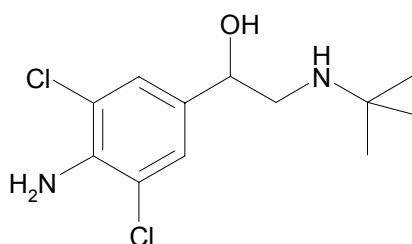


Fig. V-4: Clenbuterol

V.B.4. Counter ion influence

In a cation exchange system any positively charged species can act as a counter ion. Previous studies revealed that its optimization is far more important than that of the co-ion (85, 113, 114). After evaluation of a reasonable acid/base ratio the base type was therefore further examined. Since its influence results from both, strength and steric nature, a primary, a secondary and a tertiary amine were inquired. A stronger base, provoking an augmented pH is expected to yield an augmented EOF due to the generation of more anionic binding sites at the monolithic surface. Simultaneously it might represent a more effective counter-ion accelerating the slow mass transfer of ion-exchange mechanisms and hence enhance peak shape/efficiency. However, it may also reduce the surface charge by effective ion-pairing leading to lower EOF.

Results and Discussion

As can be gathered from Fig. V-6, the Clenbuterol enantiomers elute the quickest when AB is employed. Hence, the counter-ion effectiveness seems to be related rather to structural properties than to the basicity of the amine. Structural similarities between the interaction sites of AB and Clenbuterol support the outcome that AB is the strongest competitor. Additionally, even hydrogen bondings between the hydroxy and amine functions of AB and Clenbuterol may occur. As expected, the most effective counter ion significantly enhanced peak shapes (Fig. V-5). Strong ion pairing between AB and the charged selector moieties is assumed to decrease EDL thickness and consequently μ_{eo} . Furthermore, a higher number of adsorption sites might be generated at an augmented pH when DEA or TEA are utilized. In this case μ_{eo}

is amplified as well. Nevertheless μ_{CEC} decelerate, because DEA and TEA are weaker competitors so that the molecular interaction is stronger than with AB at the same concentration.

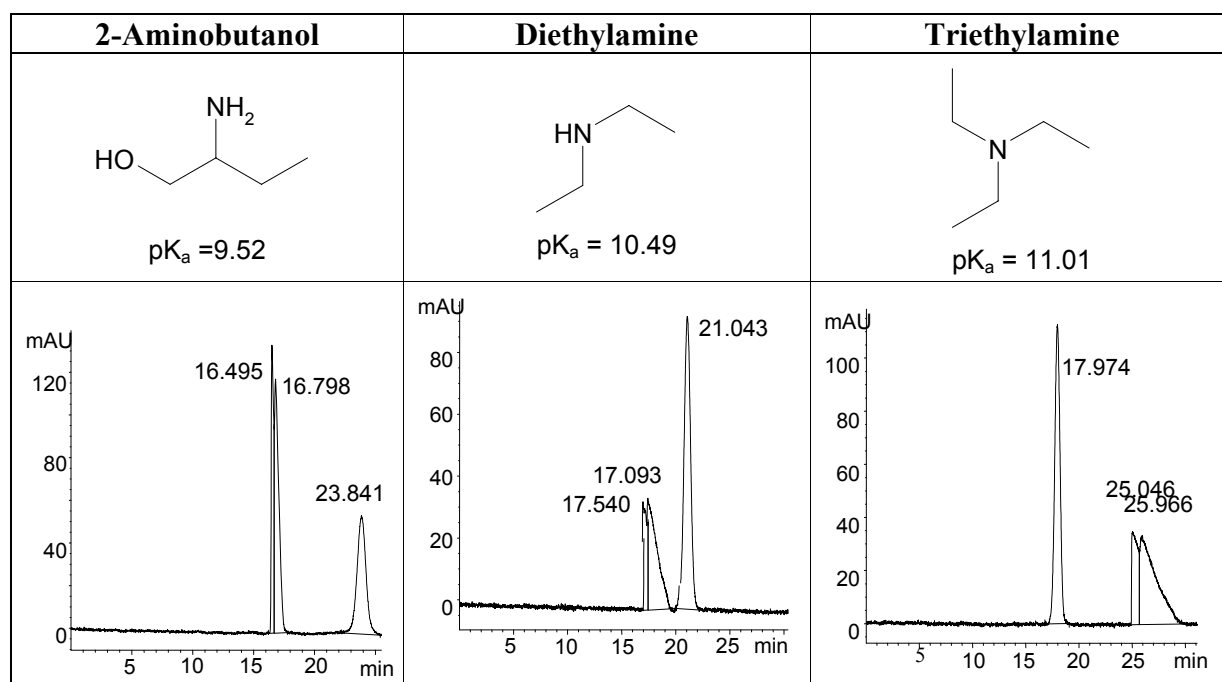


Fig. V-5: Repertory of tested bases. Sample concentration: 1 mg/ml. Mobile phase: MeOH/ACN (20/80; v/v) + 10 mM FA + 10 mM amine. Voltage: 5 kV. Inj. time: 20 sec. Temp.: 30 °C. ---EOF marker: Acetone.

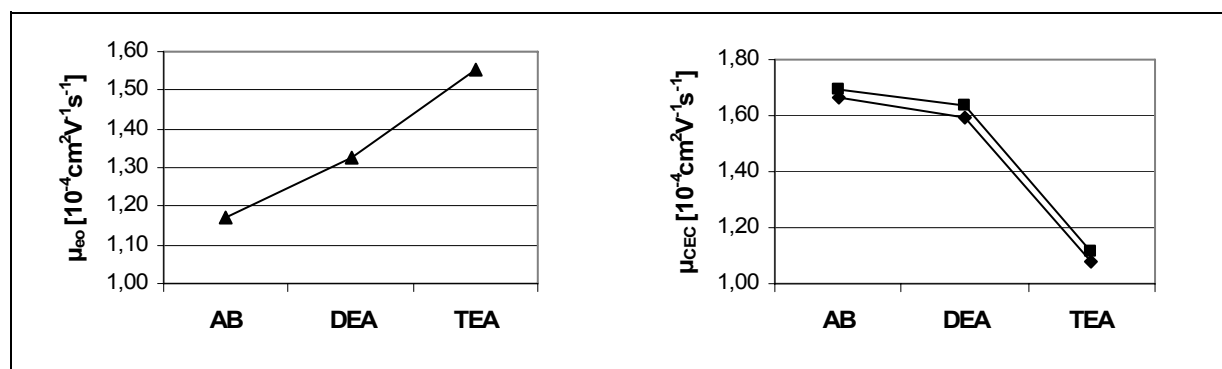


Fig. V-6: Electrophoretic mobilities with various amines. Sample concentration: 1 mg/ml. Mobile phase: MeOH/ACN (20/80; v/v) + 10 mM FA + 10 mM amine. Voltage: 5 kV. Inj. time: 20 sec. Temp.: 30 °C. ---EOF marker: Acetone.

V.B.5. Total electrolyte concentration

Variation of the total electrolyte concentration is a most important and convenient tool to balance strong ionic interactions. As has been set out more precisely in chapter V.B.2., the mobility of the EOF can directly be enlarged by lowering the ionic strength of the mobile phase on the square root of which it depends. A reduced counter-ion concentration in turn is supposed to strengthen the ionic interaction. A dilution series prepared from a stock solution

containing equimolar amounts of FA and AB was used to confirm the applicability of these theories.

Results and Discussion

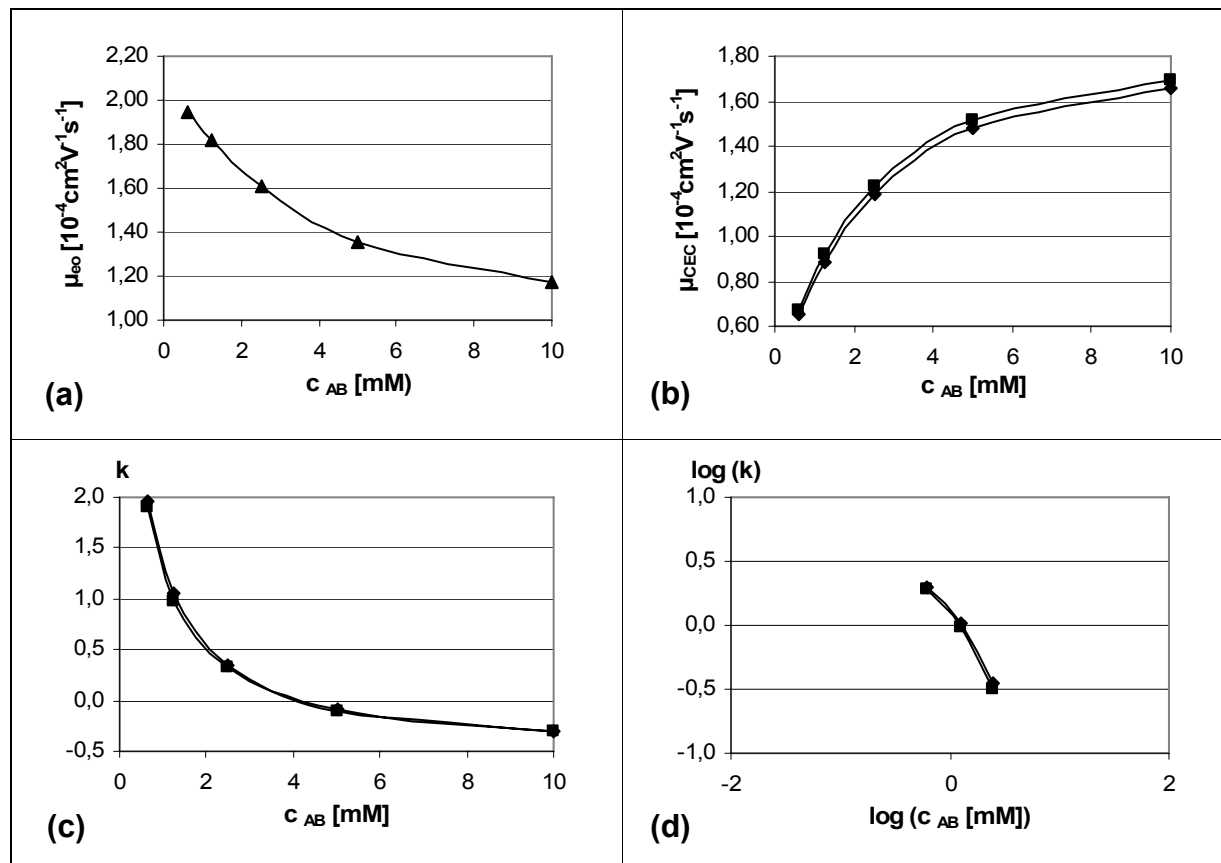


Fig. V-7: Plots of μ_{eof} , μ_{CEC} and k ($\log k$) vs. AB concentration ($\log c_{AB}$). Sample concentration: 1 mg/ml. Mobile phase: MeOH/ACN (20/80; v/v) + 10 mM FA + 10 mM amine. Voltage: 5 kV. Inj. time: 20 sec. Temp.: 30 °C. --- EOF marker: Acetone.

The FA/AB ratio was kept constant, while the solvent was diluted. Mobilities fulfilled theoretical expectations well. Fig. V-7 (a) illustrates that the higher the ζ -potential (the lower the ionic strength, respectively) the stronger the EOF. Fig. V-7 (b) displays the dependency of the mobility of the enantiomers on the counter-ion concentration. Since ion-exchange is supposed to be the dominating interaction, the positively charged solutes elute earlier when a higher number of competitors are present and indeed, enantiomer mobilities exceed EOF velocity at the two highest electrolyte concentrations. In ion exchange systems the logarithm of retention factor plotted vs the logarithm of counter ion concentration typically shows linear dependencies and parallel lines for enantiomers. This indicates that the number of charges involved in the separation mechanism is the same for both molecules. So, the ionic interaction is essentially a non-enantioselective contribution. In the present study plot (d) can only be established for three data points, which is not very representative. Besides, they may already be in the critical, non-linear concentration scale.

Deviations from linearity would be expected in low counter ion concentration ranges. It has been reported that in case of electrolyte concentrations around and below 1 mM the electric double layer thickness has reached a value in the magnitude of the mesopore diameter (115). Subsequently EDL overlap and concentration polarization may occur. The mesopores become charge selective, accumulating counter-ions and excluding co-ions. These effects are also referred to as “elektrokinetic effects of the 2nd kind”. It has been found that they can be used to drastically improve efficiencies in low concentration ranges (116). It can be inferred from Fig. V-8 that this is obviously not the case herein. Furthermore, electrokinetic effects of the 2nd kind are known to provoke a non-linear correlation between electro-osmotic mobility (and retention factors) and applied voltage. The absence of these phenomena was explored in chapter V.B.8, adding to the supposition that ion exchange constitutes the predominant interaction mechanism.

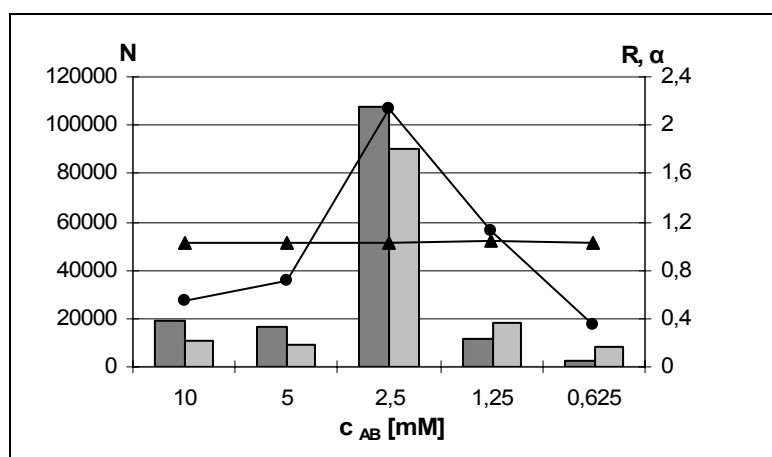


Fig. V-8: Plate numbers, resolution (●) and selectivity (▲) as a function of counter ion concentration. Sample concentration: 1 mg/ml. Mobile phase: MeOH/ACN (20/80; v/v) + 10 mM FA + 10 mM amine. Voltage: 5 kV. Inj. time: 20 sec. Temp.: 30 °C. --- EOF marker: Acetone.

By virtue of the outstanding resolution at an electrolyte concentration of 2.5 mM each, these conditions were further employed. As Fig. V-8 illustrates, this peak results from an efficiency maximum at 2.5 mM, whereas selectivity remains relatively constant over the whole examined electrolyte concentration range.

V.B.6. Organic Modifier

While reflecting upon the influence of MeOH percentage, a large number of manifold effects have to be contemplated. The predominant ion-exchange mechanism and further hydrophilic interactions like H-bonding are presumed to be strengthened in more hydrophobic media, in mixtures containing mainly ACN, precisely. Hence, the more ACN is present, the stronger the interaction with the selector and thus, retention. Besides, ACN causes larger pH shifts towards

higher apparent pH than MeOH. This evokes distinct pH/pK_a scales in distinct solvent compositions, resulting in different dissociation degrees of BGE, analyte and chiral selector. The dependency of the electro-osmotic flow on the permittivity/viscosity ratio, which is greater in ACN rich mixtures, has to be taken into account as well. From this point of view μ_{eo} should be maximized at such conditions.

Results and Discussion

The MeOH content of the mobile phase has been varied from 0 to 100 % in ACN and 2.5 mM FA and AB each were added as electrolytes.

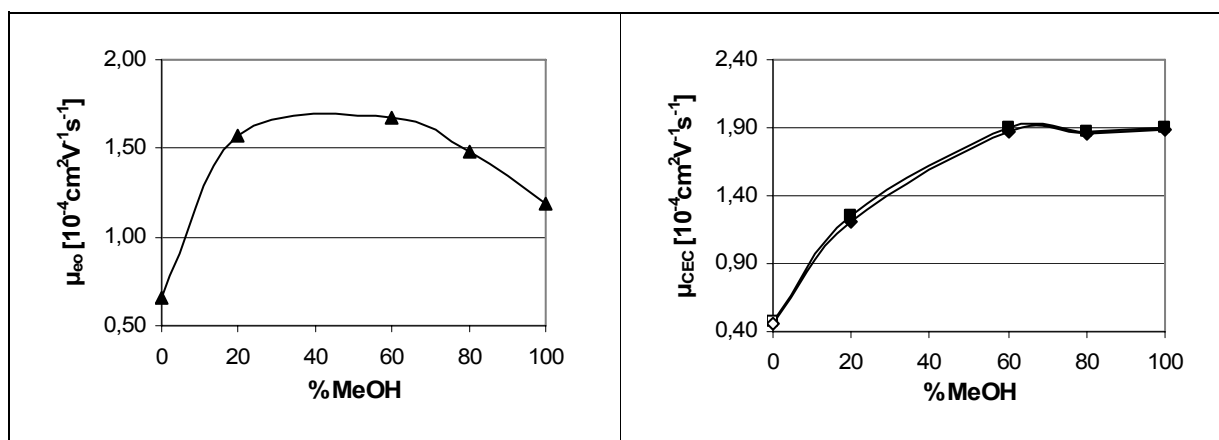


Fig. V-9: Influence of organic modifier concentration on mobilities. Sample conc.: 1 mg/ml. Mobile phase: MeOH/ACN + 2.5 mM FA + 2.5 mM AB. Voltage: 5 kV. Inj. time: 20 sec. Temp.: 30 °C. EOF-marker: Acetone.

A detailed interpretation is complicated, as μ_{ep} of the cationic solutes needs to be considered and depends on the MeOH/ACN ratio as well. At 60 % and more MeOH μ_{ec} remains largely constant, although μ_{eo} decelerates rapidly. This confirms the assumption that hydrophilic ionic interactions between analytes and selector are weakened in more polar media and the Clenbuterol enantiomers are less retarded. Considering EOF behaviour, a mobility maximum should be reached at 80 % ACN as this composition was found to exhibit the highest ε/η ratio (117). Nonetheless maxima around 60 % have been determined previously in similar studies (107, 113). The explanation could be stronger ion pairing in ACN rich media, causing a decrease of the EDL thickness and, consequently, EOF mobility. At 100 % ACN μ_{eo} is lowest. Clenbuterol enantiomers did not elute within one hour, indicating a μ_{ec} below $0.47 \text{ cm}^2 \text{ V}^{-1} \text{ s}^{-1}$. As has been stated above, the relation between retention factors and organic modifiers (Fig. V-10) can hardly be predicted. With regard to Eq. (1) it is plausible that retention factors decrease when void time increases, which is the case in MeOH-rich compositions where μ_{eo} diminishes.

Surprisingly, selectivity values remained unchanged. An improvement of the chromatographic performance was achieved *via* enhanced resolution at 20 % MeOH.

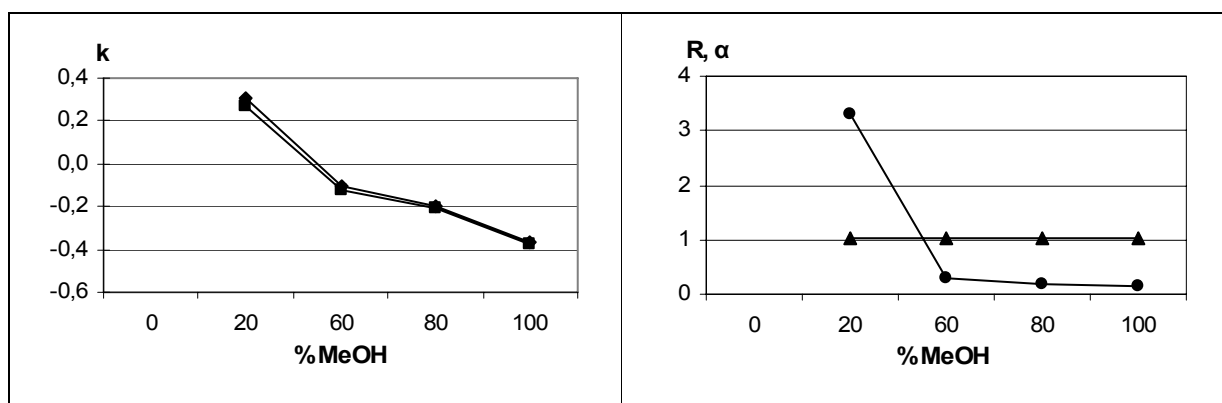


Fig. V-10: Influence of organic modifier concentration on retention factors, resolution (●) and selectivity (▲). Sample conc.: 1 mg/ml. Mobile phase: MeOH/ACN + 2.5 mM AcOH + 2.5 mM AB. Voltage: 5 kV. Inj. time: 20 sec. Temp.: 30 °C. EOF-marker: Acetone.

V.B.7. Optimized mobile phase conditions

The optimized mobile phase composition yielded the following separation:

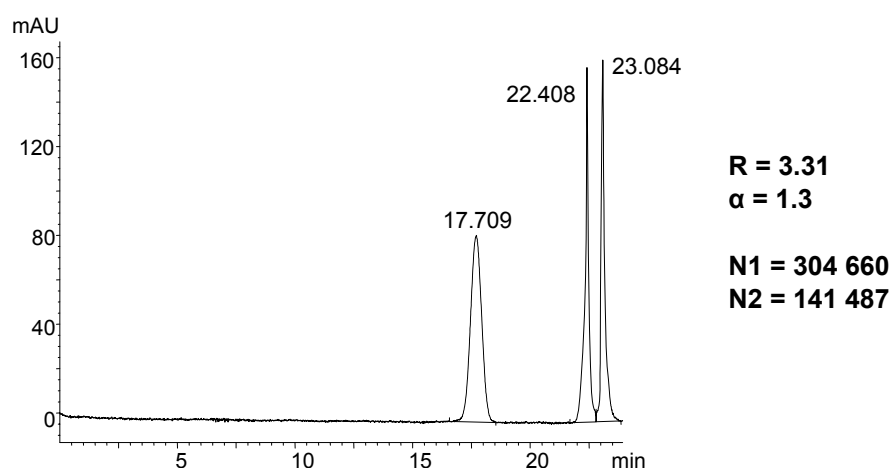


Fig. V-11: Separation of Clenbuterol enantiomers at optimized conditions: Sample concentration: 1mg/ml. Mobile phase: MeOH/ACN (20/80; v/v) + 2.5 mM FA + 2.5 mM AB. Voltage: 5kV. Inj. time: 20 sec. Temp.: 30 °C. --- EOF-marker: Acetone

V.B.8. Van Deemter Curves

The next topic to be explored was the dependency of the plate height on the observed EOF velocity. The main parameters have already been pointed out in chapter IV.A. and shall therefore only briefly be reviewed. In HPLC the Van Deemter equation (Eq. 4) constitutes a relation between linear flow velocity and plate height.

The first term, A, comprises eddy diffusion and is largely independent from u . Secondly, a summand containing a factor B, regarding diffusional mass transfer in the flow direction of the

mobile phase, divided by the flow velocity, is included. Eventually, there is a third parameter, C , representing mass transfer resistance according to the stationary phase, multiplied by u .

As has been stated above, H is supposed to be relatively declined in comparison to liquid chromatography due to an amplified mass transfer and a flat electro-osmotic flow profile in CEC. In the present study the A and C terms are additionally expected to decrease, because monolithic capillaries are used instead of particle packed material. According to theory, the absence of particles is expected to particularly flatten the C -term which is directly proportional to the square of the particle diameter. Furthermore, the silica monolith provides macropores ($\sim 2 \mu\text{m}$) guaranteeing satisfactorily fast mobile phase movement. The present silica monoliths possess relatively thin skeletons, yielding short diffusion distances in the intraskeletal mesopores, being responsible for the high efficiency of such monolithic support.

Results and Discussion

The applied voltage has been varied between 2.5 and 25 kV at optimized mobile phase conditions.

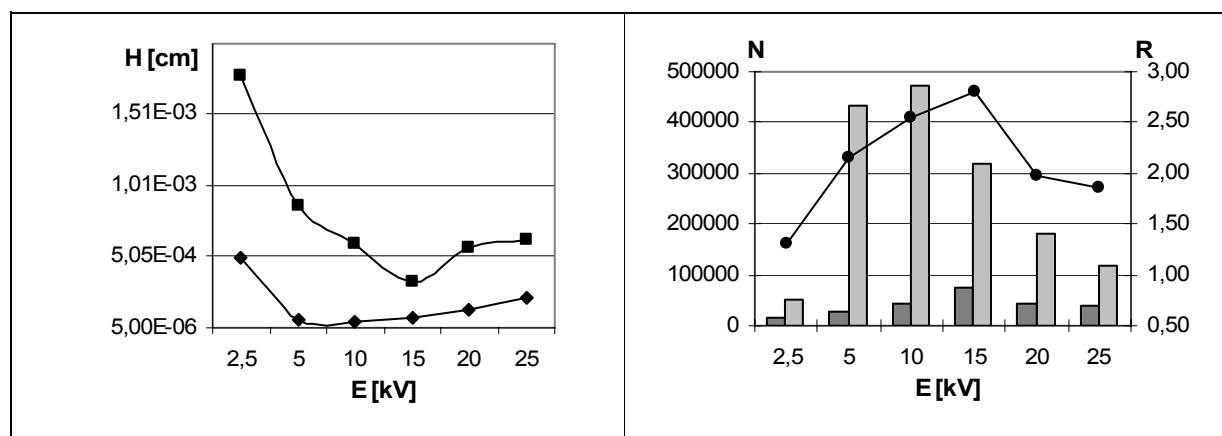


Fig. V-12: H/E curve of Clenbuterol and influence of applied voltage on plate numbers and resolution. Sample concentration: 1mg/ml. Mobile phase: MeOH/ACN (20/80; v/v) + 2.5 mM FA + 2.5 mM AB. Inj.: 20 sec. at 5 kV. Temp.: 30 °C

N -values of the more strongly retarded enantiomer are obviously significantly higher than for the first and consequently yield lower plate heights. This is the formal expression of a focussing of the stronger retarded peak. Such effects have been observed before (118).

In order to evaluate the absence of electrokinetic effects of the second kind, delved into in a more detailed way in chapter V.B.5., the correlations in Fig. V-13 were established. No deviations from the linear correlation between electro-osmotic mobility and applied voltage are found. Therefore, it is assumed that no Joule heat effects exist in the capillary and no concentration polarization occurs inside monolithic mesopores.

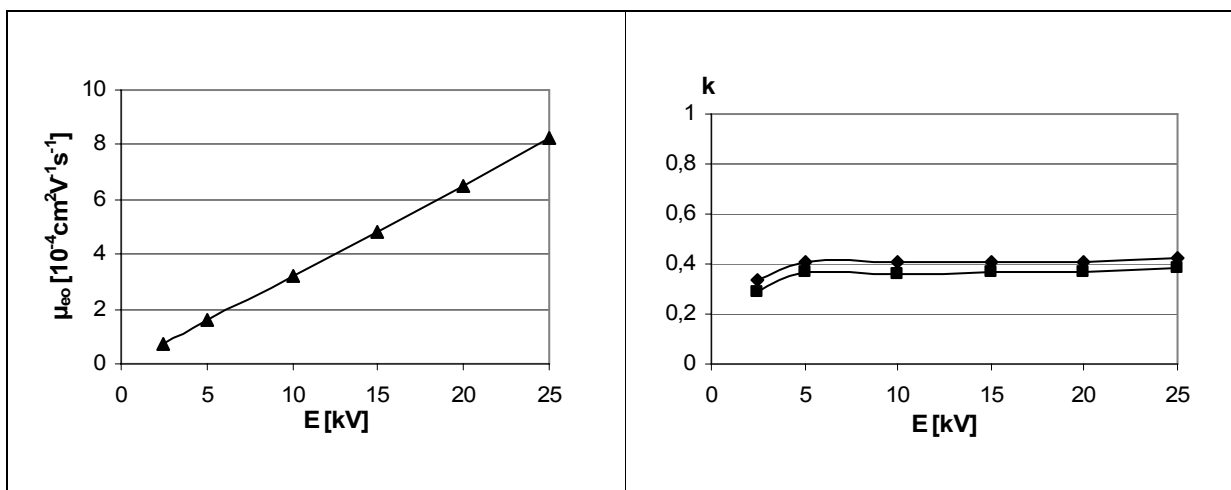


Fig. V-13: EOF mobility and retention factors of Clenbuterol vs applied voltage. Sample concentration: 1mg/ml. Mobile phase: MeOH/ACN (20/80; v/v) + 2.5 mM FA + 2.5 mM AB. Inj.: 20 sec. at 5 kV. Temp.: 30 °C

Besides, Clenbuterol retention factors do not vary as the voltage is augmented, although the ionic strength of the BGE is rather low. So, as has been stated when exploring the total electrolyte concentration, ion-exchange is the dominating interaction mechanism.

V.B.9. Conclusion

The previous experiments, showing the successful separation of Clenbuterol enantiomers, indicate the potential of phosphonic acid pseudo-dipeptide selectors. Further research employing this selector class will be done in the future.

References

- (1) Klebe, G., *Wirkstoffdesign, Entwurf und Wirkung von Arzneistoffen*, Spektrum Akad. Verlag 2009, 69.
- (2) Brenna, E., Fuganti, C., Serra, S., *Tetrahedron: Asymmetry* 2003, 14, 1-42.
- (3) Guth, H., *Helvetica Chimica Acta* 1996, 79, 1559-1571.
- (4) Belitz, H. D., Grosch, W., Schieberle, P., *Lehrbuch der Lebensmittelchemie*, Springer 2007, 35.
- (5) Knoche, B., Blaschke, G., *Chirality* 1994, 6, 221-224.
- (6) De Andres, F., Castaneda, G., Rios, A., *Chirality* 2009, 21, 751-759.
- (7) Lewis, D. L., Garrison, A. W., Wommack, K. E., Whitemore, A., *Nature (London)* 1999, 401, 898-901.
- (8) Mueller, D., Klepel, H., Macholz, R. M., Lewerenz, H. J., Engst, R., *Bulletin of Environmental Contamination and Toxicology* 1981, 27, 704-706.
- (9) Schneiderheinze, J. M., Armstrong, D. W., Berthod, A., *Chirality* 1999, 11, 330-337.
- (10) Greig-Smith, P. W., Thompson, H. M., Hardy, A. R., Bew, M. H., *et al.*, *Crop Protection* 1994, 13, 567-581.
- (11) Testa, B., *Grundlagen der Organischen Stereochemie*, Verlag Chemie Weinheim 1983.
- (12) Dale, J. A., Dull, D. L., Mosher, H. S., *Journal of Organic Chemistry* 1969, 34, 2543-2549.
- (13) Lin, C.-E., Ko, T.-C., Kuo, C.-M., Trapp, O., *et al.*, *Electrophoresis* 2009, 30, 3071-3078.
- (14) Mikus, P., Marakova, K., Valaskova, I., Havranek, E., *Pharmazie* 2009, 64, 423-427.
- (15) Scriba, Gerhard K. E., *Journal of Separation Science* 2008, 31, 1991-2011.
- (16) Haginaka, J., *Pharm Tech Japan* 1995, 11, 1643-1652.
- (17) Preinerstorfer, B., Bicker, W., Lindner, W., Lammerhofer, M., *Journal of Chromatography, A* 2004, 1044, 187-199.
- (18) Domling, A., *Current opinion in chemical biology* 2000, 4, 318-323.
- (19) Domling, A., Ugi, I., *Angewandte Chemie, International Edition* 2000, 39, 3168-3210.
- (20) Zhu, J., *European Journal of Organic Chemistry* 2003, 1133-1144.
- (21) Lack, O., Weber, L., *Chimia* 1996, 50, 445-447.
- (22) Veiderma, M., *Proceedings of the Estonian Academy of Sciences, Chemistry* 2007, 56, 98-102.
- (23) Zhang, J., Jacobson, A., Rusche, J. R., Herlihy, W., *Journal of Organic Chemistry* 1999, 64, 1074-1076.
- (24) El Kaim, L., Grimaud, L., Oble, J., *Angewandte Chemie, International Edition* 2005, 44, 7961-7964.
- (25) Schneekloth, J. S., Jr., Kim, J., Sorensen, E. J., *Abstracts of Papers, 236th ACS National Meeting, Philadelphia, PA, United States, August 17-21, 2008* 2008, AEI-068.
- (26) Ugi, I., Steinbrückner, C., *Angew. Chem.* 1959, 71, 386.
- (27) Ugi, I., *Journal fuer Praktische Chemie/Chemiker-Zeitung* 1997, 339, 499-516.
- (28) Ugi, I., Steinbrückner, C., DE-B 1,103,337 1959.
- (29) Godet, T., Bonvin, Y., Vincent, G., Merle, D., *et al.*, *Organic Letters* 2004, 6, 3281-3284.
- (30) Marcaccini, S., Torroba, T., *Nature Protocols* 2007, 2, 632-639.
- (31) Bienayme, H., *Tetrahedron Letters* 1998, 39, 4255-4258.
- (32) Bossio, R., Marcaccini, S., Pepino, R., *Liebigs Annalen der Chemie* 1990, 935-937.
- (33) Ugi, I., Meyr, R., *Angew. Chem.* 1958, 70, 702-703.
- (34) Hardy, P. M., Lingham, I. N., *International Journal of Peptide & Protein Research* 1983, 21, 392-405.
- (35) Ugi, I., Marquarding, D., Urban, R., *Chemistry and Biochemistry of Amino Acids, Peptides, and Proteins* 1982, 6, 245-289.
- (36) Doemling, A., Kehagia, K., Ugi, I., *Tetrahedron* 1995, 51, 9519-9522.
- (37) Gedey, S., Van der Eycken, J., Fuloep, F., *Organic Letters* 2002, 4, 1967-1969.
- (38) Gokel, G., Luedke, G., Ugi, I., *Isonitrile Chem.* 1971, 145-199.
- (39) Dai, W.-M., Li, H., *Tetrahedron* 2007, 63, 12866-12876.

- (40) Bossio, R., Marcaccini, S., Pepino, R., Torroba, T., *Heterocycles* 1999, 50, 463-467.
- (41) Domling, A., Herdtweck, E., Ugi, I., *Acta Chemica Scandinavica* 1998, 52, 107-113.
- (42) Ugi, I., Demharter, A., Hoerl, W., Schmid, T., *Tetrahedron* 1996, 52, 11657-11664.
- (43) Kunz, H., Pfrengle, W., Sager, W., *Tetrahedron Letters* 1989, 30, 4109-4110.
- (44) Ross, G. F., Herdtweck, E., Ugi, I., *Tetrahedron* 2002, 58, 6127-6133.
- (45) Mumm, O., Hesse, H., Volquartz, H., *Berichte der Deutschen Chemischen Gesellschaft* 1915, 48, 379-391.
- (46) Mumm, O., Moller, F., *Berichte der Deutschen Chemischen Gesellschaft [Abteilung] B: Abhandlungen* 1937, 70B, 2214-2227.
- (47) Kingston, H. M., Haswell, S. J., *Microwave-Enhanced Chemistry*, American Chemical Society, 1997
- (48) Feinberg, M. H., *Analysis* 1991, 19, 47-55.
- (49) Schnitzer, G., Pain, M., Testu, C., Chafey, C., *Analysis* 1990, 18, i20-i22.
- (50) Ali, M., Bond, S. P., Mbogo, S. A., McWhinnie, W. R., Watts, P. M., *Journal of Organometallic Chemistry* 1989, 371, 11-13.
- (51) Bose, A. K., Manhas, M. S., Ghosh, M., Shah, M., *Journal of Organic Chemistry* 1991, 56, 6968-6970.
- (52) Gedye, R. N., Smith, F. E., Westaway, K. C., *Canadian Journal of Chemistry* 1988, 66, 17-26.
- (53) Giguere, R. J., Bray, T. L., Duncan, S. M., Majetich, G., *Tetrahedron Letters* 1986, 27, 4945-4948.
- (54) Majetich, G., Hicks, R., *Radiation Physics and Chemistry* 1995, 45, 567-579.
- (55) Margolis, S. A., Jassie, L., Kingston, H. M., *Journal of Automatic Chemistry* 1991, 13, 93-95.
- (56) Subbaraju, G. V., Manhas, M. S., Bose, A. K., *Tetrahedron Letters* 1991, 32, 4871-4874.
- (57) Laurent, R., Laporterie, A., Dubac, J., Berlan, J., *et al.*, *Journal of Organic Chemistry* 1992, 57, 7099-7102.
- (58) Raner, K. D., Strauss, C. R., Vyskoc, F., Mokbel, L., *Journal of Organic Chemistry* 1993, 58, 950-953.
- (59) Blackwell, H. E., *Organic & Biomolecular Chemistry* 2003, 1, 1251-1255.
- (60) Hoel, A. M. L., Nielsen, J., *Tetrahedron Letters* 1999, 40, 3941-3944.
- (61) Tye, H., Whittaker, M., *Organic & Biomolecular Chemistry* 2004, 2, 813-815.
- (62) Pirrung, M. C., Das Sarma, K., *Journal of the American Chemical Society* 2004, 126, 444-445.
- (63) Brahmachary, E., Ling, F. H., Svec, F., Frechet, J., *Journal of Combinatorial Chemistry* 2003, 5, 441-450.
- (64) Bradley, J.-C., Mirza Khalid, B., Osborne, T., Wiliams, A., Owens, K., *Journal of visualized experiments : JoVE* 2008.
- (65) Passerini, M., *Gazzetta Chimica Italiana* 1921, 51, 181-189.
- (66) Cheng, J.-F., Chen, M., Arrhenius, T., Nadzan, A., *Tetrahedron Letters* 2002, 43, 6293-6295.
- (67) Lee, D., Sello, J. K., Schreiber, S. L., *Organic Letters* 2000, 2, 709-712.
- (68) Xu, P., Lin, W., Zou, X., *Synthesis* 2002, 1017-1026.
- (69) Bicker, W., Kacprzak, K., Kwit, M., Laemmerhofer, M., *Tetrahedron: Asymmetry* 2009, 20, 1027-1035.
- (70) Auger, G., Heijenoort, J., *Journal für Praktische Chemie* 1995, 337, 351-357.
- (71) Holy, A., Rosenberg, I., *Collection of Czechoslovak Chemical Communications* 1987, 52, 2775-2791.
- (72) Gross, H., Boeck, C., Costisella, B., Gloede, J., *Journal fuer Praktische Chemie (Leipzig)* 1978, 320, 344-350.
- (73) Yonemitsu, O., Cerutti, P., Witkop, B., *Journal of the American Chemical Society* 1966, 88, 3941-3945.
- (74) Dyatkina, N. B., Theil, F., von Janta-Lipinski, M., *Tetrahedron* 1995, 51, 761-772.
- (75) Kohyama, N., Hayashi, T., Yamamoto, Y., *Bioscience, Biotechnology, and Biochemistry* 2005, 69, 836-838.
- (76) Shirokova, E. A., Tarusova, N. B., *Journal of Medicinal Chemistry* 1994, 37, 3739-3748.
- (77) Hanessian, S., Delorme, D., Dufresne, Y., *Tetrahedron Letters* 1984, 25, 2515-2518.
- (78) Rabinowitz, R., *Journal of the American Chemical Society* 1960, 82, 4564-4567.
- (79) De Lombaert, S., Singh, K., Blanchard, L., Soliman, V. F., *Bioorganic & Medicinal Chemistry Letters* 1994, 4, 899-902.
- (80) De Lombaert, S., Erion, M. D., Tan, J., Blanchard, L., *Journal of Medicinal Chemistry* 1994, 37, 498-511.

- (81) Wallace, E. M., Moliterni, J. A., Moskal, M. A., Neubert, A. D., *et al.*, *Journal of Medicinal Chemistry* 1998, *41*, 1513-1523.
- (82) Hebenstreit, D., Bicker, W., Laemmerhofer, M., Lindner, W., *Electrophoresis* 2004, *25*, 277-289.
- (83) Hoffmann, C. V., Laemmerhofer, M., Lindner, W., *Analytical and Bioanalytical Chemistry* 2009, *393*, 1257-1265.
- (84) Hoffmann, C. V., Pell, R., Laemmerhofer, M., Lindner, W., *Analytical Chemistry (Washington, DC, United States)* 2008, *80*, 8780-8789.
- (85) Preinerstorfer, B., Hoffmann, C., Lubda, D., Laemmerhofer, M., Lindner, W., *Electrophoresis* 2008, *29*, 1626-1637.
- (86) Bogdal, D., Pielichowski, J., Jaskot, K., *Organic Preparations and Procedures International* 1998, *30*, 427-432.
- (87) Chatti, S., Bortolussi, M., Loupy, A., *Tetrahedron Letters* 2000, *41*, 3367-3370.
- (88) Sarju, J., Danks, T. N., Wagner, G., *Tetrahedron Letters* 2004, *45*, 7675-7677.
- (89) Meyer, V. R., *Praxis der Hochleistungs-Flüssigchromatographie*, Wiley-VCH Verlag 2004, 23.
- (90) van Deemter, J. J., Zuiderweg, F. J., Klinkenberg, A., *Chemical Engineering Science* 1956, *5*, 271-289.
- (91) Schwedt, G., *Analytische Chemie, Grundlagen, Methoden und Praxis*, Wiley - VCH Verlag GmbH & Co KGaA, 2008, 363
- (92) Scoog, D., West, D., Hollar, F., Crouch, S., *Fundamentals of Analytical Chemistry*, Brooks/Cole 2004.
- (93) von Smoluchowski, M., *Bull. Int. Acad. Sci. Cracovie* 1903, *8*, 182-200.
- (94) Dell'mour, M., Findeisen, A., Kaml, I., Baatz, W., Kenndler, E., *Open Analytical Chemistry Journal* 2008, *2*, 67-73
- (95) Preinerstorfer, B., *Department of Analytical and Food Chemistry*, University of Vienna, Vienna 2006.
- (96) Helles, W., *Untersuchungsmethoden in der Chemie, Einführung in die moderne Analytik*, Georg Thieme Verlag 1997.
- (97) Lammerhofer, M., Enantioseparations by Capillary Electrochromatography, in: *Chiral Separations by Capillary Electrophoresis*. A. Van Eeckhaut, Y. Michotte (Eds.), Taylor and Francis, 2009.
- (98) Lammerhofer, M., *Journal of chromatography. A* 2005, *1068*, 31-57.
- (99) Noel, R., Sanderson, A., Spark, L., *Cellulosics* 1993, 17-24.
- (100) Svec, F., Tennikova, T. B., Deyl, Z., *Monolithic Materials*, Journal of Chromatography Library, *67*, 2003.
- (101) Svec, F., Frechet, J. M. J., *Industrial & Engineering Chemistry Research* 1999, *38*, 34-48.
- (102) Viklund, C., Svec, F., Frechet, J. M. J., Irgum, K., *Chemistry of Materials* 1996, *8*, 744-750.
- (103) Allen, D., El Rassi, Z., *Electrophoresis* 2003, *24*, 3962-3976.
- (104) Lammerhofer, M., Peters, E. C., Yu, C., Svec, F., Frechet, J. M., *Analytical chemistry* 2000, *72*, 4614-4622.
- (105) Lammerhofer, M., Svec, F., Frechet, J. M., *Analytical chemistry* 2000, *72*, 4623-4628.
- (106) Lammerhofer, M., Svec, F., Frechet, J. M. J., Lindner, W., *Journal of Microcolumn Separations* 2000, *12*, 597-602.
- (107) Tobler, E., Lammerhofer, M., Lindner, W., *Journal of chromatography. A* 2000, *875*, 341-352.
- (108) Görlitz, B. D., *Lehrbuch der Pharmakologie und Toxikologie in der Veterinärmedizin*, Enke 2007, 219.
- (109) Bruchhausen, F., Ebel, S., Frahm, A. W., Hackenthal, E., *Hagers Handbuch der pharmazeutischen Praxis*, Springer 1993, 990.
- (110) Singler, A., Treutlein, G., *Doping im Spitzensport*, Meyer & Meyer Sport 2006, 72.
- (111) Agency, W. A.-D., *The 2008 Prohibited List, International Standard* 2007, 11111 http://multimedia.olympic.org/pdf/en_report_1315.pdf.
- (112) Langendijk, P., Bouwman, E. G., Soede, N. M., Taverne, M. A. M., Kemp, B., *Theriogenology* 2002, *57*, 1563-1577.
- (113) Preinerstorfer, B., Lindner, W., Laemmerhofer, M., *Electrophoresis* 2005, *26*, 2005-2018.
- (114) Preinerstorfer, B., Lubda, D., Lindner, W., Laemmerhofer, M., *Journal of Chromatography, A* 2006, *1106*, 94-105.
- (115) Nischang, I., Tallarek, U., *Electrophoresis* 2004, *25*, 2935-2945.

- (116) Tallarek, U., Leinweber, F. C., Nischang, I., *Electrophoresis* 2005, 26, 391-404.
- (117) Tjornelund, J., Bazzanella, A., Lochmann, H., Bachmann, K., *Journal of Chromatography, A* 1998, 811, 211-217.
- (118) Zarbl, E., Lammerhofer, M., Woschek, A., Hammerschmidt, F., *et al.*, *Journal of Separation Science* 2002, 25, 1269-1283.

Abstract

The present diploma thesis aims at presenting a new class of chiral selectors, phosphonic acid pseudo-peptides, for enantiomer separation in capillary electrochromatography (CEC), as well as their synthesis. Enantiomer separation is an eminent task in analytical chemistry, because biological systems can respond differently to distinct enantiomeric forms.

The focus herein lay on environmental issues. Agrochemicals are most often applied as racemates, although a growing number of studies indicate that in many cases primarily one enantiomer has the intended impact. The other is an avoidable contamination of water, sediments and soil as well as living organisms. Examples are pyrethroids, synthetic pesticides used for controlling insects in crop production, or racemic herbicides like Mecoprop and Dichlorprop.

Since distinct enantiomers can have different effects in patients, the importance of chirality in drug discovery has been recognized for a (relatively) long time. However, pharmaceuticals have to be considered as an environmental issue as well, because degradation (also of metabolites) may take place enantioselectively (e.g. in sewage plants and following surroundings, like sediments and soil).

The biomimetics herein were prepared in an Ugi reaction, a multicomponent reaction which was found to be suitable for the generation of whole compound libraries in a short time. The primary test compound was methyl 3,3-dimethyl-2-[4-allyloxy- α -(2,6-dimethylanilido)-benzylamino]-butane phosphonate, a novel zwitter-ionic pseudo-peptide. Preliminary experiments were performed to choose the best support and to explore immobilization chemistry. Concerning the support, silica monoliths were provided by Merck and organic polymer monoliths (OPMs) were produced in-house.

Generally, monolithic capillaries are a modern miniaturized separation material. With regard to environmentally friendly separation techniques, they are favourable over classical columns due to their low solvent consumption in the range of a few millilitres.

The OPMs as well as the silica monoliths revealed epoxy groups at their surfaces, which can be thiolized and subsequently subjected to radical addition of a selector. Immobilization chemistry *via* thiolization from epoxy groups had been investigated on OPMs before, but was tested for the first time on silica monoliths. For this reason, preliminary experiments evaluating the adoption of this immobilization technique for silica monoliths and comparing the performance to OPMs were carried out. Since the yield of the selector synthesis is still to be optimized in the future, a readily available selector, *tert*-butylcarbamoylequinidine (*t*-BuCQD), was employed as chromatographic test selector in CEC. Better separation results

were obtained with silica monolithic support which could successfully be employed for the separation of aryloxy carboxylic acid herbicides (amongst others Mecoprop and Dichlorprop) that could not be separated on the OPM. These results were eventually compared to those of high-density *t*-BuCQD loaded organic polymer monoliths prepared earlier by Lämmerhofer et al. The resulting manuscript has been accepted for publication (Buchinger et al., *Electrophoresis* 2009).

Subsequently, a silica monolith was used for the immobilization of enantiopure methyl 3,3-dimethyl-2-[4-allyloxy- α -(2,6-dimethylanilido)-benzylamino]-butane phosphonate. The enantiomers of Clenbuterol, a β_2 -sympathomimeticum, could successfully be baseline-separated, indicating the potential of phosphonic acid pseudo-peptide selectors. Thus, more intensive research on this new selector class is to follow in the future.

Zusammenfassung

Die vorliegende Diplomarbeit stellt eine neue Klasse chiraler Selektoren für die Enantiomerentrennung in der Kapillarelektrochromatographie (CEC), Phosphonsäurepseudopeptide, sowie deren Synthese, vor. Enantiomerentrennung ist eine bedeutende Aufgabe in der analytischen Chemie, da biologische Systeme unterschiedlich auf verschiedene Enantiomere reagieren können. Der Fokus dieser Arbeit lag auf umweltrelevanten Fragestellungen. Agrochemikalien werden meist als Racemate angewandt, obwohl eine zunehmende Anzahl an Studien darauf hinweist, dass in vielen Fällen hauptsächlich ein Enantiomer die gewünschte Wirkung erzielt. Das andere stellt eine vermeidbare Belastung von Wasser, Sedimenten und Boden, sowie lebender Organismen, dar. Beispiele sind Pyrethroide, synthetische Pestizide, die in der Getreideproduktion verwendet werden, oder racemische Herbizide, wie Mecoprop und Dichlorprop.

Da unterschiedliche Enantiomere verschiedene Wirkungen in Patienten haben können, wurde die Bedeutung von Chiralität in der Arzneimittelentwicklung schon vor (relativ) langer Zeit erkannt. Pharmaka müssen jedoch auch als umweltrelevante Thematik wahrgenommen werden, da ihr Abbau und der ihrer Metabolite in der Umwelt enantioselektiv erfolgen kann (in Kläranlagen und nachfolgenden Umgebungen, wie Sedimenten und Böden).

Die hier gezeigten Biomimetika wurden in einer Ugi Reaktion hergestellt, einer Multikomponentenreaktion, welche sich als geeignet zur Herstellung ganzer Komponenten-„Bibliotheken“ in kurzer Zeit erwiesen hat. Die Haupttestkomponente war Methyl 3,3-dimethyl-2-[4-allyloxy- α -(2,6-dimethylanilido)-benzylamino]-butan-phosphonat, ein neues zwitterionisches Pseudopeptid. Vorstudien wurden durchgeführt, um das beste Trägermaterial festzustellen und die Immobilisierungsschemie zu untersuchen bzw. zu optimieren. Betreffend das Trägermaterial wurden Silica Monolithe von Merck zur Verfügung gestellt und organische Polymermonolithe (OPMs) wurden selbst hergestellt.

Allgemein sind monolithische Kapillaren ein modernes miniaturisiertes Trennmaterial. In Hinblick auf umweltfreundliche Trenntechniken sind sie aufgrund ihres geringen Lösungsmittelverbrauchs von ein paar Millilitern der klassischen Säulenchromatographie vorzuziehen.

Die OPMs exponieren ebenso wie die Silica Monolithe Epoxygruppen an ihrer Oberfläche, welche thiolisiert und anschließend der Selektorimmobilisierung über radikalische Addition unterworfen werden können. Immobilisierungsschemie *via* Thiolisierung von Epoxygruppen ausgehend ist bereits früher an OPMs untersucht worden, wurde jedoch zum ersten Mal an Silica Monolithen getestet. Aus diesem Grund wurden vorangehende Experimente bezüglich

der Evaluierung der Adaption dieser Immobilisierungstechnik für Silica Monolithe und zum Vergleich der Trennleistung zu jener von OPMs durchgeführt.

Da die Ausbeute der Selektorsynthese noch optimierungsbedürftig ist, wurde ein anderer Selektor, *tert*-Butylcarbamoylchinidin, als chromatographischer Testselektor in CEC Testläufen verwendet. Das Silica Trägermaterial lieferte bessere Resultate, Aryloxy-carbonsäure-Herbizide (u.a. Mecoprop und Dichlorprop) konnten erfolgreich basisliniengetrennt werden, was an einem vergleichbaren OPM nicht gelang. Diese Ergebnisse wurden letztlich mit früheren eines dicht *t*-BuCQD beladenen OPM, welcher bereits von Lämmerhofer et al hergestellt und getestet worden war, verglichen. Das daraus folgende Manuskript wurde für zukünftige Veröffentlichung akzeptiert (Buchinger et al., Electrophoresis 2009).

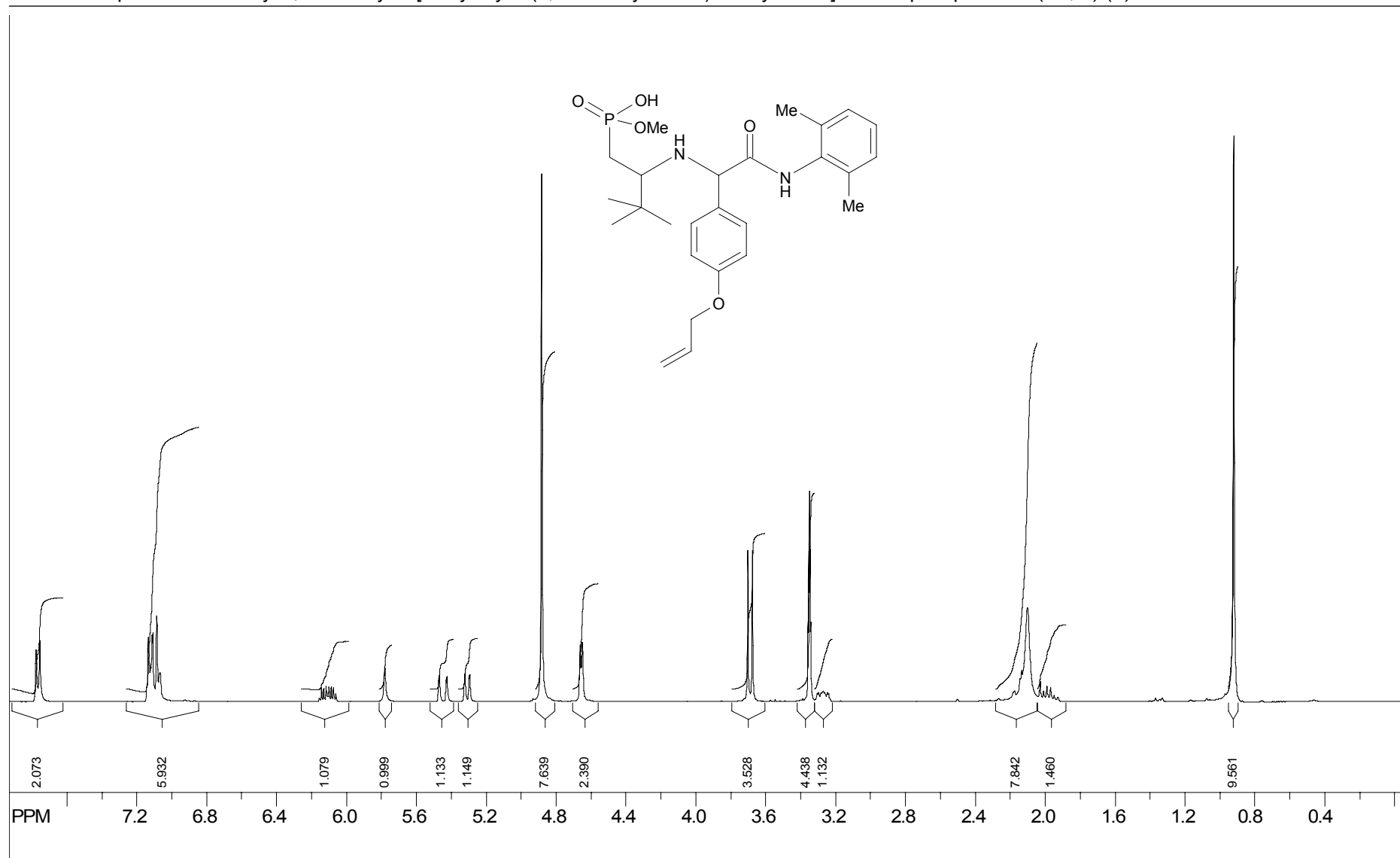
Im Anschluss wurde ein Silica Monolith für die Immobilisierung von enantiomerenreinem Methyl 3,3-dimethyl-2-[4-allyloxy- α -(2,6-dimethylanilido)-benzylamino]-butan-phosphonat verwendet. Die Enantiomere von Clenbuterol (einem β_2 -Sympathomimetikum), konnten erfolgreich basisliniengetrennt werden, was auf das Potential von Phosphonsäurepseudopeptidselektoren hinweist. Folglich wird an dieser neuen Selektorklasse künftig weitergeforscht werden.

APPENDIX

NMR and IR spectra

methyl 3,3-dimethyl-2-[4-allyloxy- α -(2,6-dimethylanilido)-benzylamino]-butane phosphonate

¹H-NMR spectrum of methyl 3,3-dimethyl-2-[4-allyloxy- α -(2,6-dimethylanilido)-benzylamino]-butane phosphonate (2R, \times)-(+)

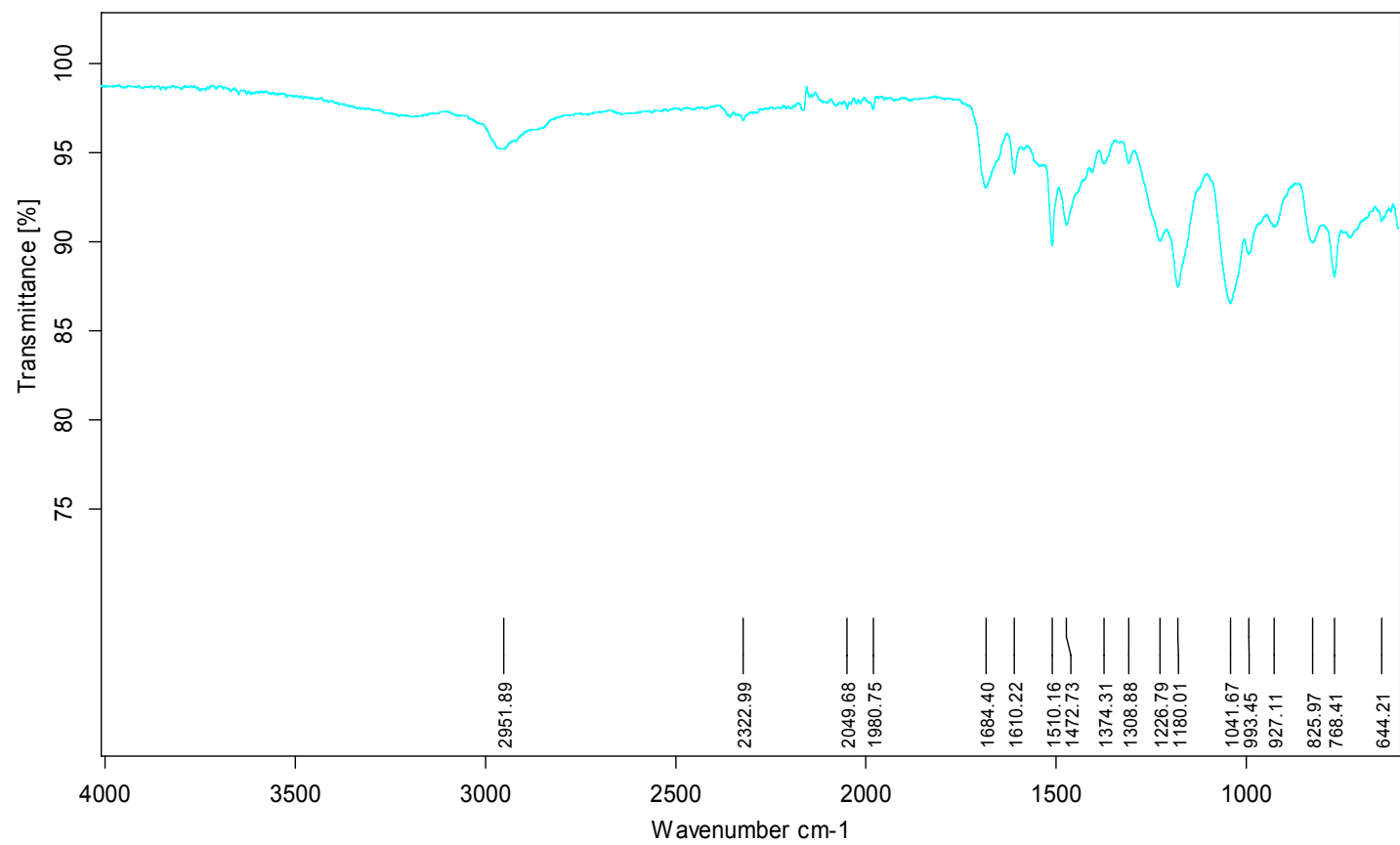


file: H:\SBA12\80\fid exp: <zg30>
 transmitter freq.: 400.132471 MHz
 time domain size: 65536 points
 width: 8278.15 Hz = 20.688513 ppm = 0.126314 Hz/pt
 number of scans: 16

freq. of 0 ppm: 400.129991 MHz
 processed size: 32768 complex points
 LB: 0.300 GB: 0.0000

¹³C-NMR spectrum of methyl 3,3-dimethyl-2-[4-allyloxy-α-(2,6-dimethylanilido)-benzylamino]-butane phosphonate (2R, x)-(+)





IR spectrum of racemic methyl 3,3-dimethyl-2-[4-allyloxy- α -(2,6-dimethylanilido)-benzylamino]-butane phosphonate

DANKE SCHÖN

DANKE DANKE DANKE DANKE DANKE DANKE DANKE DANKE DANKE DANKE DANKE

Auf der Uni...

Mein herausragender Dank gilt **Professor Michael Lämmerhofer**, nicht nur für die gewissenhafte Betreuung dieser Diplomarbeit, sondern insbesondere für die Diskussionsbereitschaft im Hinblick auf die Themenwahl – **DANKE FÜR ALLES!!!**

Bei **Professor Wolfgang Lindner** bedanke ich mich für die Bereitstellung der materiellen und finanziellen Ressourcen, sowie dafür, dass sich unter seiner Leitung eine nette und gleichzeitig hochmotivierte Arbeitsgruppe herausgebildet hat. Ich bin stolz, Teil dieser gewesen zu sein.

Dieter Lubda bzw. der **Firma Merck** danke ich für die Ermöglichung dieses Projektes durch die Bereitstellung der Silica Monolith.

Herzlich danke ich **Dr. Beatrix Follrich**, die mir jederzeit mit Rat und Tat zur Seite stand - **Trixi, DANKE!**

Generell danke ich den **Kollegen der Arbeitsgruppe** Lindner für ihre stete Hilfsbereitschaft und Ermutigungen – insbesonere **Mag. Marek Mahut** für die organisatorische Hilfestellung am Ende.

Weiters bin ich **Professor Josef Tomiska** zu großem Dank verpflichtet, der mein Interesse an der Mathematik während des Studiums erkannt und gefördert hat. Auch seine Ratschläge im Hinblick auf wissenschaftliches Schreiben weiß ich sehr zu schätzen.

Zu Hause...

Zuvorderst danke ich **meinen Eltern und meiner Familie**, die mir dieses Studium ermöglicht haben, ebenso wie meiner Taufpatin und deren Mann, **Margit und Walter Flechsig**, die stets reges Interesse an meiner Arbeit bekundeten.

Des weiteren vielen Dank an **Babsi und Michi Schrefl**, sowie **Ka Köllner**, die durch ihre Unterstützung und Motivation jede auf ihre Art und Weise zum Entstehen dieser Arbeit beigetragen haben.

Ein augenzwinkerndes Danke schön auch an **Marcus Paryzek** und **Thomas Dworak**, die zur richtigen Zeit am richtigen Ort waren.

Die letzten Zeilen dieser Danksagung widme ich meinen **Studienkollegen**:

Ich will euch auch in Zukunft nicht missen!!!

Stefanie Buchinger
Jakob Schefzikgasse 37/3/1, A-3430 Tulln
Telefon: +43(0)6801103276
E-Mail: stefanie.buchinger@gmx.net

CURRICULUM VITAE



Name: Stefanie Buchinger
Adresse: Jakob Schefzikgasse 37/3/1
3430 Tulln an der Donau
Geburtsdatum: 23. März 1986
Geburtsort: Tulln an der Donau
Familienstand: ledig, kinderlos
Staatsbürgerschaft: Österreich

AUSBILDUNG

1992 bis 1996: Volksschule I, Tulln
1996 bis 2000: BG/BRG Tulln, Unterstufe
2000 bis 2004: BG/BRG Tulln, Oberstufe (naturwissenschaftlicher Zweig)
Matura im Juni 2004 mit ausgezeichnetem Erfolg bestanden
seit Oktober 2004: Diplomstudium Chemie an der Universität Wien
seit März 2008: Diplomstudium der Rechtswissenschaften an der Universität Wien
Juni 2008: Erhalt eines Leistungsstipendiums der Universität Wien für das Kalenderjahr 2007 für die Studienrichtung Chemie
Juli 2009: Beginn der Diplomarbeit am Institut für Analytische Chemie

FREMDSPRACHENKENNTNISSE

Englisch fließend in Sprache und Schrift
Französisch und Spanisch auf Alltagsniveau

EDV KENNTNISSE

Windows Office (Word, Excel, Power Point)
Verschiedene fachspezifische (instrumentell-analytische)
Programme
Computergestützte Recherche chemischer Fachliteratur
(SciFinder u.ä.)

FACHBEZOGENE FERIAL- UND NEBENBESCHÄFTIGUNGEN

Juli, August 2006:	Praktikantin beim <i>Amt für Verbraucherschutz</i> des Kantons Aargau in der Schweiz
WS 2007/08 und WS 2008/09:	Anstellung als Tutorin für die LVA <i>Mathematik</i> <i>Chemiker</i> am Institut für Physikalische Chemie